

**Technical University of Crete – School of Mineral Resources
Engineering**

**Comparison of Density Calculation Methods
Applied to Real Reservoir Fluids**

An MSc Thesis submitted in partial fulfillment of the requirements for the degree of
MASTER OF SCIENCE in Petroleum Engineering

Charalampos Poulis

23/10/2018

© Copyright by Charalampos Poulis

All Rights Reserved

Acknowledgements

I wish to express my sincerest gratitude to my supervisor, Professor Vassilis Gaganis, for his excellent guidance, invaluable suggestions and comments throughout my work for this Thesis. I do also wish to express my sincerest thanks to all the professors of the Master's course, for their technical guidance and fruitful discussions throughout the course's duration.

I would like to acknowledge the contribution of Hellenic Petroleum Company for sponsoring the whole Course and made it possible for all of us to attend.

I am indebted to my parents who always encouraged higher studies and supported me in any way possible.

Abstract

Gas density as well as its derivative, are necessary in almost every upstream petroleum engineering calculation. Calculations in the wellbore are directly related to the hydrostatic head and hence directly related to the petroleum fluid density. Calculations in the reservoir are on the other hand mostly related to the fluid's compressibility or in other words density's first derivative with respect to pressure.

Density calculation is directly related to compressibility z factor calculation and therefore the one problem reduces into another. The most common sources of compressibility z factor values are experimental measurement, equations of state and empirical correlations. Necessity for z factor values prediction arises when there is no available experimental data for the required composition, pressure and temperature conditions. In the present master thesis, a large database of real reservoir fluid PVT properties is utilized, where the z factor has been experimentally measured for various pressure values above the dew point pressure in the monophasic region.

Industry's most commonly used z factor calculation methods were implemented using Microsoft Excel® and Mathworks Matlab® where appropriate. The results from the various methods implemented were compared to the experimental measurements while the methods were finally evaluated in terms of their quality and performance.

Table of Contents

ACKNOWLEDGEMENTS	III
ABSTRACT	IV
TABLE OF CONTENTS	V
LIST OF FIGURES	VIII
LIST OF TABLES	X
NOMENCLATURE	XI
LIST OF ABBREVIATIONS	XIV
CHAPTER 1 INTRODUCTION.....	1
1.1 PREFACE.....	1
1.2 THESIS’S OBJECTIVE.....	2
1.3 THESIS OUTLINE.....	2
CHAPTER 2 REVIEW OF GAS PROPERTIES	4
2.1 BACKGROUND	4
2.2 CLASSIFICATION OF NATURAL GASES.....	5
2.2.1 <i>Dry Gas</i>	7
2.2.2 <i>Wet Gas</i>	8
2.2.3 <i>Gas Condensate</i>	9
2.3 CRITICAL AND REDUCED GAS PROPERTIES	10
2.3.1 <i>Critical Properties of the Heavy End</i>	12
2.3.2 <i>Mixing Rules</i>	16
CHAPTER 3 EMPIRICAL CORRELATIONS BASED ON THE CORRESPONDING STATES PRINCIPLE .	21
3.1 BACKGROUND	21
3.2 CORRELATIONS BASED ON THE CORRESPONDING STATES PRINCIPLE	29
3.2.1 <i>Hall and Yarborough</i>	33
3.2.2 <i>Dranchuk and Abou-Kassem</i>	34
3.2.3 <i>Brill and Beggs</i>	36
3.2.4 <i>Azizi, Behbahani and Isazedeh</i>	37
3.2.5 <i>Shell Oil Company</i>	39
3.2.6 <i>Niger Delta</i>	40
3.2.7 <i>Heidaryan et al.</i>	40
CHAPTER 4 CUBIC EQUATIONS OF STATE	44

4.1	BACKGROUND	44
4.2	VAN DER WAALS EOS.....	46
4.3	REDLICH-KWONG EOS.....	48
4.4	SOAVE-REDLICH-KWONG (SRK) EOS	50
4.5	PENG-ROBINSON (PR) EOS.....	52
4.6	BINARY INTERACTION COEFFICIENT (BICs).....	55
4.7	SOLUTION OF THE CUBIC POLYNOMIAL.....	57
4.7.1	<i>Cardano</i>	58
4.8	VOLUME SHIFT CORRECTION	61
CHAPTER 5	EXPERIMENTAL COMPRESSIBILITY FACTOR VALUES	64
5.1	BACKGROUND	64
5.2	FLUID'S DATABASE PROPERTIES.....	64
5.2.1	<i>Pressure Discretization</i>	65
5.2.2	<i>Reservoir Temperature Distribution</i>	66
5.2.3	<i>Composition Distribution</i>	67
CHAPTER 6	RESULTS AND DISCUSSION.....	71
6.1	STATISTICAL TOOLS	71
6.1.1	<i>Mean Absolute Deviation</i>	71
6.1.2	<i>Mean Square Error</i>	71
6.1.3	<i>Root Mean Square Error</i>	72
6.1.4	<i>Mean Absolute Relative Deviation</i>	72
6.1.5	<i>Mean Relative Deviation</i>	72
6.1.6	<i>Outliers Removal</i>	73
6.2	RESULTS COMPARISON	73
6.2.1	<i>Correlations</i>	73
6.2.2	<i>Equation of State Results</i>	87
6.2.3	<i>Discussion</i>	90
6.3	CONCLUSIONS.....	92
APPENDIX.....	94
REFERENCES	119

List of Figures

Figure 1.1 – Procedure for the calculation of the z factor with the various methods.	3
Figure 2.1 - Phase diagram of multicomponent mixture.....	6
Figure 2.2 – Typical phase diagram of a dry gas.....	7
Figure 2.3 – Typical phase diagram of a wet gas.....	8
Figure 2.4 – Typical phase diagram of a gas condensate.....	9
Figure 3.1 - Deviation factor z chart for low pressure gases (GPA Copyright).....	22
Figure 3.2 - The Standing-Katz generalized z factor chart.....	24
Figure 3.3 - z factor of pure substances at reduced conditions ($T_r=0.65$).....	24
Figure 3.4 - z factor of pure substances at reduced conditions ($T_r=0.75$).....	25
Figure 3.5 - z factor of pure substances at reduced conditions ($T_r=0.85$).....	25
Figure 3.6 - z factor of pure substances at reduced conditions ($T_r=1.02$).....	26
Figure 3.7 - z factor of pure substances at reduced conditions ($T_r=1.07$).....	26
Figure 3.8 - z factor of pure substances at reduced conditions ($T_r=1.13$).....	27
Figure 3.9 - z factor of pure substances at reduced conditions ($T_r=1.24$).....	27
Figure 3.10 - z factor of pure substances at reduced conditions ($T_r=1.55$).....	28
Figure 3.11 - z factor of pure substances at reduced conditions ($T_r=1.98$).....	28
Figure 3.12 - z factor of pure substances at reduced conditions ($T_r=2.03$).....	29
Figure 3.13 – Comparison of Standing and Sutton correlations for the calculation of pseudo-critical temperature and pressure.....	32
Table 3.3: Tuned coefficients of the Azizi et al. correlation.....	38
Table 3.4: Tuned coefficients of Heidaryan et al. z factor correlation (Eq. 3.37).....	41
Table 4.1: Binary Interaction Coefficients (BICs) for the PR EoS and SRK EoS.....	56
Figure 4.1 – p-V diagram of a pure component as calculated by a cubic EoS illustrating the van der Waals’s “loop” defining vapor pressure by the equal-area rule.....	63
Figure 5.1 – ΔP frequency distribution for the natural gases of the database.....	66
Figure 5.2 – T_{res} frequency distribution for the natural gases of the database ($^{\circ}F$).....	68
Figure 5.3 – C_{7+} concentration distribution for the natural gases of the database.....	68
Figure 5.4 – H_2S concentration distribution for the natural gases of the database.....	69
Figure 5.5 – CO_2 concentration distribution for the natural gases of the database.....	69
Figure 5.6 – CH_4 concentration distribution for the natural gases of the database.....	70
Figure 6.1 – MRD of the Azizi, Elsharkawy combination.....	74
Figure 6.2 – MRD of the Aziz, Elsharkawy, Wichert combination.....	75
Figure 6.3 – MRD of the Azizi, Kays combination.....	75

Figure 6.4 – MRD of the Azizi, Kays, Wichert combination.....	76
Figure 6.5 – MRD of the Brill and Beggs, Elsharkawy combination.....	77
Figure 6.6 – MRD of the Brill and Beggs, Elsharkawy, Wichert combination	78
Figure 6.7 – MRD of the Brill and Beggs, Kays combination.....	78
Figure 6.8 – MRD of the Brill and Beggs, Kays, Wichert combination	79
Figure 6.9 – MRD of the Shell, Elsharkawy combination	80
Figure 6.10 – MRD of the Shell, Elsharkawy, Wichert combination.....	81
Figure 6.11 – MRD of the Shell, Kays combination	81
Figure 6.12 – MRD of the Shell, Kays, Wichert combination	82
Figure 6.13 – MRD of the Heidaryan, Elsharkawy combination	83
Figure 6.14 – MRD of the Heidaryan, Elsharkawy, Wichert combination.....	83
Figure 6.15 – MRD of the Heidaryan, Kays combination	84
Figure 6.16 – MRD of the Heidaryan, Kays, Wichert combination	84
Figure 6.17 – MRD of the Hall and Yarborough, Elsharkawy combination.....	85
Figure 6.18 – MRD of the Hall and Yarborough, Elsharkawy, Wichert combination	86
Figure 6.19 – MRD of the Hall and Yarborough, Kays combination	86
Figure 6.20 – MRD of the Hall and Yarborough, Kays, Wichert combination.....	87
Figure 6.21 – MRD of the PR, Volume shift, nonzero BICs	88
Figure 6.22 – MRD of the PR, nonzero BICs	88
Figure 6.23 – MRD of the PR, Volume shift.....	89
Figure 6.24 – MRD of the PR.....	89

List of Tables

- Table 2.1:** *Typical compositions of various reservoir fluids.*
- Table 2.2:** *Critical properties of pure substances*
- Table 2.3:** *Constants of the El Sharkawy mixing parameters*
- Table 3.1:** *Correlations for the calculation of z factor*
- Table 3.2:** *Constants of the Dranchuk and Abou-Kassem z factor correlation*
- Table 3.3:** *Tuned coefficients of the Aziz, Behbahani, Isazedehe z factor correlation*
- Table 3.4:** *Tuned coefficients of Heidaryan et al. z factor correlation (Eq. 3.37)*
- Table 4.1:** *Binary Interaction Coefficients (BICs) for the PR EoS and SRK EoS*
- Table 4.2:** *Binary Interaction Parameters (BICs) adopted by this work.*
- Table 6.1:** *Recommended application ranges for the correlations*
- Table 6.2:** *Statistical metrics for the different combinations (Azizi et al.)*
- Table 6.3:** *Statistical metrics for the different combinations (Brill and Beggs)*
- Table 6.4:** *Statistical metrics for the different combinations (Shell correlation)*
- Table 6.5:** *Statistical metrics for the different combinations (Heidaryan et al.)*
- Table 6.6:** *Statistical metrics for the different combinations (Hall and Yarborough)*
- Table 6.7:** *Statistical metrics for the different combinations of the PR EoS*
- Table 6.8:** *MARD range for gases with experimental error*
- Table 6.9:** *MARD error of selected natural gases*

Nomenclature

A_{bb}	:	parameter of the Brill and Beggs correlation for the calculation of z factor
A_{car}	:	coefficient of the 3 rd order term in the cubic Cardano polynomial
A_{mix}	:	EoS constant describing molecular attractive forces, dimensionless
A_i	:	EoS constant calculated by compound describing molecular attractive forces, dimensionless
b	:	dimensional PR-EoS constant describing molecular repulsive forces, L^3/n , $ft^3/lbm\ mol$, VdW covolume
B_{car}	:	coefficient of the 2 nd order term in the cubic Cardano polynomial
b_{car}	:	cubic Cardano polynomial coefficient after the transformation
B_{mix}	:	EoS constant describing molecular repulsive forces, dimensionless
B_i	:	EoS constant calculated by compound describing molecular repulsive forces, dimensionless
B_{bb}	:	parameter of the Brill and Beggs correlation for the calculation of z factor
C_{bb}	:	parameter of the Brill and Beggs correlation for the calculation of z factor
C_{car}	:	coefficient of the 1 st order term in the cubic Cardano polynomial
c_{car}	:	cubic Cardano polynomial coefficient after the transformation
D_{bb}	:	parameter of the Brill and Beggs correlation for the calculation of z factor
D_{car}	:	coefficient of the 0 th order term in the cubic Cardano polynomial
E_{car}	:	cubic Cardano polynomial coefficient after division of both sides with A_{car}
F_{car}	:	cubic Cardano polynomial coefficient after division of both sides with A_{car}
f_p	:	Twu correlation parameter for critical pressure
f_T	:	Twu correlation parameter for critical temperature
f_V	:	Twu correlation parameter for critical volume
G_{car}	:	cubic Cardano polynomial coefficient after division of both sides with A_{car}
k_{ij}	:	binary interaction coefficient (<i>BIC</i>) used in the mixing rules of A parameter of the PR EoS
m	:	correlating function in correction term α for EOS constant A , parameter of the SRK EoS
MW	:	molecular weight, m/n or $lbm/lbm\ mol$

MW_p	:	molecular weight of the paraffin hydrocarbon at Twu correlation, m/n or lbm/lbm mol
P	:	pressure at the examined conditions, psia
P_c	:	fluid's critical pressure, psia, m/Lt ²
P_d	:	dewpoint pressure, psia
P_{ci}	:	critical pressure of the i^{th} component in gas mixture, psia
P_{cP}	:	critical pressure of paraffin hydrocarbons, m/Lt ² , psia
P_{cric}	:	cricondenbar, psia
p_{pc}	:	fluid's pseudo-critical pressure, psia
p_{pr}	:	fluid's pseudo-reduced pressure, dimensionless
R	:	universal gas constant, 10.73146 psia-ft ³ /°R-lbm mol
T	:	temperature at the examined conditions, psia
t	:	parameter of the Hall and Yarborough equation for the calculation of z factor, inverse absolute temperature ($1/T$)
T_b	:	normal boiling point temperature at 1 atm, °R
T_c	:	gas mixture critical temperature, °R
T_{ci}	:	critical temperature of the i^{th} component in gas mixture, °R
T_{cP}	:	critical temperature of paraffin hydrocarbons, °R
T_{cric}	:	cricondentherm temperature, °R
t_{HY}	:	parameter of the Hall and Yarborough correlation for the calculation of z factor
T_{pc}	:	fluid's pseudo-critical temperature, °R
T_{pr}	:	fluid's pseudo-reduced temperature, dimensionless
V_a	:	volume of the real gas, ft ³
V_c	:	critical volume, Lt ³ , ft ³ or bbl
V^{cor}	:	corrected by volume translation molar volume
V_{cP}	:	critical volume of paraffin hydrocarbons, Lt, cu.ft.
v^{EOS}	:	molar volume as calculated by the EoS, prior to volume translation
V_i	:	volume of the ideal gas
v_m	:	molar volume, defines the ratio of volume per mole
y	:	Reduced-density parameter used in the Hall and Yarborough eq. for the calculation of z factor
z	:	real gas deviation (compressibility) factor
Z_{RA}	:	Rackett compressibility factor
α	:	numerical constant(s) used in the PR EoS; describes molecular attractive forces, psia/(ft ³ -lbm mol) ²
γ_g	:	specific gravity, air=1 or water=1
γ_p	:	specific gravity of paraffin hydrocarbons, water=1
Δ	:	discriminant of the depressed cubic Cardano polynomial
$\Delta\gamma_P$:	parameter in the Twu critical-pressure correlation
$\Delta\gamma_T$:	parameter in the Twu critical-temperature correlation
$\Delta\gamma_V$:	parameter in the Twu critical-volume correlation
ρ_g	:	density of gas, lb _m /ft ³

θ : generic symbol for any component property; Twu property correlation parameter

ω : acentric factor (dimensionless)

List of Abbreviations

BIC	:	binary interaction coefficient
EoS	:	equation of state
MAD	:	mean absolute deviation
MARD	:	mean absolute percentage error
MSE	:	mean squared error
PR	:	Peng-Robinson equation of state
RK	:	Redlich-Kwong equation of state
RMSE	:	root mean squared error
SBV	:	Stewart-Burckhardt-Voo mixing rule
SRK	:	Soave-Redlich-Kwong equation of state
VdW	:	van der Waals
VLE	:	vapor-liquid equilibria

Chapter 1 Introduction

1.1 Preface

The knowledge of density of natural gases is necessary in the majority of petroleum and natural gas engineering calculations. Some of these calculations include gas metering, gas compression, design of processing and transport units, and design of pipeline, separation and surface facilities. Properties of natural gases are also important in the calculation of gas flow rate through the reservoir medium, material balance calculations, estimation of natural gas reserves, and eventually reservoir simulations. Most commonly the natural gas properties are experimentally measured in the laboratory but occasionally however, this kind of data becomes unavailable. There comes the necessity to estimate natural gas properties, such as compressibility and density by other means rather than experimental measurements. The reasons for unavailability of experimental data are that it is hard to determine experimentally measured z factor values for all compositions of natural gases on the whole ranges of pressures and temperatures and also that the laboratory measurements are costly and most of the time these measurements are performed at reservoir temperatures exclusively.

Heavy natural gases such as sour gases and gas condensates have been increasingly gaining in popularity as a number of fields have been discovered around the world in the past three decades. For these natural gases the available methods in the literature for the calculation of density and z factor are considered to be producing unsatisfactory predictions. These methods can be classified into three major families [Erdogmus et al, 1997]. The first family of methods utilizes the natural gas composition or natural gas gravity to calculate pseudo-critical gas properties and predicts natural gas properties from empirical correlations. Commonly in such a kind of method, gas viscosity calculation involves the use of gas density and hence prediction of viscosity is dependent

on the choice of the method that is used to estimate the natural gas density. The second family of methods receives as input the natural gas composition to estimate gas properties by utilizing the principle of corresponding states. The third family of methods which is the most recent one is based on equation of state models and has the advantage of using a single equation to calculate k-values, the z factor, and natural gas density [Guo et al, 2001]. Last but not least, stable convergence in the vicinity of the fluid's critical point is guaranteed by this last group of methods.

1.2 Thesis's Objective

Today's upstream petroleum engineering and wellbore calculations are directly related to the hydrostatic head which is also directly related to natural gas density. The calculation of gas density and its derivative requires the determination of z factor and pseudo-critical properties of the natural gas mixture. Furthermore, as more and more acid and sour environment reservoirs are being discovered, it becomes increasingly important to have simple and robust techniques to be able to accurately determine z factor and hence gas density of natural gases with high concentrations of non-hydrocarbons such as carbon dioxide, nitrogen and hydrogen sulfide.

The present thesis investigates the most widely used natural gas density calculation methods which can be implemented in a computer. For natural gases containing large quantities of non-hydrocarbons common correction techniques are applied. The results of each natural gas density calculation method are quality checked and the performance of each calculation method is evaluated against real gas density measurements.

1.3 Thesis Outline

In this master thesis, some of the most widely used compressibility z factor calculation methods were implemented. These methods are either based on the approaches of cubic equations of state or on the Standing – Katz compressibility factor chart and the corresponding states principle. The Peng-Robinson equation of state along with its variations and corrections, which is routinely being used in reservoir calculations as well as five improved pseudo critical property correlations for the Standing-Katz chart, are

utilized to match the experimentally obtained compressibility z factor of two hundred thirty four real reservoir gases and condensates of the database, including highly sour and acid gases (high concentration of H_2S and CO_2), slightly sour gases, lean and rich natural gases (significant amount of C_{12+}). The steps followed for the completion of the present work are shown in the flowchart in Fig. 1.1 below.

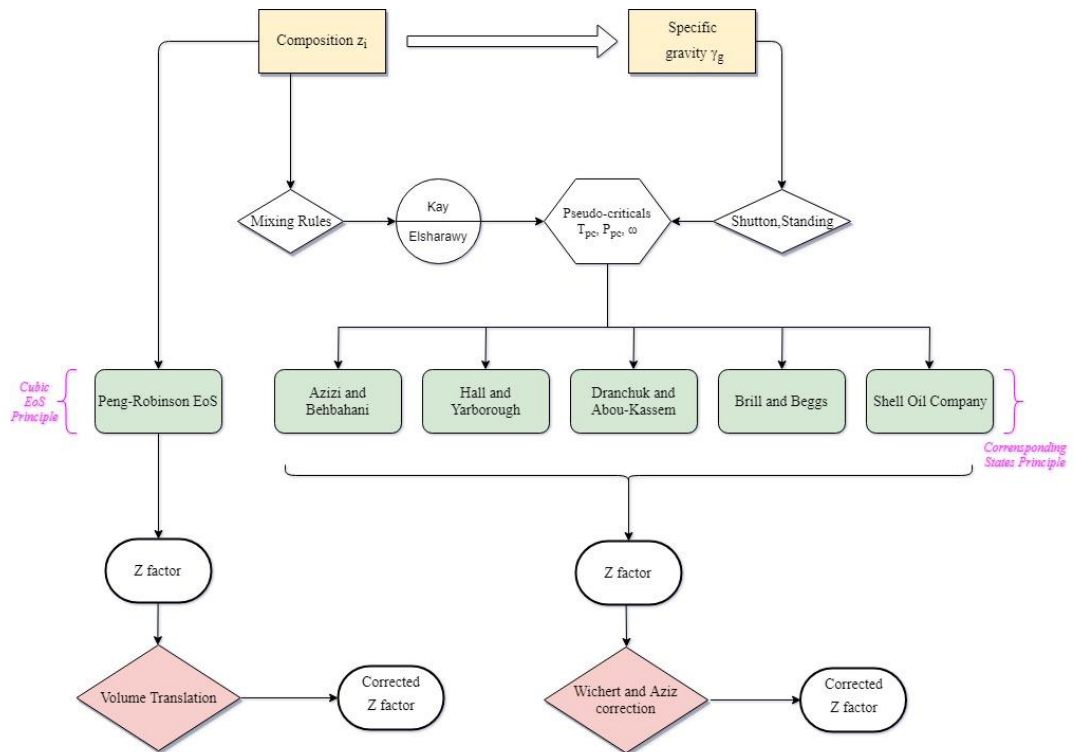


Figure 1.1 – Procedure for the calculation of the z factor with the various methods.

Chapter 2 Review of Gas Properties

2.1 Background

Compressibility factor z , or deviation factor as it is commonly also called, is a measure of the amount that a real gas deviates from the ideal gas behavior. It is a dimensionless property and by definition it is equal to the ratio of the volume actually occupied by a real gas at a given set of pressure and temperature conditions over the volume that it would occupy if it behaved like an ideal gas at the same conditions. A value of unity for the z factor would represent that the real gas behaves ideally.

$$z = \frac{V_{actual}}{V_{ideal}} = \frac{\text{Actual volume of } n \text{ moles of gas at } p \text{ and } T}{\text{Ideal volume of } n \text{ moles of gas at the same } p \text{ and } T}$$

According to the kinetic theory of gases, which laid the foundations for the Ideal gas law, neither the attractive forces between the gas molecules nor the repulsive forces are taken into account when describing gas behavior. In nature however, ideal gases do not really exist and gases behave as real ones. The molecules of real gases accept two kind of forces: to move apart from each other due to their perpetual kinetic motion, and to come close to each other because of electrostatic attractive forces between them.

At standard conditions, or at conditions close to that, gas molecules are quite far apart from each other and the attractive forces are negligible. Attractive forces are also very weak at high temperatures, due to the molecules increased kinetic energy. Under such aforementioned conditions, real gases tend to approach ideal gas behavior. This approximation is not valid however in case that the real gas is under elevated pressure as the molecules are very close to each other which results in significant attractive forces between them. What has been described so far qualitatively explains the behavior of

ideal and real gases and general representations of the ideal and real gas behaviors are given in Eqs. 2.1 and 2.2 respectively.

$$\text{Ideal Gas Law: } PV = nRT \quad (2.1)$$

$$\text{Real Gas Law: } PV = z nRT \quad (2.2)$$

2.2 Classification of Natural Gases

Fig. 2.1 is a typical phase diagram of a reservoir fluid which can be conveniently used to describe various types of reservoir fluids. A reservoir contains natural gas if its temperature is higher than the fluid's critical temperature. The depletion of the reservoir will result in retrograde condensation if the reservoir temperature lies between the critical temperature and the cricondentherm (T_{crit}), whereas no liquid will appear if the temperature is greater than the cricondentherm. Additionally, the oil in a reservoir with a temperature close to its critical point is more volatile than that at a lower temperature. A small reduction in pressure below its bubble point, in a reservoir with a temperature just below the fluid's critical one, will lead to vaporization of some quantity of the oil. It is profound thereby that the location of reservoir temperature isotherm on the phase diagram can be used to classify reservoir fluids.

Reservoir's temperature is mainly determined by its depth. The phase behavior of a reservoir fluid is determined by its composition. In Table 2.1 typical compositions of various classes of reservoir hydrocarbon fluids are given. Critical temperatures of heavy hydrocarbons are higher than those of the lighter. The pseudo-critical temperature of a hydrocarbon mixture containing predominantly large quantities of heavier hydrocarbons will be therefore higher compared to that of a mixture which contains lighter components.

Table 2.1: Typical compositions of various reservoir fluids.

Component, mole %	Dry Gas	Gas Condensate	Volatile Oil	Black Oil
N ₂	6.25	0.29	0.12	0.16
CO ₂	2.34	1.72	1.50	0.91
C ₁	81.13	79.14	69.59	36.47
C ₂	7.24	7.48	5.31	9.67
C ₃	2.35	3.29	4.22	6.95
iC ₄	0.22	0.51	0.85	1.44
nC ₄	0.35	1.25	1.76	3.93
iC ₅	0.09	0.36	0.67	1.44
nC ₅	0.03	0.55	1.12	1.41
C ₆	-	0.61	1.22	4.33
C ₇₊	-	4.80	16.64	33.29

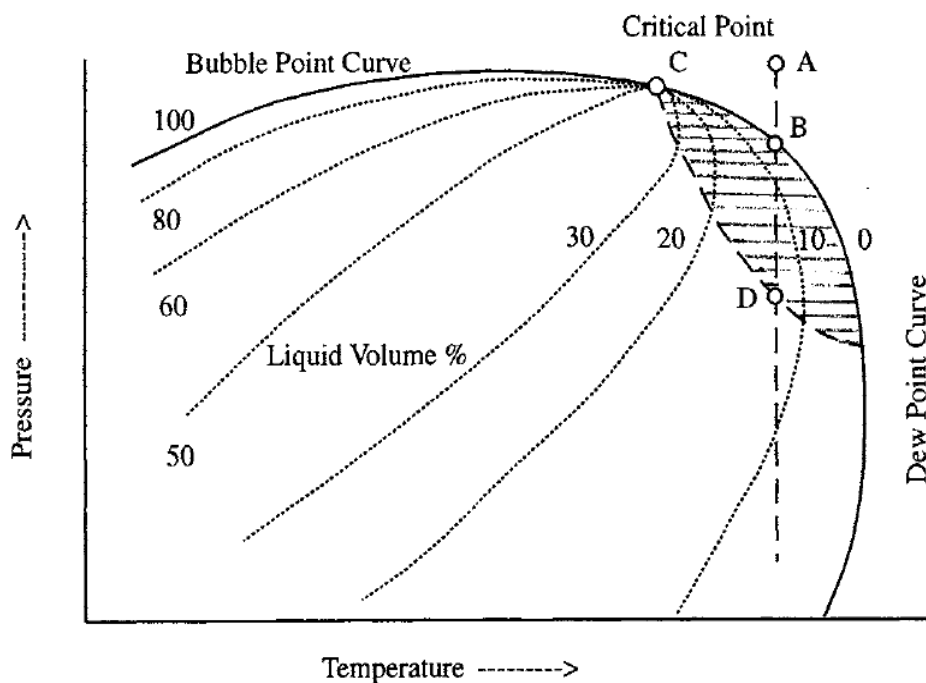


Figure 2.1 - Phase diagram of multicomponent mixture

2.2.1 Dry Gas

Fig. 2.2 shows the phase diagram of a typical dry gas. Dry gases are predominantly composed of methane and light non-hydrocarbons such as nitrogen and carbon dioxide. The phase envelope is relatively tight and mostly located below the reservoir temperature. The gas remains single phase from the reservoir to the separator conditions, while the contained water however may condense at standard conditions due to the cooling of the gas. PVT tests in the laboratory are limited to the gas compressibility measurement.

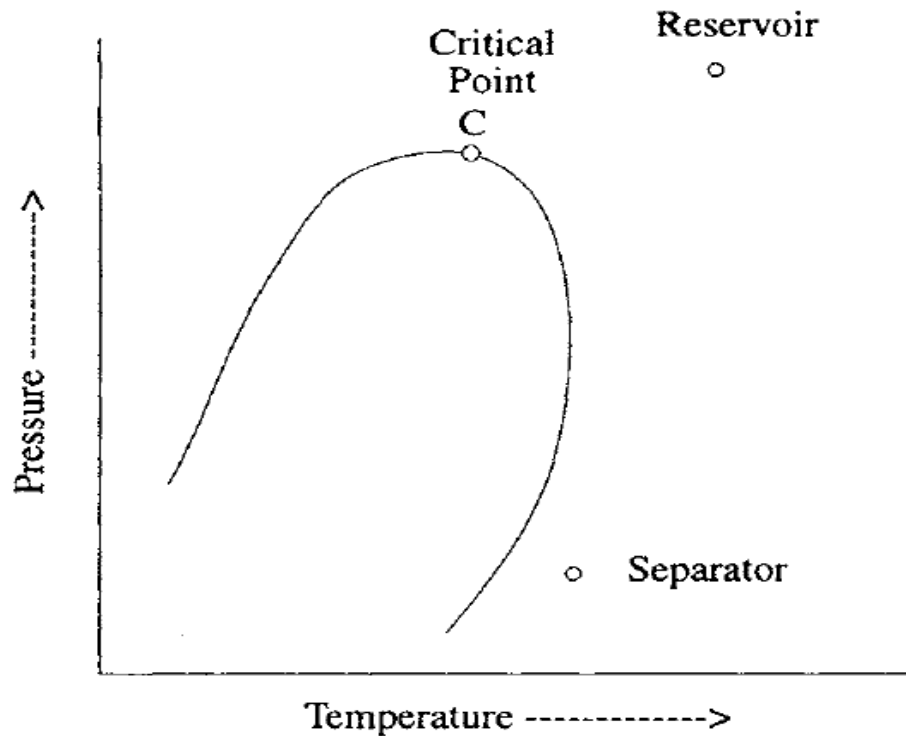


Figure 2.2 – Typical phase diagram of a dry gas

2.2.2 Wet Gas

A wet gas is mainly composed by methane and other light hydrocarbons. As it was the case with dry gases, its phase envelope is located entirely over a temperature range below that of the reservoir, as shown in Fig. 2.3. A wet gas therefore will not form condensate in the reservoir during depletion. Separator conditions lie however within the phase envelope, producing in this way some quantity of condensate at standard conditions. The only PVT test applicable at reservoir conditions is the gas compressibility measurement, while separator tests are generally conducted to determine the amount and the properties of the condensed phase at standard conditions.

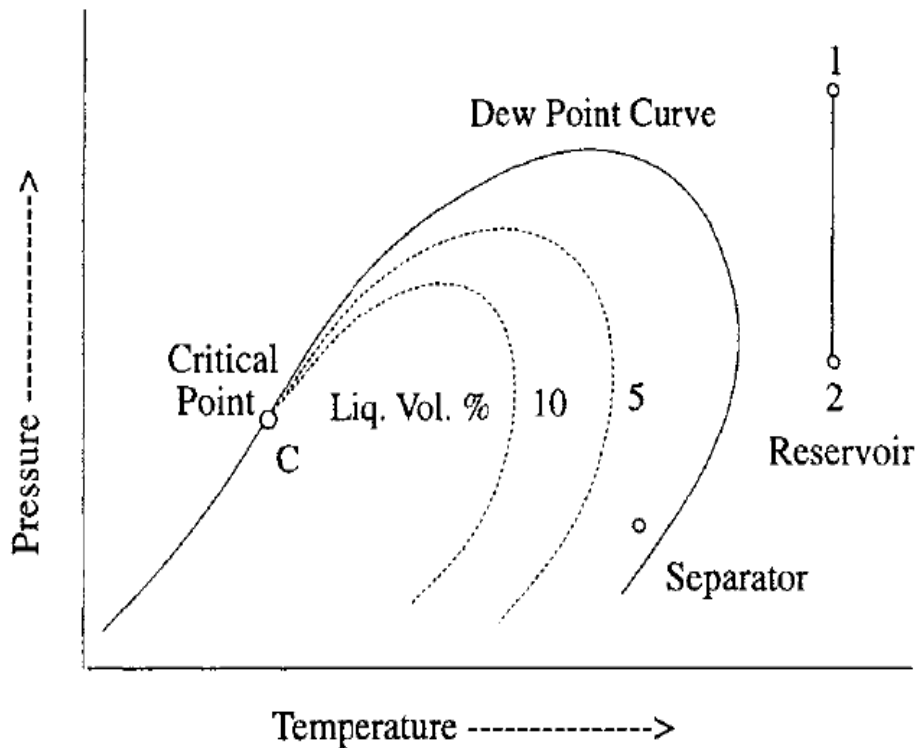


Figure 2.3 – Typical phase diagram of a wet gas

2.2.3 Gas Condensate

A typical phase diagram of a gas condensate is shown in Fig. 2.4. The presence of heavier hydrocarbons expands the phase envelope and rotates it clockwise compared to that of a wet gas and the reservoir temperature is between the critical one and the cricondentherm. Liquid droplets will be formed due to retrograde condensation in the reservoir when the pressure falls below the fluid's dewpoint. Moreover at separator conditions, further condensation will take place due to the fluid's cooling. The amount of potentially condensable hydrocarbons in the reservoir increases with the richness of the natural gas, as more heavy components shift the critical temperature towards the reservoir temperature, while a gas with a cricondentherm near the reservoir temperature will behave very similar to a wet gas.

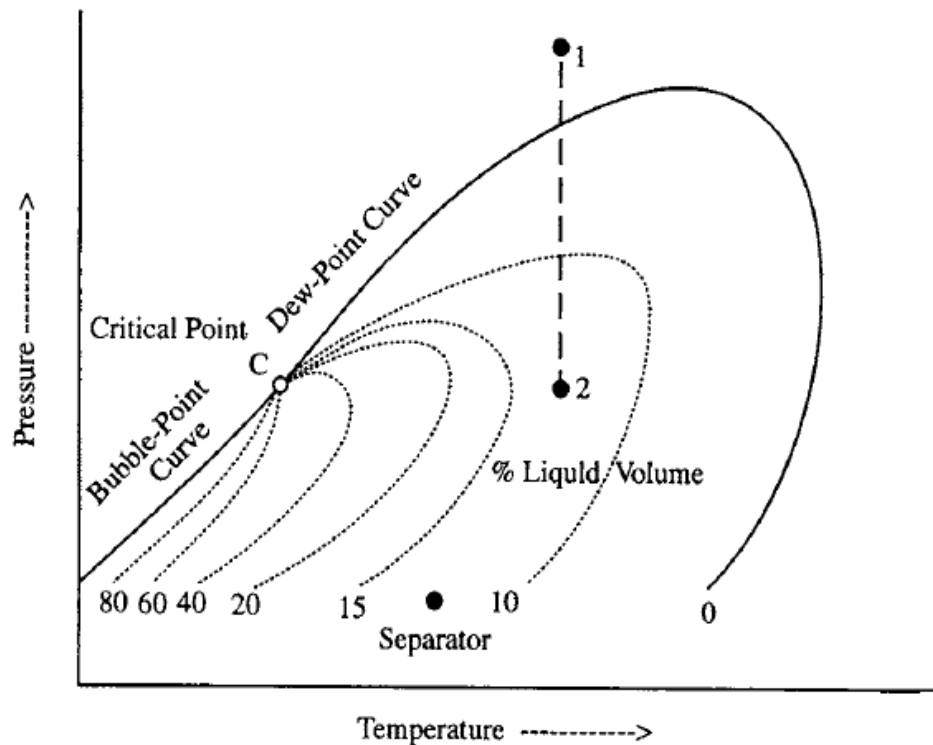


Figure 2.4 – Typical phase diagram of a gas condensate

The concentration of heptanes plus is generally less than 12% mole in gas condensates fluids, as fluids that contain more than that almost always behave like liquids in the reservoir. However, a number of exceptions have been reported with condensates exhibiting heptanes plus fraction as high as 15.5% mole and oils with as low as 10%. The condensate color can be water-white or dark. Dark condensates usually have relatively high specific gravity and are associated with high dewpoint gases. The specific gravity of condensates ranges from 0.74 to 0.82, although values as high as 0.88 have been reported.

2.3 Critical and Reduced Gas Properties

Most equations of state and correlations do not incorporate gas pressure and temperature explicitly to define the state of a system, but instead they utilize two or more reduced properties, according to corresponding states theory, which are dimensionless. The corresponding states theory is described in detail in the next chapter. Reduced pressure, temperature and reduced density are calculated by Eqs. 2.3a, 2.3b and 2.3c respectively.

$$P_r = P/P_c \quad (2.3a)$$

$$T_r = T/T_c \quad (2.3b)$$

$$\rho_r = \rho/\rho_c \quad (2.3c)$$

Absolute units must be used for the calculation of reduced pressure and temperature. P_c , T_c and ρ_c refer either to the true critical properties of a pure compound, or some average calculated by means of a mixing rule for the case of mixtures. The reduced pressure for the majority of hydrocarbon gases applications varies from 0.02 to 30; reduced temperature commonly ranges from less than 1 to 2.5 for hydrocarbon gases.

Reduced density may vary from zero at very low pressures to 3.5 at elevated pressures for hydrocarbon fluids.

Critical properties are well known for pure compounds (like oxygen, nitrogen, carbon dioxide, methane, ethane and up to C₅) and can be found in the literature. Regarding the hydrocarbon pseudo-components from C₆ up to C₁₁ average values from the literature can be used with only tiny deviations from the real ones. The discussed critical properties are presented tabulated in Table 2.2. The determination of the critical properties of the heavy end fraction is presented in a following section.

Note that pseudo-critical properties are not necessarily approximations of the true critical properties, but are chosen instead so that mixture properties can be estimated correctly by means of various corresponding states based correlations.

Table 2.2: *Critical properties of pure substances*

Compound	Formula	Molar mass	Liquid density	Pc (MPa)	Tc (K)	Omega
Oxygen	O ₂	0.031999	0.00	5.04	154.6	0.025
Nitrogen	N ₂	0.028013	0.0	3.39	77.40	0.039
Carbon dioxide	CO ₂	0.044010	0.0	7.38	304.1	0.239
Hydrogen sulfide	H ₂ S	0.034080	0.0	8.94	373.2	0.081
Methane	CH ₄	0.016043	300	4.60	190.4	0.011
Ethane	C ₂ H ₆	0.030070	356	4.88	305.4	0.099
Propane	C ₃ H ₈	0.044097	508	4.25	369.8	0.153
iso-Butane	i-C ₄ H ₁₀	0.058124	567	3.65	408.2	0.183
normal Butane	n-C ₄ H ₁₀	0.058124	586	3.80	425.2	0.199
iso-Pentane	i-C ₅ H ₁₂	0.072451	625	3.39	460.4	0.227
normal Pentane	n-C ₅ H ₁₂	0.072451	631	3.37	469.7	0.251
Hexane	C ₆ H ₁₄	0.084000	690	3.33	512.8	0.250
Heptanes	C ₇ H ₁₆	0.096000	727	3.12	547.2	0.280
Octane	C ₈ H ₁₈	0.107000	749	2.89	575.6	0.312
Nonane	C ₉ H ₂₀	0.121000	768	2.64	602.8	0.348
Decane	C ₁₀ H ₂₂	0.134000	782	2.42	626.7	0.385
Undecane	C ₁₁ H ₂₄	0.147000	793	2.24	647.8	0.419

2.3.1 Critical Properties of the Heavy End

Nearly all naturally occurring gas fluids contain some heavy fractions that are not well defined. There arises the need of adequately characterizing those undefined plus fractions in terms of their critical properties [Gastón, 2007]. Several correlations have been developed to estimate the physical properties of petroleum fractions and are in principal function of the specific gravity, the normal boiling point temperature and the molecular weight. Some of the most important correlations are the *Riazi-Daubert* (1987), *Twu* (1984), *Ahmed* (1985), *Kesler-Lee* (1976), and *Edmister* (1958).

2.3.1.1 *Riazi-Daubert's Correlation*

Riazi and Daubert (1987) developed a set of equations to evaluate properties of undefined petroleum fractions. This correlation is the one mostly used by the Industry to obtain physical properties of the heavy end fraction using the laboratory reported molecular weight and specific gravity as heavy fraction parameters. In this study, the Riazi-Daubert's correlation was implemented for the calculation of the normal boiling point of the fluids under examination and is given by Eq. 2.4.

$$T_b = 6.77857 MW^{0.401673} SG^{-1.58262} \exp [0.00377409 MW + 2.984936 SG - 0.00425288 MW SG] \quad (2.4)$$

2.3.1.2 *Twu Correlation*

This correlation is based on a perturbation-expansion model with normal paraffins as the reference system. To calculate critical pressure, for example, critical temperature, critical volume, and specific gravity of the paraffin with the same normal boiling point as the heavy hydrocarbon fraction must be calculated in advance. Kesler et al. first used the perturbation expansion method (with n-alkanes as the reference fluid) to develop a suite of critical-property and acentric factor correlations. Twu uses the same approach to develop a set of correlations for the calculation of critical properties and the acentric

factor of heavy petroleum ends. Below the normal paraffin correlations are given first, followed by the correlations for petroleum fractions. The critical temperature of the paraffin is given by Eq. 2.5. The critical pressure of the paraffin is given by Eq. 2.6. The critical volume of the paraffin is given by Eq. 2.7. Parameter γ_p of the correlation is given by Eq. 2.8. The boiling temperature of the paraffin, which is assumed to be equal to that of the hydrocarbon mixture, is finally given by Eq. 2.9.

$$T_{cP} = T_b \left[0.533272 + (0.191017 \cdot 10^{-3})T_b + (0.779681 \cdot 10^{-7})T_b^2 - (0.284376 \cdot 10^{-10})T_b^3 + \frac{(0.959468 \cdot 10^2)}{(0.01 T_b)^{13}} \right]^{-1} \quad (2.5)$$

$$P_{cP} = (3.83354 + 1.19629 \alpha^{0.5} + 34.8888 \alpha + 36.1952 \alpha^2 + 104.193 \alpha^4)^2 \quad (2.6)$$

$$V_{cP} = [1 - (0.419869 - 0.505839 \alpha - 1.5643 \alpha^3 - 9481.7 \alpha^{14})]^{-8} \quad (2.7)$$

$$\gamma_p = 0.843593 - 0.12862 \alpha - 3.36159 \alpha^3 - 13749.5 \alpha^{12} \quad (2.8)$$

$$T_b = \exp(5.71419 + 2.71579 \theta - 0.28659 \theta^2 - 39.8544 \theta^{-1} - 0.122488 \theta^{-2}) - 247522 \theta + 35.3155 \theta^2 \quad (2.9)$$

In the above equations, α and θ parameters are given by Equations 2.10 and 2.11 respectively.

$$\alpha = 1 - \frac{T_b}{T_{cP}} \quad (2.10)$$

$$\theta = \ln (MW_p) \quad (2.11)$$

The molecular weight of the hydrocarbon paraffin MW_p cannot be computed explicitly with respect to T_b and Eqs. 2.5 through 2.11 must be solved iteratively. An initial approximation of the solution is however given by Eq. 2.12.

$$MW_p \approx \frac{T_b}{10.44 - 0.0052 T_b} \quad (2.12)$$

It is claimed that the Twu normal paraffin correlation is valid for C_1 through C_{100} but the properties at higher carbon numbers are only approximate because experimental data for paraffins heavier than approximately C_{20} do not essentially exist. Hydrocarbon heavy fraction properties are calculated by the formulas given below. Critical temperature of the heavy end fraction is calculated by Equations 2.13 to 2.15.

$$f_T = \Delta\gamma_T \left[\frac{-0.362456}{\sqrt{T_b}} + \left(0.0398285 - \frac{0.948125}{\sqrt{T_b}} \right) \Delta\gamma_T \right] \quad (2.13)$$

$$\Delta\gamma_T = e^{5(\gamma_p - \gamma)} - 1 \quad (2.14)$$

$$T_c = T_{cp} \left(\frac{1 + 2 f_T}{1 - 2 f_T} \right)^2 \quad (2.15)$$

Critical volume of the heavy end fraction is calculated by Equations from 2.16 to 2.18.

$$f_V = \Delta\gamma_V \left[\frac{0.466590}{\sqrt{T_b}} + \left(-0.182421 + \frac{3.01721}{\sqrt{T_b}} \right) \Delta\gamma_V \right] \quad (2.16)$$

$$\Delta\gamma_V = e^{4(\gamma_p^2 - \gamma^2)} - 1 \quad (2.17)$$

$$V_c = V_{cP} \left(\frac{1 + 2 f_V}{1 - 2 f_V} \right)^2 \quad (2.18)$$

Critical pressure of the heavy end fraction is calculated by Equations from 2.19 to 2.21.

$$f_P = \Delta\gamma_P \left[\left(2.53262 - \frac{46.1955}{\sqrt{T_b}} - 0.00127885 T_b \right) + \left(-11.4277 + \frac{252.14}{\sqrt{T_b}} + 0.00230535 T_b \right) \Delta\gamma_P \right] \quad (2.19)$$

$$\Delta\gamma_V = e^{0.5(\gamma_p - \gamma)} - 1 \quad (2.20)$$

$$P_c = P_{cP} \left(\frac{T_c}{T_{cP}} \right) \left(\frac{V_{cP}}{V_c} \right) \left(\frac{1 + 2 f_P}{1 - 2 f_P} \right)^2 \quad (2.21)$$

2.3.1.3 Edmister Correlation

In the present work, the Riazi-Daubert's correlation is used for the calculation of the normal boiling point of the hydrocarbon paraffin, since it is the one mostly used by the industry; for calculating the acentric factor, Riazi-Daubert uses the Edmister's correlation [Riazi, M. R., Daubert, T. E. (1987)]. The Edmister's correlation for the acentric factor, which depends on critical temperature and critical pressure, is given by Eq. 2.22 [Edmister, W.C., 1958].

$$\omega = \frac{3}{7} \frac{\log(P_c/14.7)}{T_c/T_b - 1} - 1 \quad (2.22)$$

2.3.2 Mixing Rules

Mixing rules are used in order to calculate average properties for gas mixtures by incorporating the fluid composition. Natural gas mixtures contain hundreds of well-defined and “undefined” components as well. These components are quantified in a composition set on the basis of mole, weight, and volume fractions. For a mixture of N components, $i=1, \dots, N$, the overall mole fractions are given by Eq. 2.23, where $\sum z_i$ always sums up to unity. Weight or mass fractions are given by Eq. 2.24 where the sum of w_i is always equal to unity.

$$z_i = \frac{n_i}{\sum_{j=1}^N n_j} = \frac{m_i/MW_i}{\sum_{j=1}^N m_j/MW_j} \quad (2.23)$$

$$w_i = \frac{m_i}{\sum_{j=1}^N m_j} = \frac{n_i MW_i}{\sum_{j=1}^N n_j MW_j} \quad (2.24)$$

Although the composition of a natural gas mixture is commonly expressed in terms of mole fractions, the measurement of composition by means of gas chromatography is usually based on mass, which is further converted to mole fraction via the molecular weight of each component.

2.3.2.1 Kay's mixing rule

The simplest and perhaps the most widely used mixing rule is the linear Kay's mixing rule, which is given by a mole-fraction average as shown in Eq. 2.25. This mixing rule is usually adequate for molecular weight, pseudo-critical temperature and acentric factor.

$$\theta_{av} = \sum_{i=1}^N z_i \theta_i \quad (2.25)$$

It can be thought of as a specific application of the generalized linear mixing rule that is given by Eq. 2.26.

$$\theta_{av} = \frac{\sum_{i=1}^N \varphi_i \theta_i}{\sum_{i=1}^N \varphi_i} \quad (2.26)$$

In the above formula, φ_i is the weighting factor and is usually one of the following: $\varphi_i = z_i$, mole fraction (Kay's mixing rule), $\varphi_i = w_i$, weight fraction or $\varphi_i = v_i$, volume fraction. Depending on the quantity that is being averaged, other mixing rules may be appropriate. In a next chapter of the present work for instance, the Elsharkawy mixing rule is presented and used. Moreover, the mixing rules that are used for the calculation of the constants of various equations of state are chosen on the basis of statistical thermodynamics.

2.3.2.2 Stewart–Burckhardt–Voo (SBV) mixing rule

This is a standard method of calculating the compressibility factor for natural gases and it is based on computing pseudo-critical properties of the gases via the mixing rules that are given by Eq. 2.27 for pseudo-critical temperature and Eq. 2.28 for pseudo-critical pressure.

$$T_{pc} = \frac{K^2}{J} \quad (2.27)$$

$$P_{pc} = \frac{T_{pc}}{J} \quad (2.28)$$

In the above equations, K and J are parameters which are calculated by Eqs. 2.29 and 2.30 respectively.

$$K = \sum [y_i \left(\frac{T_c}{P_c^{0.5}} \right)_i] \quad (2.29)$$

$$J = \left(\frac{1}{3} \right) \left[\sum y_i \left(\frac{T_c}{P_c} \right) \right] + \left(\frac{2}{3} \right) \left[\sum y_i \left(\frac{T_c}{P_c} \right)_i^{0.5} \right]^2 \quad (2.30)$$

2.3.2.3 El Sharkawy mixing rule

This simple mixing rule was developed by implementing multiple regression analysis to experimental compressibility factor data. The outcomes are two six-constant mixing parameters (J_{inf} and K_{inf}) that involve only molar fraction of gas (y_i) and critical temperature (T_c) and critical pressure (P_c) of pure components. These mixing parameters are calculated by Eqs. 2.31 and 2.32 for J_{inf} and K_{inf} respectively.

$$J_{inf} = a_0 + \left[a_1 \left(\frac{y_i T_c}{P_c} \right) \right] H_2S + \left[a_2 \left(\frac{y_i T_c}{P_c} \right) \right] CO_2 + \left[a_3 \left(\frac{y_i T_c}{P_c} \right) \right] N_2 \\ + \left[a_4 \sum y_i \left(\frac{T_c}{P_c} \right) \right] C_1 - C_{n-1} + [a_5(y_i MW)]C_{7+} \quad (2.31)$$

$$K_{inf} = \beta_0 + \left[\beta_1 \left(\frac{y_i T_c}{P_c^{0.5}} \right) \right] H_2S + \left[\beta_2 \left(\frac{y_i T_c}{P_c^{0.5}} \right) \right] CO_2 + \left[\beta_3 \left(\frac{y_i T_c}{P_c^{0.5}} \right) \right] N_2 + \left[\beta_4 \sum y_i \left(\frac{T_c}{P_c^{0.5}} \right) \right] C_1 - C_{n-1} + [\beta_5 (y_i MW)] C_{7+} \quad (2.32)$$

The constants α_0 to α_5 and β_0 to β_5 of the equations above were determined by the authors using multiple regression analysis and are listed in Table 2.3. In these mixing parameters one can distinguish three parts. The first part contains non-hydrocarbons (e.g. hydrogen sulfide, carbon dioxide, nitrogen), the second part comprises of the pure hydrocarbons from methane to C_{n-1} whose critical properties and acentric factor are well known, or at least can be estimated safely. The last part contains the heavy end C_{n+} whose molecular weight is experimentally measured. The necessity of estimating explicitly the critical properties and the acentric factor of the heavy end is eliminated by means of the present mixing method.

Table 2.3: Constants of the El Sharkawy mixing parameters

Constant	Value	Constant	Value
α_0	0.036983	β_0	-0.7765003
α_1	1.043902	β_1	1.0695317
α_2	0.894942	β_2	0.9850308
α_3	0.792231	β_3	0.8617653
α_4	0.882295	β_4	1.0127054
α_5	0.018637	β_5	0.4014645

Having calculated the above mixing parameters, critical pressure and temperature of the gas mixture can be determined by the following relationships:

$$T_{pc} = \frac{K_{inf}^2}{J_{inf}} \quad (2.33)$$

$$P_{pc} = \frac{T_{pc}}{J_{inf}} \quad (2.34)$$

Chapter 3 Empirical Correlations based on the Corresponding States Principle

3.1 Background

The principle of corresponding states suggests that pure but similar gases exhibit the same deviation from the ideal gas behavior, or equivalently, the z factor value, at the same values of reduced pressure and temperature. After decades since its development, the Standing-Katz z factor chart (Fig. 3.1), is still widely used as a practical source of natural gas z factor values. The Standing-Katz chart was developed using data for binary mixtures of methane with propane, ethane, butane and other natural gases with a wide range of compositions. None of the gas mixtures had molecular weights in excess of 40. The Standing-Katz chart is actually a modification and extension of the generalized z factor chart developed by Brown and Holcomb (Fig. 3.2) and is identical to that at reduced pressures less than 4. For greater values of the reduced pressure, the Brown-Holcomb chart was found to be consistently inaccurate; thereby, Standing and Katz used data from 16 natural gas mixtures, along with methane z factors as a guide, to extend the chart to reduced pressure as high as 15. The Standing-Katz z factor chart correlates the z factor as a function of pseudo-reduced pressure and pseudo-reduced temperature.

The theory of corresponding states proposes that all gases will exhibit the same behavior (e.g. the z factor), when viewed in terms of reduced pressure, reduced volume and reduced temperature. Mathematically, this principle can be expressed as:

$$z = z_c \Psi(p_r, T_r) \quad (3.1)$$

The mathematical derivation of the expression above is as follows. By multiplying and dividing the left-hand-side of the real gas law (Eq. 1.2) by $p_c V_c$ we get:

$$p_c V_c \frac{pV}{p_c V_c} = \frac{zRT}{T_c} z_c T_c = \frac{pV}{p_c V_c} = zR \frac{T_c}{z_c T_c} \frac{T}{T_c} \quad (3.2)$$

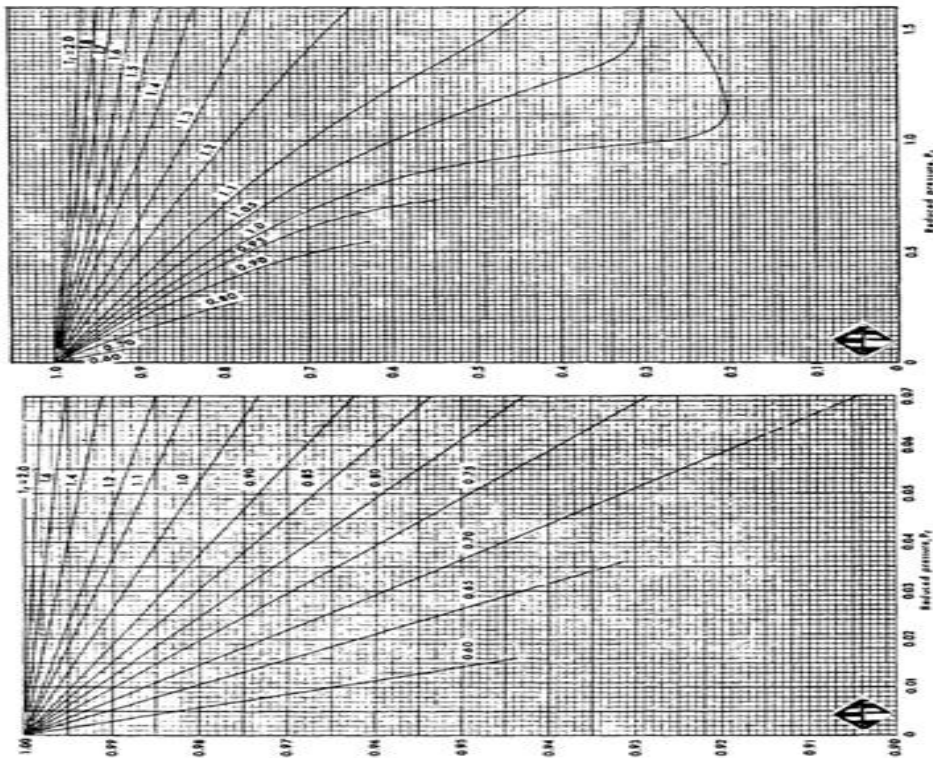


Figure 3.1 - Deviation factor z chart for low pressure gases (GPA Copyright)

By definition it is valid that:

$$p_r = \frac{p}{p_c} \text{ \& } T_r = \frac{T}{T_c} \leftrightarrow p_r V_r = \frac{z}{z_c} \frac{z_c T_c}{p_c V_c} T_r \quad (3.3)$$

From the real gas law (Eq. 1.2) we have:

$$\frac{z_c T_c}{p_c V_c} = \frac{1}{R} = p_r V_r = \frac{z}{z_c} \frac{p_r}{T_r} V_r = z = z_c \frac{T_r}{p_r V_r} \quad (3.4)$$

$$z = z_c \Psi(p_r, T_r) \quad (3.5)$$

Based on the derivation above, the following relationship can be established:

$$\frac{p_{r1} V_{r1}}{z_{r1} T_{r1}} = \frac{p_{r2} V_{r2}}{z_{r2} T_{r2}} \quad (3.6)$$

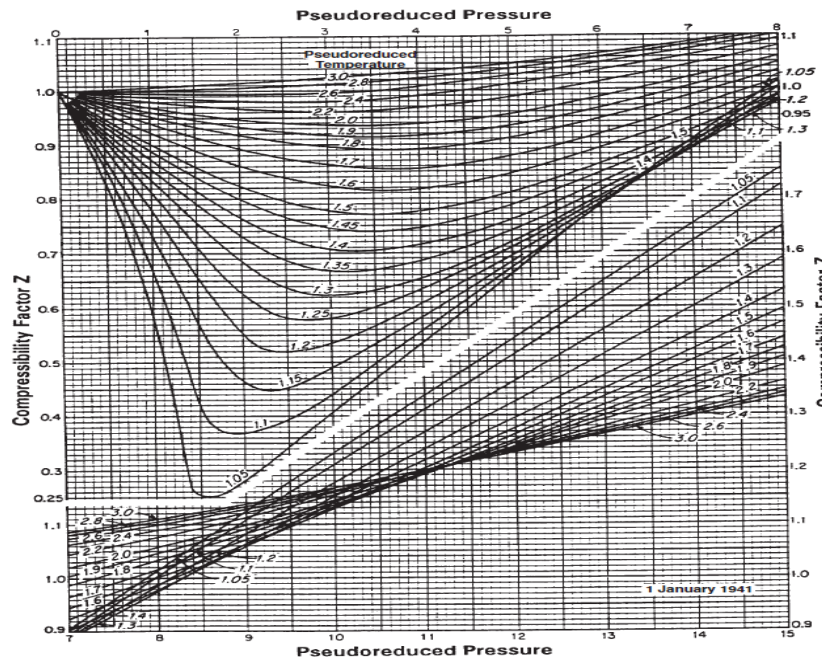


Figure 3.2 - The Standing-Katz generalized z factor chart

From Fig. 3.3 to Fig. 3.12 that follow, various compressibility z factor curves are shown for pure substances and at various reduced conditions.

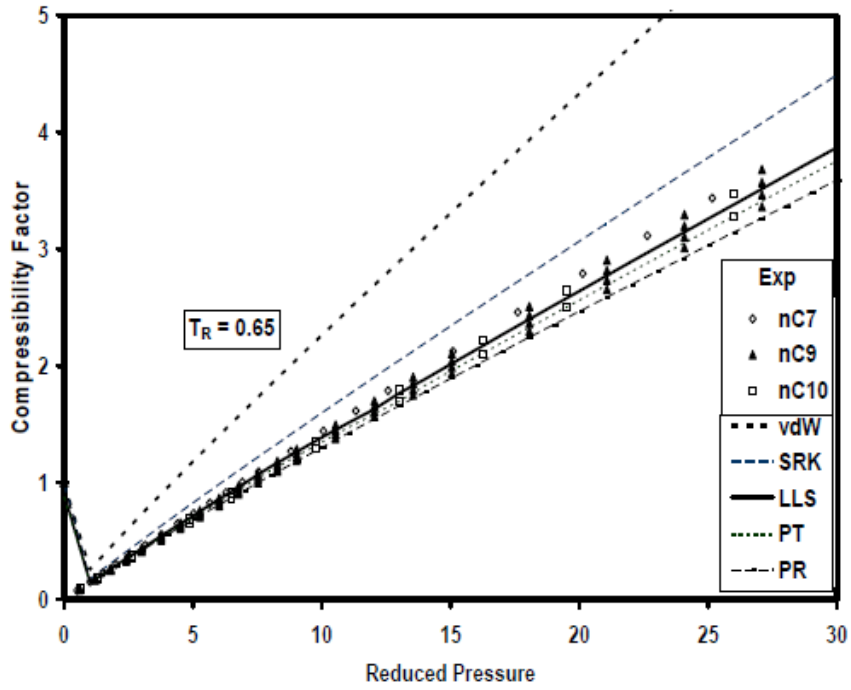


Figure 3.3 - z factor of pure substances at reduced conditions ($T_r=0.65$)

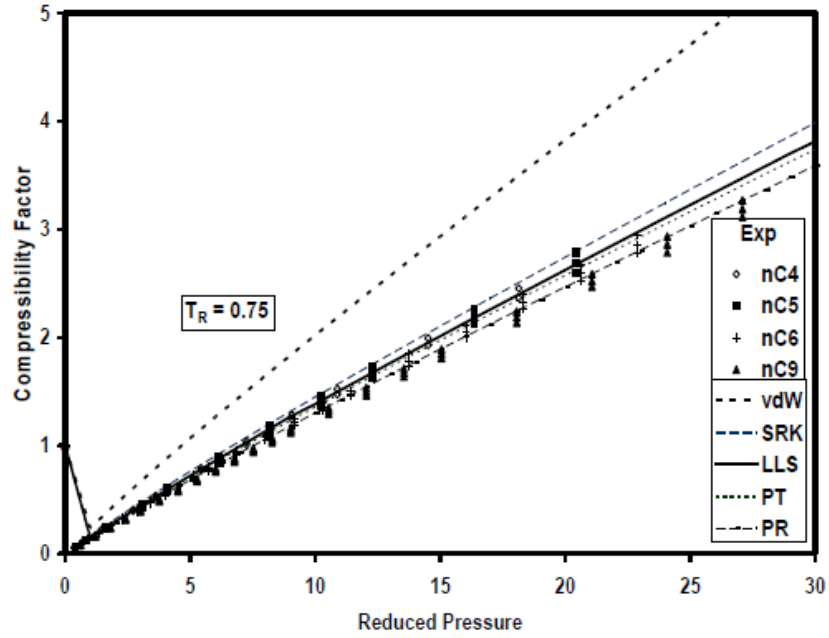


Figure 3.4 - z factor of pure substances at reduced conditions ($T_r=0.75$)

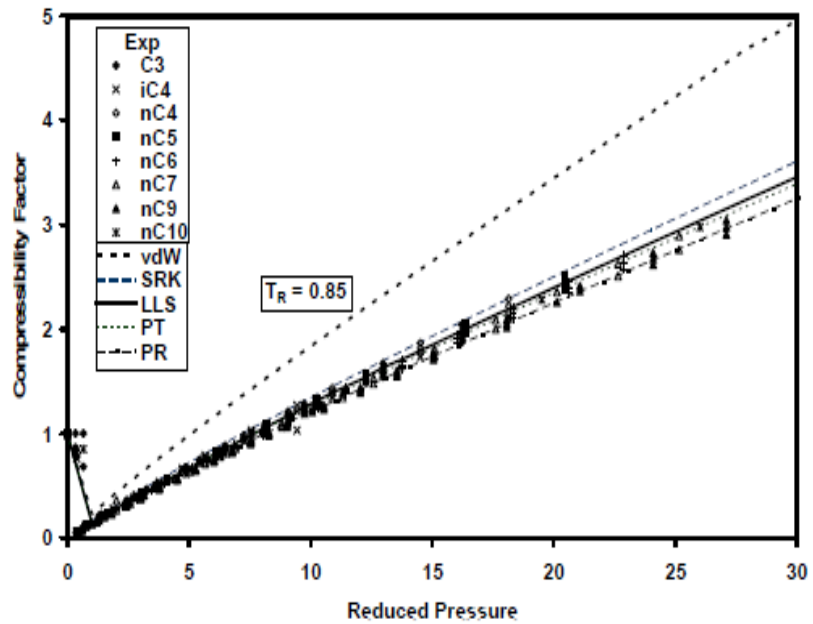


Figure 3.5 - z factor of pure substances at reduced conditions ($T_r=0.85$)

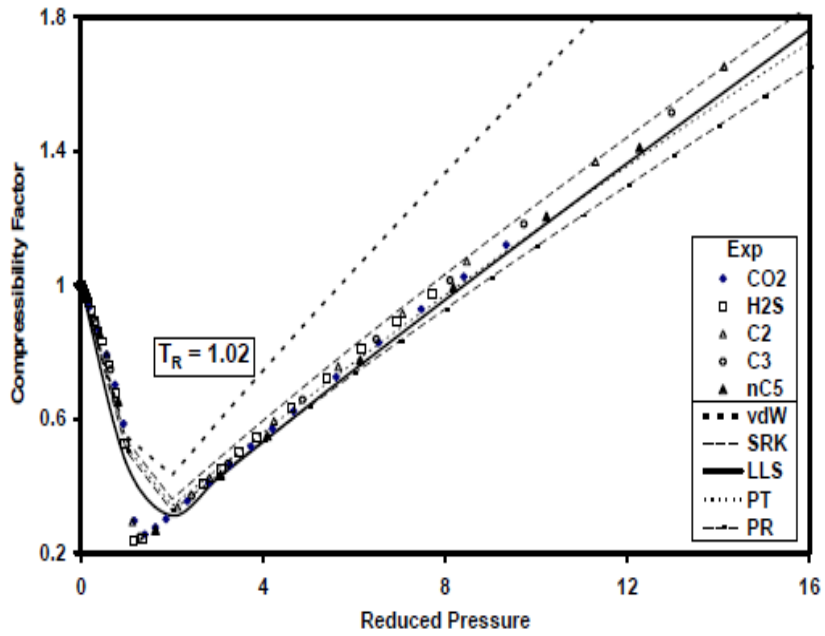


Figure 3.6 - z factor of pure substances at reduced conditions ($T_r=1.02$)

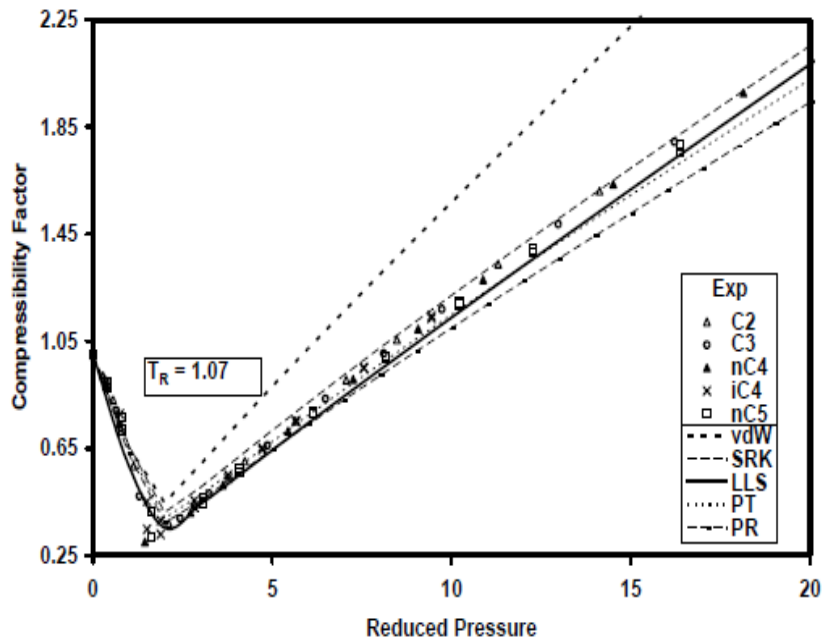


Figure 3.7 - z factor of pure substances at reduced conditions ($T_r=1.07$)

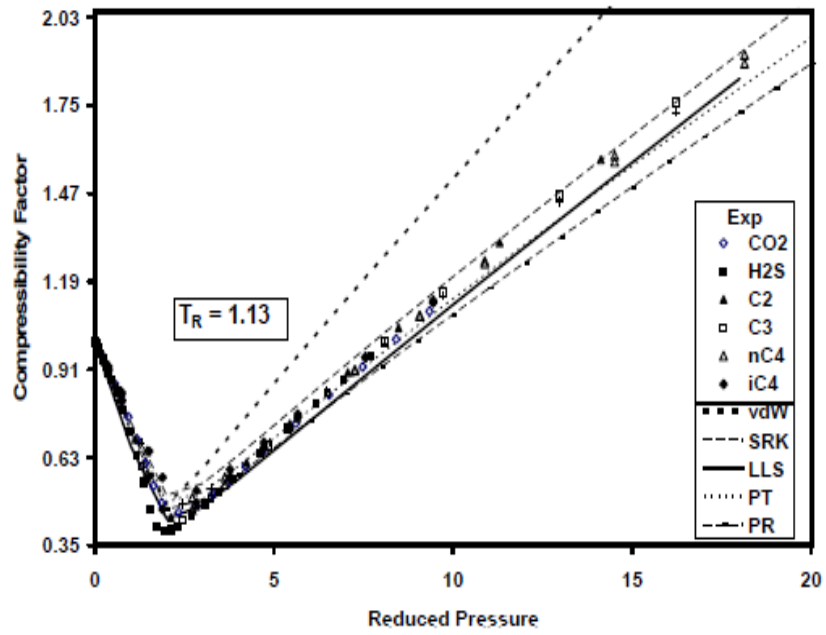


Figure 3.8 - z factor of pure substances at reduced conditions ($T_r=1.13$)

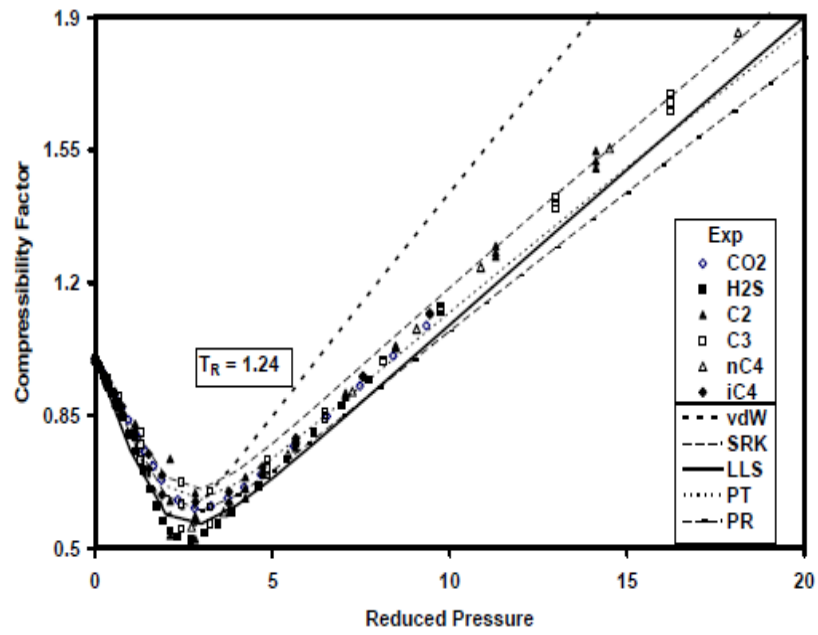


Figure 3.9 - z factor of pure substances at reduced conditions ($T_r=1.24$)

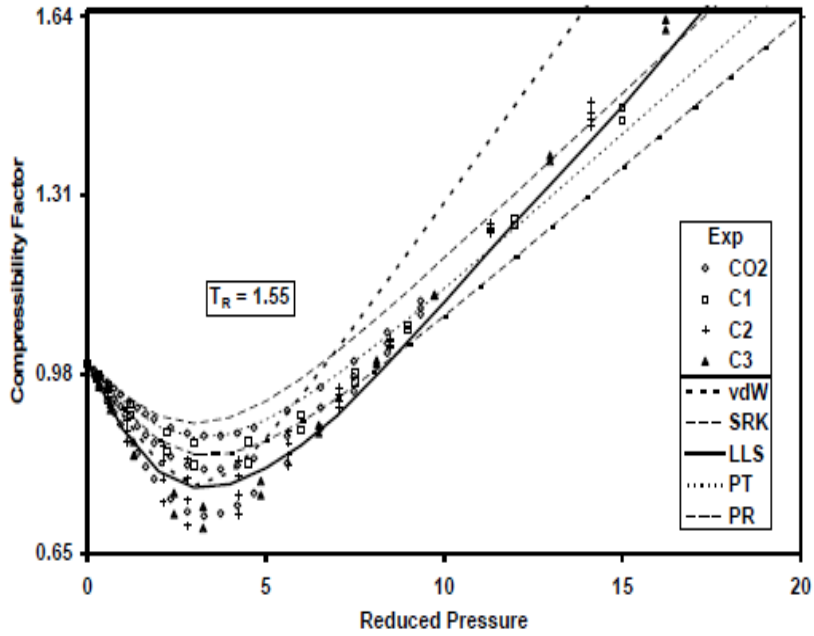


Figure 3.10 - z factor of pure substances at reduced conditions ($T_r=1.55$)

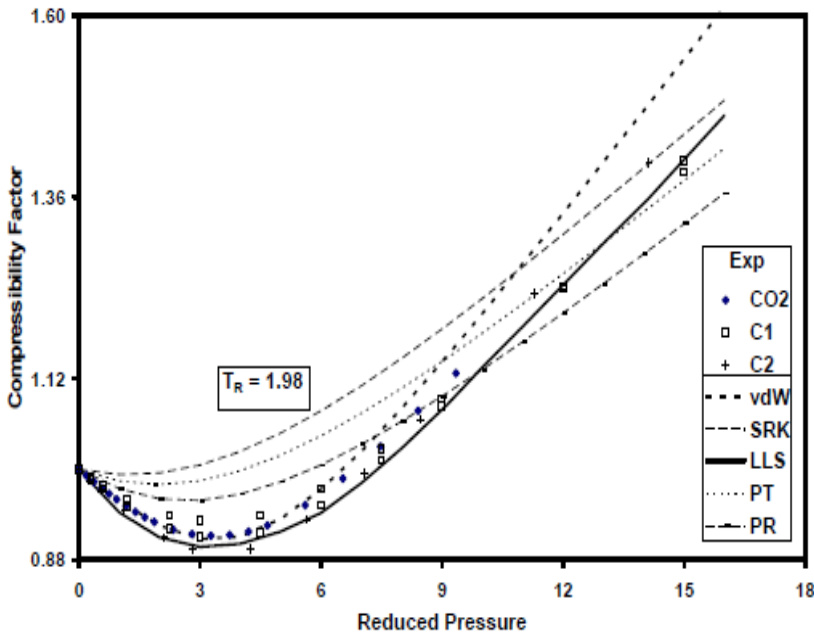


Figure 3.11 - z factor of pure substances at reduced conditions ($T_r=1.98$)

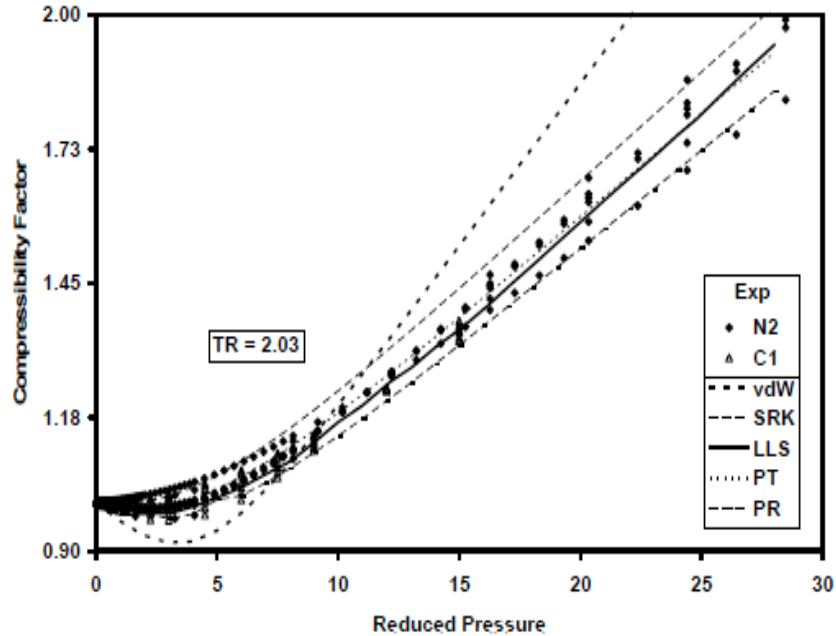


Figure 3.12 - z factor of pure substances at reduced conditions ($T_r=2.03$)

3.2 Correlations Based on the Corresponding States Principle

Since the Standing-Katz chart firstly appeared in the literature in 1941, there was an apparent need for a simple mathematical description which would effectively reproduce and extend the chart. For years, engineers had been using empirical correlations instead of tables and charts for determining the gas z factor. The effective use of the correlations however, lies in an understanding of the way they were derived and the knowledge of their limitations.

Today, numerous rigorous mathematical expressions have been proposed to accurately reproduce the Standing-Katz chart. This section presents a literature review of some of the most widely used empirical correlations for the calculation of z factor. The correlations presented here are divided into two groups, shown in Table 3.1: direct (explicit) and iterative (implicit) relationships. Most of these expressions have been

designed to be solved for the gas z factor at any pseudo-reduced pressure and pseudo-reduced temperature.

Table 3.1: Correlations for the calculation of z factor

Iterative Relations:	Hall and Yarborough
	Dranchuk and Abou-Kassem
Direct Relations:	Brill and Beggs
	Azizi, Behbahani and Isazede
	Shell Oil Company
	Niger Delta
	Heidaryan et al.

The pseudo-critical properties of a natural gas mixture can readily be determined from gas composition and mixing rules or from correlations which yield pseudo-critical properties given the natural gas specific gravity γ_g . If the natural gas composition is known, the pseudo-critical pressure and temperature can be determined by using Kay's linear mixing rule [Bradley, 1987] according to Eqs. 3.7a and 3.7b respectively. In these formulas, subscript i stands for the different components of the natural gas mixture.

$$P_{pc} = \sum z_i P_{ci} \quad (3.7a)$$

$$T_{pc} = \sum z_i T_{ci} \quad (3.7b)$$

For natural gases whose detailed chemical composition is not known, as it is the case at early production stages, numerous correlations have been proposed over the years to predict pseudo-critical properties as a function of their specific gravity solely, a property which is readily available in most cases. *Standing* for example developed two sets of such correlations: one for dry hydrocarbon natural gases with $\gamma_{gHC} < 0.75$ (Eqs. 3.8a and 3.8b for pseudo-critical temperature and pressure respectively) and one for wet natural

gases with $\gamma_{gHC} > 0.75$ (Eqs. 3.9a and 3.9b for pseudo-critical temperature and pressure respectively).

$$T_{pcHC} = 168 + 325 \gamma_{gHC} - 12.5 \gamma_{gHC}^2 \quad (3.8a)$$

$$P_{pcHC} = 667 + 15.0 \gamma_{gHC} - 37.5 \gamma_{gHC}^2 \quad (3.8b)$$

$$T_{pcHC} = 187 + 330 \gamma_{gHC} - 71.5 \gamma_{gHC}^2 \quad (3.9a)$$

$$P_{pcHC} = 706 - 51.7 \gamma_{gHC} - 11.1 \gamma_{gHC}^2 \quad (3.9b)$$

Similar correlations were also developed by *Sutton* for hydrocarbon natural gas mixtures (Eqs. 3.10a and 3.10b for pseudo-critical temperature and pressure respectively). The author claims that these correlations are the most reliable for the calculation of pseudo-critical properties with the Standing-Katz z factor chart. He even claims that his correlations are more accurate even than methods which use composition and mixing rules to calculate pseudo-critical properties.

Fig. 3.13 illustrates a comparison of Standing and Sutton correlations for the calculation of pseudo-critical pressure and temperature. The Sutton and the Standing wet gas correlation for T_{pc} yield basically the same results, whereas the three correlations for the calculation of P_{pc} demonstrate significant deviations for $\gamma_{gHC} > 0.85$.

$$T_{pcHC} = 169.2 + 349.5 \gamma_{gHC} - 74.0 \gamma_{gHC}^2 \quad (3.10a)$$

$$P_{pcHC} = 756.8 - 131 \gamma_{gHC} - 3.6 \gamma_{gHC}^2 \quad (3.10b)$$

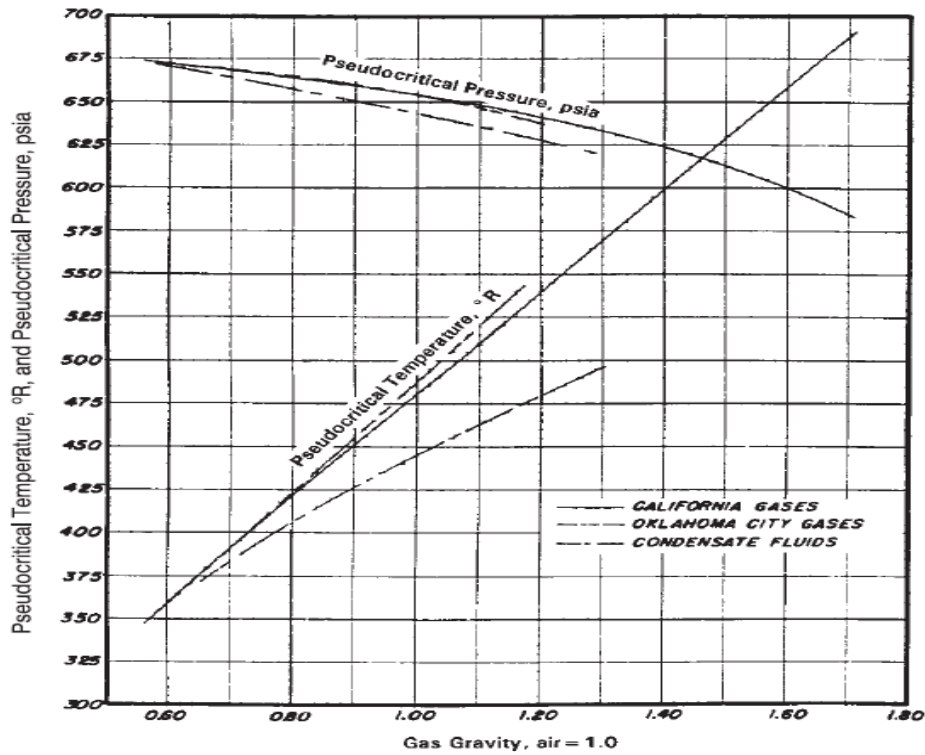


Figure 3.13 – Comparison of Standing and Sutton correlations for the calculation of pseudo-critical temperature and pressure

An important point to be stressed here is that the correlations described in this paragraph predict pseudo-critical ‘average’ values, which are evidently not fully accurate estimates of the natural gas mixtures property values. Moreover, the existing correlations are characterized by poor accuracy when predicting values of pseudo-critical properties for natural gases which contain significant quantities of non-hydrocarbon components such as nitrogen (N_2), carbon dioxide (CO_2) and hydrogen sulfide (H_2S). Improved prediction techniques for the calculation of pseudo-critical properties of natural gases, as well as corrections which can be applied to the outcomes of the aforementioned correlations are discussed later in this work.

3.2.1 Hall and Yarborough

Hall and Yarborough (1973) published a method that can accurately predict the Standing-Katz z factor chart by using a Carnahan-Starling hard-sphere EoS model. Based on data taken from the Standing-Katz chart the authors derived best fit mathematical expressions. The mathematical formula of the Hall and Yarborough equation is:

$$Z = a p_{pr}/y \quad (3.11)$$

where,

$$a = 0.06125 t \exp[-1.2 (1 - t)^2] \quad (3.12)$$

In Eq. 3.12, t is the reciprocal of the pseudo-reduced temperature ($t=T_{pc}/T$). The reduced density parameter y of Eq. 3.11 which is a product of the VdW covolume times the density is calculated by Eq. 3.12.

$$f(y) = 0 = -a p_{pr} + \frac{y + y^2 + y^3 - y^4}{(1 - y)^3} - (14.76 t - 9.76 t^2 + 4.58 t^3)y^2 + (90.7 t - 242.2 t^2 + 42.4 t^3)y^{2.18+2.82 t} \quad (3.13)$$

The first derivative of $f(y)$ is given by:

$$\frac{df(y)}{dy} = \frac{1 + 4y + 4y^2 - 4y^3 + y^4}{(1 - y)^4} - (29.52 t - 19.52t^2 + 9.16t^3)y + (2.18 + 2.82t)(90.7t - 242.2t^2 + 42.4 t^3)y^{1.18+2.82t} \quad (3.14)$$

Since Eq. 3.13 contains both z and ρ_M (which is a function of z) the solution is thus obtained by using an iterative method. Whitson suggests the use of a Newton-Raphson method with an initial guess of $y=0.001$ with the convergence to be achieved in 3 to 10 iterations for $|f(y)| = 1 \times 10^{-8}$. Hall and Yarborough pointed out that the method is not recommended for application if the pseudo-reduced temperature is less than one.

3.2.2 Dranchuk and Abou-Kassem

In 1975 Dranchuk and Abou-Kassem proposed an equation of state with eleven constants C_1 to C_{11} for calculating the deviation factor z of natural gases. The equation is as follows:

$$z = \left[C_1 + \frac{C_2}{T_{pr}} + \frac{C_3}{T_{pr}^3} + \frac{C_4}{T_{pr}^4} + \frac{C_5}{T_{pr}^5} \right] \rho_r + \left[C_6 + \frac{C_7}{T_{pr}} + \frac{C_8}{T_{pr}^2} \right] \rho_r^2 - C_9 \left[\frac{C_7}{T_{pr}} + \frac{C_8}{T_{pr}^2} \right] \rho_r^5 + C_{10} (1 + C_{11} \rho_r^2) \frac{\rho_r^2}{T_{pr}^3} 3 \exp(-C_{11} \rho_r^2) + 1 \quad (3.15)$$

In Eq. 3.15, ρ_r is the reduced natural gas density which is defined by the following relationship:

$$\rho_r = \frac{0.27 p_{pr}}{z T_{pr}} \quad (3.16)$$

The constants C_1 to C_{11} of Eq. 3.15 were determined by fitting the equation, using non linear regression models, to 1500 points from the Standing-Katz z factor chart. The values of the constants are listed in Table 3.2.

As can be noticed from Eqs. 3.15 and Eq. 3.16, the calculation of z involves z value itself, hence in order to obtain a solution for Eq. 3.15, an iterative numerical method such as Newton-Raphson should be implemented. Dranchuk and Abou-Kassem method

has been found to be applicable over the ranges of $0.2 < p_{pr} < 30$ and $1.0 < T_{pr} < 3.0$, with an average absolute error of 0.585 percent.

Table 3.2: Constants of the Dranchuk and Abou-Kassem z factor correlation

Constant	Value
C_1	0.32650
C_2	1.07000
C_3	-0.5339
C_4	0.01569
C_5	-0.05165
C_6	0.54750
C_7	-0.73610
C_8	0.18440
C_9	0.10560
C_{10}	0.61340
C_{11}	0.72100

The Newton-Raphson method regarding Eq. 3.15 is implemented as follows. Firstly, we state a new function $f(z)$ by moving both parts of Eq. 3.15 on the left-hand side. Eq. 3.17 corresponds to that $f(z)$ function.

$$\begin{aligned}
 f(z) = & A_1 \left(\frac{0.27P_{pr}}{T_{pr}} \right) \left(\frac{1}{Z} \right) + A_2 \left(\frac{0.27P_{pr}}{T_{pr}} \right)^2 \left(\frac{1}{Z} \right)^2 + A_3 \left(\frac{0.27P_{pr}}{T_{pr}} \right)^5 \left(\frac{1}{Z} \right)^5 \\
 & + \frac{C_{10}}{T_{pr}^3} \left(\frac{0.27P_{pr}}{T_{pr}} \right)^2 \left(\frac{1}{Z} \right)^2 3 \exp \left[-C_{11} \left(\frac{0.27P_{pr}}{T_{pr}} \right)^2 \left(\frac{1}{Z} \right)^2 \right] \\
 & + \frac{C_{10}C_{11}}{T_{pr}^3} \left(\frac{0.27P_{pr}}{T_{pr}} \right)^4 \left(\frac{1}{Z} \right)^4 3 \exp \left[-C_{11} \left(\frac{0.27P_{pr}}{T_{pr}} \right)^2 \left(\frac{1}{Z} \right)^2 \right] + 1
 \end{aligned} \tag{3.17}$$

- z

By substituting Eq. 3.16 to Eq. 3.17 and differentiating with respect to the

compressibility z factor we get the first derivative of Eq. 3.17.

$$\begin{aligned}
& \frac{df}{dz} \\
&= A_1 \left(\frac{0.27P_{pr}}{T_{pr}} \right) \left(-\frac{1}{Z^2} \right) + A_2 \left(\frac{0.27P_{pr}}{T_{pr}} \right)^2 \left(-\frac{2}{Z^3} \right) + A_3 \left(\frac{0.27P_{pr}}{T_{pr}} \right)^5 \left(-\frac{5}{Z^6} \right) \\
&+ \frac{C_{10}}{T_{pr}^3} \left(\frac{0.27P_{pr}}{T_{pr}} \right)^2 \left(-\frac{2}{Z^3} \right) 3 \exp \left[-C_{11} \left(\frac{0.27P_{pr}}{T_{pr}} \right)^2 \left(\frac{1}{Z} \right)^2 \right] \\
&+ \frac{C_{10}}{T_{pr}^3} \left(\frac{0.27P_{pr}}{T_{pr}} \right)^2 \left(\frac{1}{Z^2} \right) 3 \left(2 C_{11} \left(\frac{0.27P_{pr}}{T_{pr}} \right) \left(\frac{1}{Z^3} \right) \right) \exp \left[-C_{11} \left(\frac{0.27P_{pr}}{T_{pr}} \right)^2 \left(\frac{1}{Z} \right)^2 \right] \\
&+ \frac{C_{10} C_{11}}{T_{pr}^3} \left(\frac{0.27P_{pr}}{T_{pr}} \right)^4 \left(-\frac{4}{Z^5} \right) 3 \exp \left[-C_{11} \left(\frac{0.27P_{pr}}{T_{pr}} \right)^2 \left(\frac{1}{Z} \right)^2 \right] \\
&+ \frac{C_{10} C_{11}}{T_{pr}^3} \left(\frac{0.27P_{pr}}{T_{pr}} \right)^4 \left(\frac{1}{Z^4} \right) 3 \left(2 C_{11} \left(\frac{0.27P_{pr}}{T_{pr}} \right) \left(\frac{1}{Z^3} \right) \right) \exp \left[-C_{11} \left(\frac{0.27P_{pr}}{T_{pr}} \right)^2 \left(\frac{1}{Z} \right)^2 \right] - 1
\end{aligned} \tag{3.18}$$

By means of the Dranchuk and Abou-Kassem correlation combined with the Elsharkawy mixing rule, the z factor is calculated with adequate accuracy, compared to that of EoS models, without in tandem the need of characterizing the heavy end fraction. This method also eliminates the need for BIC calculations that are necessary in the case of EoS models, as it is discusses in next sections.

3.2.3 Brill and Beggs

Brill and Beggs (1986) proposed a best-fit equation to the Standing-Katz z factor chart which is as follows:

$$Z = A + (1 - A)e^{-B} + c P_{pr}^D \tag{3.19}$$

where

$$A = 1.39 (T_{pr} - 0.92)^{0.5} - 0.36T_{pr} - 0.101 \quad (3.20)$$

$$B = (0.62 - 0.23 T_{pr})P_{pr} + \left[\left(\frac{0.066}{T_{pr} - 0.86} \right) - 0.037 \right] P_{pr}^2 + \left[\frac{0.32}{10^9 (T_{pr} - 1)} \right] P_{pr}^6 \quad (3.21)$$

$$C = 0.132 - 0.32 \log (T_{pr}) \quad (3.22)$$

$$D = 10^{0.3106 - 0.49 T_{pr} + 0.1824 T_{pr}^2} \quad (3.23)$$

For many petroleum engineering calculations, the Brill and Beggs correlation gives a satisfactory representation (± 1 to 2%) of the original Standing-Katz z factor chart for the range of $1.2 < T_{pr} < 2$. The major advantage of the Brill and Beggs correlation is that it can be solved explicitly with respect to z and thus not requiring an iterative approach. The main limitations are that reduced temperature must be $T_{pr} > 1.2$ (≈ 540 °R) and $T_{pr} < 2$ (≈ 800 °R) and reduced pressure must be $P_{pr} < 15$ (≈ 10000 psia).

3.2.4 Azizi, Behbahani and Isazede

In 2010, Azizi, Behbahani and Isazede proposed a new correlation (Eq. 3.24) for the calculation of z factor, which is based on 3038 points from the Standing-Katz z factor chart.

$$Z = A + \frac{B + C}{D + E} \quad (3.24)$$

In the above equation, A , B , C , D and E are parameters which are computed in various pressure and temperature conditions according to the following formulas:

$$A = a T_r^{2.16} + b P_r^{1.028} + c P_r^{1.58} T_r^{-2.1} + d \ln (T_r)^{-0.5} \quad (3.25)$$

$$B = e + f T_r^{2.4} + g P_r^{1.56} + h P_r^{0.124} T_r^{3.033} \quad (3.26)$$

$$C = i \ln (T_r)^{-1.28} + j \ln (T_r)^{1.37} + k \ln(P_r) + l \ln (P_r)^2 + m \ln(P_r) \ln(T_r) \quad (3.27)$$

$$D = 1 + n T_r^{5.55} + o P_r^{0.68} T_r^{0.33} \quad (3.28)$$

$$E = p \ln (T_r)^{1.18} + q \ln (T_r)^{2.1} + r \ln(P_r) + s \ln (P_r)^2 + t \ln(P_r) \ln(T_r) \quad (3.29)$$

The tuned coefficients used in the above equations were determined by the authors with the utilization of curve-fitting software and are listed in Table 3.3.

The advantage of this correlation is that it is explicit in z and thus does not require an iterative solution as is required by other methods such as the Hall and Yarborough and the Dranchuk and Abou-Kassem. The Azizi, Behbahani and Isazedeh z factor correlation has proven to be accurate for sweet natural gases over the range of $0.2 < P_p r < 11$ and $1.1 < T_{pr} < 2$.

Table 3.3: Tuned coefficients of the Azizi et al. correlation

Constant	Value
a	0.0373142485385592
b	-0.01408071514853
c	0.0163263245387186
d	-0.03077764788198
e	13843575480.943800
f	-16799138540.7637
g	1624178942.6497600

h	13702270281.086900
i	-41645509.8964740
j	237249967625.0130
k	-24449114791.1530
l	19357955749.32740
m	-126354717916.600
n	623705678.3857840
o	17997651104.33300
p	151211393445.0640
q	139474437997.1720
r	-24233012984.0950
s	18938047327.52050
t	-141401620722.689

3.2.5 Shell Oil Company

Kumar (2004) proposed the explicit shell company correlation for the estimation of z factor as follows:

$$z = A + B P_{pr} + (1 - A) \exp(-C) - D \left(\frac{P_{pr}}{10}\right)^4 \quad (3.28)$$

In the above equation, A , B , C and D are correlation parameters which are given from the following formulas:

$$A = -0.101 - 0.36 T_{pr} + 1.3868 \sqrt{T_{pr} - 0.919} \quad (3.29)$$

$$B = 0.21 + \frac{0.04275}{T_{pr} - 0.85} \quad (3.30)$$

$$C = P_{pr}(E + F P_{pr} + G P_{pr}^4) \quad (3.31)$$

$$D = 0.122 \exp(-11.3 (T_{pr} - 1)) \quad (3.32)$$

$$E = 0.6222 - 0.224 T_{pr} \quad (3.33)$$

$$F = \frac{0.0657}{T_{pr} - 0.85} - 0.037 \quad (3.34)$$

$$G = 0.32 \exp(-19.53 (T_{pr} - 1)) \quad (3.35)$$

3.2.6 Niger Delta

The Niger Delta correlation (2013) for the calculation of z factor is a simple explicit expression of the following form:

$$z = 6.41824 - 0.013363 P_{pr} - 3.351293 T_{pr} \quad (3.36)$$

3.2.7 Heidaryan et al.

In 2010, Heidaryan et al. presented the following correlation (Eq. 3.37) which is based on the Standing-Katz chart and is explicit to z .

$$z = \ln \left(\frac{A_1 + A_3 \ln(P_{pr}) + \frac{A_5}{T_{pr}} + A_7 (\ln(P_{pr}))^2 + \frac{A_9}{T_{pr}^2} + \frac{A_{11}}{T_{pr}} \ln(P_{pr})}{1 + A_2 \ln(P_{pr}) + \frac{A_4}{T_{pr}} + A_6 (\ln(P_{pr}))^2 + \frac{A_8}{T_{pr}^2} + \frac{A_{10}}{T_{pr}} \ln(P_{pr})} \right) \quad (3.37)$$

This model was derived from 1260 points of the Standing-Katz chart while multiple regression analysis was carried out to identify the relationships between the independent variables and the dependent one (z factor). In fact, the authors generated a multiple rational regression equation that provides z factor as a function of P_{pr} and the reciprocal of T_{pr} as follows:

$$z = f \left(P_{pr}, \frac{1}{T_{pr}} \right) \quad (3.38)$$

Table 3.4: Tuned coefficients of Heidaryan et al. z factor correlation (Eq. 3.37)

Coefficient	$0.2 \leq P_{pr} \leq 3$	$3 \leq P_{pr} \leq 15$
A1	2.827793	3.252838
A2	-0.4688191	-0.1306424
A3	-1.262288	-0.6449194
A4	-1.536524	-1.518028
A5	-4.535045	-5.391019
A6	0.06895104	-0.01379588
A7	0.1903869	0.06600633
A8	0.6200089	0.6120783
A9	1.838479	2.317431

A10	0.4052367	0.1632223
A11	1.073574	0.5660595

For increased accuracy, the authors introduced two sets of tuned coefficients A_I through A_{11} which are given in Table 3.4 for different ranges of the pseudo-reduced pressure of the gas system. These coefficients were determined by minimizing the sum of squares of the residuals of Eq. 3.37 and may be changed if more accurate data in sensitive region of the Standing-Katz chart are available by another numerical method.

3.3 Corrections Applied to Sour Natural Gases

If hydrogen sulfide H_2S is present, the natural gas mixture is termed sour natural gas. The existing methods of calculating z factor values when significant amounts of compounds like carbon dioxide (CO_2) and hydrogen sulfide (H_2S) are present in the natural gas mixtures incur high deviations from the actual values.

Sour and acid natural gases which contain hydrogen sulfide and/or carbon dioxide frequently exhibit different z factor behavior than sweet natural gases do. Although Kay's mixing rule is usually adequate for lean natural gases that contain no, or small quantities of non-hydrocarbons, this is not the case when the natural gas under examination contains significant quantities of the aforementioned compounds. Wichert and Aziz (1972) developed a calculation procedure to account for these differences. They introduced a pseudo-critical temperature adjustment factor ϵ shown in Eq. 3.39, which is a function of CO_2 and H_2S concentrations in the natural gas mixture. After calculating the correction term ϵ , the mixture's pseudo-critical temperature T_{pc}^* and pressure P_{pc}^* which have been calculated in advance based on Kay's mixing rule are further corrected by using Eqs. 3.40 and 3.41 respectively.

$$\epsilon = 120 [(y_{CO_2} + y_{H_2S})^{0.9} - (y_{CO_2} + y_{H_2S})^{1.6} + 15 (y_{H_2S}^{0.5} - y_{H_2S}^4)] \quad (3.39)$$

$$T_{pc} = T_{pc}^* - \epsilon \quad (3.40)$$

$$P_{pc} = \frac{P_{pc}^* (T_{pc}^* - \epsilon)}{T_{pc}^* + y_{H_2S} (1 - y_{H_2S}) \epsilon} \quad (3.41)$$

The Wichert and Aziz correction method has proven to be providing pseudo-critical properties that will yield reliable z factor values from the Standing-Katz chart. The method was developed from extensive data from natural gases containing nonhydrocarbons with CO_2 molar concentrations ranging from 0% to 55% and H_2S molar concentrations ranging from 0% to 74 %.

Chapter 4 Cubic Equations of State

4.1 Background

Cubic equations of state (EoSs) are simple polynomial equations relating pressure, volume, and temperature (PVT). They accurately describe the volumetric and phase behavior of pure compounds and mixtures, requiring only the critical properties and the acentric factor of each component. The same equation is used to calculate the properties of all hydrocarbon phases, thereby ensuring consistency in reservoir processes that approach critical conditions (e.g., miscible-gas injection and depletion of volatile-oil/gas-condensate reservoirs). Problems involving multiphase behavior, such as low-temperature CO_2 flooding, can be treated with an EoS. Volumetric behavior is calculated by solving a simple cubic equation, usually expressed in terms of the form below.

$$z^3 + A_2 z^2 + A_1 z + A_0 = 0 \quad (4.1)$$

where

$$z = \frac{pV}{RT} \quad (4.2)$$

In Eq. 4.1, A_0 , A_1 , A_2 and A_3 are constants-functions of pressure, temperature and phase composition.

Phase equilibria can also be treated with an EoS by satisfying the condition of chemical equilibrium. For a two-phase system, the chemical potential of each component in the liquid phase $\mu_i(x)$, computed by means of an EoS, must be equal to the chemical

potential of each component in the vapor phase $\mu_i(y)$. Chemical potential is usually expressed in terms of fugacity, f_i , which is calculated by Eq. 4.3.

$$\mu_i = RT \ln f_i + \lambda_i(T) \quad (4.3)$$

Constant $\lambda_i(T)$ terms drop out in most problems. For systems that do not react chemically, it can be readily shown that the condition $\mu_i(x) = \mu_i(y)$ is satisfied by the equal-fugacity constraint, $f_{Li} = f_{vi}$, where fugacity is given by Eq. 4.4. below.

$$\ln \varphi_i = \ln \frac{f_i}{y_i p} = \frac{1}{RT} \int_V^\infty \left(\frac{\theta p}{\theta n_i} - \frac{RT}{V} \right) dV - \ln z \quad (4.4)$$

Since the introduction of the van der Waals EoS, many cubic equations of state have been proposed. The Redlich and Kwong EoS (RK) in 1949, the Peng and Robinson EoS (PR) in 1976, and the Martin EoS in 1979, to name only a few. Most of these equations retain the original van der Waals repulsive term $RT / (v-b)$, modifying only the denominator in the attractive term. The Redlich - Kwong equation has been the most popular basis for developing new equations of state. Another trend has been to propose generalized three-, four-, and five-constant cubic equations that can be simplified to the PR EoS, RK EoS, or other familiar forms. Kumar and Starling use the most general five-constant cubic EoS to fit volumetric and phase behavior of nonpolar compounds, although they do not apply the equation to mixtures.

Most petroleum engineering applications rely on the PR EoS or a modification of the RK EoS. Several modified Redlich-Kwong equations have found acceptance, with Soave's modification (SRK EoS) being the simplest and most widely used. Unfortunately the SRK EoS yields poor liquid densities. Zudkevitch and Joffe proposed a modified RK EoS, the ZJRK EoS, where both EoS constants are corrected by temperature-dependent functions, resulting in improved volumetric predictions. Yarborough proposed a generalized form of the ZJRK EoS for petroleum reservoir mixtures.

The PR EoS is comparable with the SRK EoS in simplicity and form. Peng and Robinson reported that their equation predicts liquid densities better than the SRK EoS, although PR EoS densities are usually inferior to those calculated by the ZJRK EoS. A distinct advantage of the Peng-Robinson and Soave-Redlich-Kwong equations where a simple temperature-dependent correction is used for EoS constant A , is reproducibility. The ZJRK EoS relies on tables or complex functions to represent the highly nonlinear correction terms for EoS constants A and B . In the sections that follow, the most commonly used EoS models are described in detail.

4.2 Van der Waals EoS

The first EoS was proposed by Van der Waals back in 1873 and had a simple and qualitatively accurate formula (Eq. 4.5) which relates pressure with temperature and molar volume.

$$p = \frac{RT}{v-b} - \frac{a}{v^2} \quad (4.5)$$

In Eq. 4.5, a is the attraction parameter and b is the repulsive parameter. Compared to the ideal gas law, the VdW EoS incorporates two important improvements. First, the prediction of liquid behavior is now possible because volume approaches a limiting value b in high pressures:

$$\lim_{p \rightarrow \infty} v(p) = b \quad (4.6)$$

Parameter b is often called as the ‘covolume’ (effective molecular volume). The term $RT/(v-b)$ dictates liquid behavior and physically represents the repulsive component of pressure on a molecular scale.

The van der Waals equation also improves the description of non ideal gas behavior, where the term $RT/(v-b)$ approximates the ideal gas behavior (pRT/v) and the term a/v^2

accounts for non ideal behavior. The a/v^2 term reduces system pressure and traditionally is interpreted as the attractive component of pressure.

Van der Waals also stated the critical criteria that are used to define the two EoS constants a and b , that is the first and second derivatives of pressure with respect to volume equal zero at the critical point of a pure component as shown in Eq. 4.7.

$$\left(\frac{\partial p}{\partial v}\right)_{P_c T_c V_c} = \left(\frac{\partial^2 p}{\partial v^2}\right)_{P_c T_c V_c} = 0 \quad (4.7)$$

Martin and Hou showed that this constraint above is equivalent to the condition $(Z_c)^3=0$ at the critical point. Fig 4.1 of the Appendix I shows the p - v relationship of a pure compound for $T < T_c$, $T = T_c$, and $T > T_c$, indicating the zero slope inflection point on the critical isotherm that represents the van der Waals critical criteria. Imposing Eq. 4.7 on Eq. 4.5 and specifying p_c and T_c (as opposed to specifying two of the other critical properties), the constants a and b in the van der Waals equation are given by:

$$a = \frac{27 R^2 T_c^2}{64 p_c} \quad (4.8)$$

$$b = \frac{1 R T_c}{8 p_c} \quad (4.9)$$

The critical volume which is given by Eq. 4.10 results in a constant critical compressibility factor as shown below.

$$v_c = \frac{\left(\frac{3}{8}\right) (R T_c)}{p_c} \rightarrow z_c = \frac{p_c v_c}{R T_c} = \frac{3}{8} = 0.375 \quad (4.10)$$

The VdW EoS can also be written in terms of the z factor by substituting $z = pv/RT$:

$$z^3 - (B + 1)z^2 + A z - AB = 0 \quad (4.11)$$

$$A = a \frac{p}{(RT)^2} = \frac{27 p_r}{64 T_r^2} \quad (4.12)$$

$$B = b \frac{p}{RT} = \frac{1 p_r}{8 T_r} \quad (4.13)$$

where for now A and B are dimensionless parameters.

4.3 Redlich-Kwong EoS

Redlich and Kwong (1948) developed an adjustment in the original van der Waals attractive term (a/V^2), which could considerably improve the prediction of the volumetric and physical properties of the vapor phase. This attractive pressure term has a temperature dependence term and their equation can be represented as follows:

$$p = \frac{RT}{v - b} - \frac{a(T)}{v(v + b)} \quad (4.14)$$

where T is the system's temperature in °R.

During the development of their equations the authors noted that as the system pressure increases largely, i.e. $p \rightarrow \infty$, the molar volume of the substance shrinks to approximately 26% of its critical volume regardless of the temperature of the system. The critical point constraint of van der Waals (Eq. 2.7) was appropriately adjusted to satisfy the condition $b = 0.26 V_c$.

Applying the critical point conditions as expressed by Eq. 4.7 on Eq. 4.8 and by solving the resulting equations simultaneously we get:

$$\alpha = \Omega_a \frac{R^2 T_c^2}{P_c} a(T_r) \quad (4.15)$$

$$b = \Omega_b \frac{R T_c}{P_c} \quad (4.16)$$

where constants Ω_a and Ω_b are equal to 0.42748 and 0.08664 respectively. By equating Eq. 4.9 with Eq.4.13 we get:

$$p_c V_c = 0.333 R T_c \quad (4.17)$$

The expression above shows that the RK EoS produces a universal critical compressibility factor z_c equal to 0.333 for all substances. In terms of the z factor Eq. 4.14 becomes:

$$z^3 - z^2 + (A - B - B^2)z - AB = 0 \quad (4.18)$$

The fugacity expression for a pure component is as follows:

$$\ln \frac{f}{p} = \ln \phi = z - 1 - \ln(z - B) - \frac{A}{B} \ln \left(1 + \frac{B}{z} \right) \quad (4.20)$$

Redlich and Kwong extended the application of their equation to hydrocarbon liquid or gas mixtures by employing the following mixing rules:

$$a_m = \left[\sum_{i=1}^n x_i a_i^{0.5} \right]^2 \quad (4.21)$$

$$b_m = \left[\sum_{i=1}^n x_i b_i \right] \quad (4.22)$$

Many scholars of the RK EoS have been intrigued by its simplicity, accuracy, and the pleasure of deriving its thermodynamic properties. This has led to innumerable attempts to improve and extend the original Redlich-Kwong equation. It is claimed that the remarkable success of the RK EoS results from its excellent prediction of the second virial coefficient (securing good performance at low densities) and reliable predictions at high densities in the supercritical region. This latter observation results from the compromise fit of densities in the near-critical region; all components have a critical compressibility factor of $Z_c=1/3$, where, in fact, Z_c ranges from 0.29 for methane to 0.2 for heavy C_7 fractions. The Redlich-Kwong value of $Z_c=1/3$ is reasonable for lighter hydrocarbons but is unsatisfactory for heavier components.

4.4 Soave-Redlich-Kwong (SRK) EoS

Several attempts have been made to improve volumetric predictions of the RK EoS by introducing a component-dependent correction term a for the constant A of the EoS. Parameter a is dimensionless and becomes equal to unity when $T = T_c$. At temperatures other than the critical one, parameter a is defined by Eq. 4.21. Soave used vapor pressures to determine the functional relationship for the correction factor used in Eq. 4.16.

$$a_c = \left[1 + m (1 - \sqrt{T_r}) \right]^2 \quad (4.21)$$

Parameter m is correlated with the acentric factor and it is given by the following formula:

$$m = 0.480 + 1.574 \omega - 0.176 \omega^2 \quad (4.22)$$

Values of the acentric factor ω for pure substances and pseudo-components are listed in the last column of Table 2.2.

For any pure substance, the constants a and b of Eq. 4.1 are founded by imposing the classical van der Waals critical point constraints (Eq. 4.7) on Eq. 4.14 and solving the resulting equations to give.

$$\alpha = \Omega_\alpha \frac{R^2 T_c^2}{P_c} a_c \quad (4.23)$$

$$b = \Omega_b \frac{R T_c}{P_c} \quad (4.24)$$

The SRK EoS is expressed with respect to the z factor as follows:

$$Z^3 - Z^2 + (A - B - B^2)Z - AB = 0 \quad (4.25)$$

where,

$$A = \frac{a a_c p}{(RT)^2} \quad (4.26)$$

$$B = \frac{b p}{RT} \quad (4.27)$$

In the above equations, Ω_a and Ω_b are the SRK dimensionless pure component parameters and have the values of 0.42747 and 0.08664 respectively.

In order to use Eq. 4.25 with mixtures, the following mixing rules were proposed by Soave:

$$(a a_c)_m = \sum_i \sum_j x_i x_j (a_i a_j a_{ci} a_{cj})^{0.5} (1 - k_{ij}) \quad (4.28)$$

$$b_m = \sum_i [x_i b_i] \quad (4.29)$$

A and B parameters in the case of a mixture are transformed as follows:

$$A = \frac{(a a_c)_m p}{(RT)^2} \quad (4.30)$$

$$B = \frac{b_m p}{RT} \quad (4.31)$$

The parameter k_{ij} is an empirically determined correction factor called binary interaction coefficient (*BIC*), characterizing the binary formed by component i and component j in the hydrocarbon mixture. In case of a pure compound, the value of binary interaction coefficient equals unity.

The Soave-Redlich-Kwong equation is the most widely used RK EoS proposed to date even though it grossly overestimates liquid volumes (and underestimates liquid densities) of petroleum mixtures. The present use of the SRK EoS results from historical and practical reasons. It offers an excellent predictive tool for systems requiring accurate predictions of VLE and vapor properties. Volume translation which is discussed later on is highly recommended, if not mandatory, when liquid densities are computed by the EoS.

4.5 Peng-Robinson (PR) EoS

This equation of state is an important two-constant variation of the Van der Waals EoS which was introduced by Peng and Robinson in 1976 and created great expectations for

more accurate liquid densities predictions compared to the SRK equation of state. That was indeed the main motivation of the authors of the PR EoS, which in general gives density predictions of superior accuracy for reservoir fluid systems.

Although this equation improves the liquid density prediction, it cannot describe volumetric behavior near the fluid's critical point. However, the PR EoS is perhaps the most popular and widely used equation of state in the petroleum Industry. In terms of the molar volume V_m , Peng and Robinson proposed the following two-constant cubic equation:

$$P = \frac{RT}{v_m - b} - \frac{a}{v_m(v_m + b) + b(v_m - b)} \quad (4.32)$$

In the equation above, a and b parameters depend on critical pressure and temperature as it is shown in Eqs. 4.33 and 4.34 respectively, by imposing the classical van der Waals critical point constraint in Eq. 4.7. Parameter's a dimensions are $psia*ft^3$ whilst parameter b is expressed at $cu.ft./lbm\ mol$.

$$a = 0.45724 \frac{R^2 T_c^2}{P_c} a_c \quad (4.33)$$

$$b = 0.07780 \frac{RT_c}{P_c} \quad (4.34)$$

The equation predicts a universal critical gas compressibility factor of 0.307 compared to 0.333 of the SRK model. Peng and Robinson also adopted Soave's approach for calculating the parameter a_c .

$$a_c = (1 + m(1 - T_r^{0.5}))^2 \quad (4.35)$$

In Eq. 4.35 m is a correlating function in correction term a and it is calculated from Eq. 4.36.

$$m = 0.374464 + 1.54226 \omega - 0.26992 \omega^2 \quad (4.36)$$

In 1979 a modified expression for m was proposed by *Robinson et al.* that is recommended for heavier components (Eq. 4.37).

$$m = 0.3796 + 1.485 \omega - 0.1644 \omega^2 + 0.01667 \omega^3 \quad (4.37)$$

When expressed in terms of the deviation factor, the Eq.4.32 becomes:

$$Z^3 + (B - 1)Z^2 + (A - 3B^2 - 2B)Z + (B^3 + B^2 - AB) = 0 \quad (4.38)$$

In the equation above, A and B are the dimensionless versions of a and b and are calculated from Eqs. 4.39 and 4.40 respectively.

$$A = \alpha \frac{p}{(RT)^2} = 0.45724 \frac{p_r}{T_r^2} a(T_r) \quad (4.39)$$

$$B = \frac{P}{RT} b = 0.08664 \frac{P_r}{T_r} \quad (4.40)$$

where $a(T_r) = T_r^{-0.5}$.

Fugacity expressions are given by:

$$\ln \frac{f}{p} = \ln \varphi = z - 1 - \ln(z - B) - \frac{A}{2\sqrt{2}B} \ln \left[\frac{z + (1 + \sqrt{2})B}{z - (1 - \sqrt{2})B} \right] \quad (4.41)$$

$$\ln \frac{f_i}{y_i P} = \ln \varphi_i = \frac{B_i}{B} (Z - 1) - \ln(Z - B) + \frac{A}{B} \left(\frac{B_i}{B} - \frac{2}{A} \sum_{j=1}^N y_j A_{ij} \right) \ln \left(1 + \frac{B}{Z} \right) \quad (4.42)$$

The mixing rules for the PR EoS are defined as follows:

$$a_m = \sum \sum x_i x_j a_i^{\frac{1}{2}} a_j^{\frac{1}{2}} k_{ij} \quad (4.43)$$

$$b_m = \sum_i x_i b_i \quad (4.44)$$

In Eq. 4.34, k_{ij} is the binary interaction coefficient and is discussed in detail in the coming section. The PR EoS does not calculate inferior saturation pressures compared to the SRK EoS equation, and the temperature-dependent correction term for EoS constant A is very similar to the Soave correction. The largest improvement offered by the PR EoS is a universal critical compressibility factor of 0.307 , which is somewhat lower than the Redlich-Kwong value of one-third and closer to experimental values for heavier hydrocarbons. Although the PR EoS is another widely used cubic EoS in petroleum engineering calculations, the difference between PR EoS and SRK EoS liquid volumetric predictions can be substantial, although, in many cases, the error in oil densities is unacceptable from both equations.

4.6 Binary Interaction Coefficient (BICs)

Binary interaction coefficient values for N_2 , CO_2 and H_2S are shown in Table 4.1 for the PR EoS and the SRK EoS as found in the literature. BICs values accounting for the interactions between hydrocarbons compounds are calculated by means of the Oellrich correlation (Eq. 4.45).

$$k_{ij} = 1 - \left(\frac{2 v_{ci}^{1/6} v_{cj}^{1/6}}{v_{ci}^{1/3} + v_{cj}^{1/3}} \right)^\theta \quad (4.45)$$

In Eq. 4.45, v_{ci} is the critical volume of component i , approximate values of which can be found in the literature for hydrocarbon compounds up to the heavy end. Parameter θ is the hydrocarbon-hydrocarbon exponent. It has been shown that a value of

Table 4.1: Binary Interaction Coefficients (BICs) for the PR EoS and SRK EoS

	PR EoS			SRK EoS		
	N2	CO2	H2S	N2	CO2	H2S
N2	-	-	-	-	-	-
CO2	0.000	-	-	0.000	-	-
H2S	0.130	0.135	-	0.120	0.120	-
C1	0.025	0.105	0.070	0.020	0.120	0.080
C2	0.010	0.130	0.085	0.060	0.150	0.070
C3	0.090	0.125	0.080	0.080	0.150	0.070
iC4	0.095	0.120	0.075	0.080	0.150	0.060
nC4	0.095	0.115	0.075	0.080	0.150	0.060
iC5	0.100	0.115	0.070	0.080	0.150	0.060
nC5	0.110	0.115	0.070	0.080	0.150	0.060
C6	0.110	0.115	0.055	0.080	0.150	0.050
C7	0.110	0.115	0.050	0.080	0.150	0.030

$\theta=1.2$ provides a good match of the paraffin-paraffin interaction coefficients of the correlation. However it is recommended that the value is obtained by matching experimental data (e.g. saturation pressure data).

Critical compressibility factor is considered as fixed and equal to 0.307 for the PR EoS, 0.333 for the RK EoS and 0.333 for the SRK EoS, as shown in previous sections. Binary interaction coefficient values between the hydrocarbon compounds and the heavy

end fraction are calculated again by Eq. 4.36 with the heavy end's critical volume to be calculated by Eq. 2.16 of the Twu correlation. Table 4.2 gathers the binary interaction coefficient values adopted by the present work.

Table 4.2: Binary Interaction Coefficients (BICs) adopted by this work.

	N2	CO2	H2S	C1	C2	C3	iC4	nC4	iC5	nC5	C6	C7	C8	C9	C10	C11	C12+
N2	0.00	0.00	0.13	0.03	0.01	0.09	0.10	0.10	0.10	0.11	0.11	0.11	0.11	0.11	0.11	0.11	0.11
CO2	0.00	0.00	0.14	0.11	0.13	0.13	0.12	0.12	0.12	0.12	0.12	0.12	0.12	0.12	0.12	0.12	0.12
H2S	0.13	0.14	0.00	0.07	0.09	0.08	0.08	0.08	0.07	0.07	0.06	0.05	0.05	0.05	0.05	0.05	0.05
C1	0.03	0.11	0.07	0.00	0.00	0.01	0.02	0.02	0.02	0.02	0.03	0.03	0.04	0.05	0.05	0.06	0.00
C2	0.01	0.13	0.09	0.00	0.00	0.00	0.01	0.01	0.01	0.01	0.01	0.02	0.02	0.03	0.03	0.04	0.00
C3	0.09	0.13	0.08	0.01	0.00	0.00	0.00	0.00	0.00	0.00	0.01	0.01	0.01	0.02	0.02	0.02	0.00
iC4	0.10	0.12	0.08	0.02	0.01	0.00	0.00	0.00	0.00	0.00	0.00	0.00	0.01	0.01	0.01	0.01	0.00
nC4	0.10	0.12	0.08	0.02	0.01	0.00	0.00	0.00	0.00	0.00	0.00	0.00	0.01	0.01	0.01	0.01	0.00
iC5	0.10	0.12	0.07	0.02	0.01	0.00	0.00	0.00	0.00	0.00	0.00	0.00	0.00	0.00	0.01	0.01	0.00
nC5	0.11	0.12	0.07	0.02	0.01	0.00	0.00	0.00	0.00	0.00	0.00	0.00	0.00	0.00	0.01	0.01	0.00
C6	0.11	0.12	0.06	0.03	0.01	0.01	0.00	0.00	0.00	0.00	0.00	0.00	0.00	0.00	0.00	0.01	0.00
C7	0.11	0.12	0.05	0.03	0.02	0.01	0.00	0.00	0.00	0.00	0.00	0.00	0.00	0.00	0.00	0.00	0.00
C8	0.11	0.12	0.05	0.04	0.02	0.01	0.01	0.01	0.00	0.00	0.00	0.00	0.00	0.00	0.00	0.00	0.00
C9	0.11	0.12	0.05	0.05	0.03	0.02	0.01	0.01	0.00	0.00	0.00	0.00	0.00	0.00	0.00	0.00	0.00
C10	0.11	0.12	0.05	0.05	0.03	0.02	0.01	0.01	0.01	0.01	0.00	0.00	0.00	0.00	0.00	0.00	0.00
C11	0.11	0.12	0.05	0.06	0.04	0.02	0.01	0.01	0.01	0.01	0.01	0.00	0.00	0.00	0.00	0.00	0.00
C12+	0.11	0.12	0.05	0.00	0.00	0.00	0.00	0.00	0.00	0.00	0.00	0.00	0.00	0.00	0.00	0.00	0.00

4.7 Solution of the Cubic Polynomial

Compressibility factor is calculated via a cubic EoS by solving a cubic polynomial expressed in terms of the z factor. This polynomial equation only slightly differs between the different EoS models. Eq. 4.11 is the cubic polynomial corresponding to the VdW EoS, Eq. 4.25 to the RK and SRK EoS ones and Eq. 4.38 corresponds to the PR EoS.

$$Z^3 - (B + 1)Z^2 + A Z - AB = 0 \quad (4.11)$$

$$Z^3 - Z^2 + (A - B - B^2)Z - AB = 0 \quad (4.25)$$

$$Z^3 + (B - 1)Z^2 + (A - 3B^2 - 2B)Z + (B^3 + B^2 - AB) = 0 \quad (4.38)$$

Constants A and B are individually calculated by each EoS as it has been described in the above paragraphs and using appropriate mixing rules. In this work, the Cardano analytical methodology was utilized in order to solve the cubic gas compressibility factor polynomials.

4.7.1 Cardano

The Cardano's formula (named after Girolamo Cardano, 1501-1576), which is similar to the perfect-square method to quadratic equations is a standard way to find a real root of a cubic equation like:

$$ax^3 + bx^2 + cx + d = 0 \quad (4.46)$$

The two remaining roots, either real or complex, are afterwards found by polynomial division and the quadratic formula. The solution has two steps, the cubic polynomial's depression and its solution.

To depress the cubic equation we firstly substitute:

$$x = y - \frac{b}{3a} \quad (4.47)$$

Then we get:

$$a\left(y - \frac{b}{3a}\right)^3 + b\left(y - \frac{b}{3a}\right)^2 + c\left(y - \frac{b}{3a}\right) + d = 0 \Leftrightarrow$$

$$ay^3 - by^3 + \frac{b^2}{3a} - \frac{b^3}{27a^3} + by^3 - \frac{2b^2}{3a}y + \frac{b^3}{9a^2} + cy - \frac{bc}{3a} + d = 0 \Leftrightarrow \quad (4.48)$$

$$ay^3 + \left(c - \frac{b^2}{3a}\right) + \left(d + \frac{2b^3}{27a^2} - \frac{bc}{3a}\right) = 0$$

The equation above has now be depressed in such a way that the term y^2 is not present anymore. The next step is to solve the depressed equation of the form:

$$y^3 + Ay = B \quad (4.49)$$

We first substitute as follows:

$$3st = A \quad (4.50)$$

$$s^3 - t^3 = B \quad (4.51)$$

Then we solve for:

$$y = s - t \quad (4.51)$$

The cubic polynomial of Eq. 4.46 has the solutions:

$$X_1 = S + T - \frac{b}{3a} \quad (4.52)$$

$$X_2 = -\frac{S+T}{2} - \frac{b}{3a} + i\frac{\sqrt{3}}{2}(S-T) \quad (4.53)$$

$$X_3 = -\frac{S+T}{2} - \frac{b}{3a} - i\frac{\sqrt{3}}{2}(S-T) \quad (4.54)$$

where:

$$S = \sqrt[3]{R + \sqrt{Q^3 + R^2}} \quad (4.55)$$

$$T = \sqrt[3]{R - \sqrt{Q^3 + R^2}} \quad (4.56)$$

$$Q = \frac{3ac - b^2}{9a^2} \quad (4.57)$$

$$R = \frac{9abc - 27a^2d - 2b^3}{54a^3} \quad (4.58)$$

In the above equations i stands for the square root of -1 . If the three roots calculated are real numbers then the largest one corresponds to a gas phase, the lowest one to a liquid one and the middle one is rejected as it lacks any physical meaning. If the roots

are comprised by a real one and a pair of complex, then the real one is selected for further calculations.

4.8 Volume Shift Correction

A comparison of the predicted liquid molar volume with the leading two-parameter EoSs with experimental data of pure compounds generally shows a systematic deviation. The deviation is almost constant over a wide pressure range away from the critical point. Hence, subtracting the predicted molar volume by a constant correction term can improve the predicted liquid density. The effect on the predicted vapor volume is generally insignificant due to its large value relative to that of liquid away from the critical point.

The concept of volume translation or volume shift was firstly introduced in 1979 by Martin et al. who attempted to ease the comparison of his proposed generalized EoS with previously published equations.

Later, Peneloux et al. published their volume translation method which modifies the two-constant cubic SRK EoS by introducing a third constant c , without changing the equilibrium calculations of the original two constant EoS. Their major contribution was indeed the fact that he showed that the volume shift applied does not affect equilibrium calculations either for pure components or mixtures and thereby does not affect the original volumetric capabilities of the SRK EoS. Jhaveri and Youngren later showed that volume translation works equally well with any other two constant EoS such as the PR EoS.

According to the volume translation method, the molar volume that is calculated by the EoS, v^{EoS} is corrected by a simple correction term which is linear with respect to the fluid's composition (Eq. 4.59).

$$v^{cor} = v^{EoS} - \sum_{i=1}^N z_i c_i \quad (4.59)$$

In the above expression z_i stands for the component's i molar concentration and c_i is the volume translation component-specific parameter which is estimated from Eqs. 4.60 and 4.61 for the SRK and the PR equations of state respectively.

$$c_i = \frac{R T_c}{P_c} (0.1156 - 0.4077 z_{RA}) \quad (4.60)$$

$$c_i = \frac{R T_c}{P_c} (0.1154 - 0.4006 z_{RA}) \quad (4.61)$$

The above equations for the calculation of c_i involve the Rackett compressibility factor z_{RA} which depends on the component's acentric factor ω and it is given by Eq. 4.62.

$$z_{RA} = 0.29056 - 0.08775 \omega \quad (4.62)$$

The shift in the EoS calculated molar volume is according to the authors actually equivalent to adding a third constant to the EoS but it is special because equilibrium conditions remain unaltered. One can readily notice that fact for a pure component, where the van der Waals 'loop' defines vapor pressure by making the areas above and below the $p = p_v$ line on a $p - v$ plot equal in Fig. 4.1. The equal area balance of fugacities does not change when the curve is shifted to the left or to the right along the volume axis of the diagram and it can be readily seen that vapor-pressure predictions are unaltered by introducing the volume translation parameter c_i .

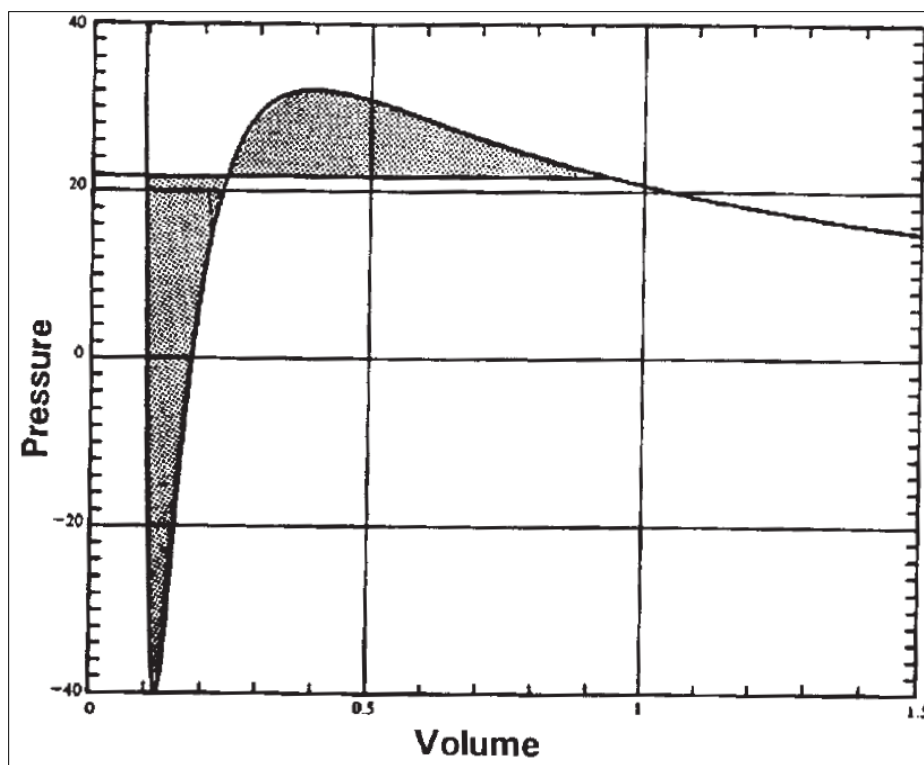


Figure 4.1 – p-V diagram of a pure component as calculated by a cubic EoS illustrating the van der Waals’s “loop” defining vapor pressure by the equal-area rule.

Although primarily the Peneloux et al. volume translation method is applicable to liquid phase hydrocarbons, the present work adopted it for correcting the volume of hydrocarbon gases and condensate gases. The effect of the implementation of the aforementioned correction method is discussed in a next chapter.

Chapter 5 Experimental Compressibility Factor Values

5.1 Background

Among the existing methods for the determination of compressibility z factor, experimental measurement is clearly the most accurate and reliable one. It is hard however to determine experimentally measured z factor values for all compositions of gases at all ranges of pressures and temperatures that might be encountered during the exploitation of a field. At the same time, this method is expensive and most of the time these measurements are made at reservoir temperature only. At this point the necessity for vigorous and accurate z factor computational methods arises that can provide reliable forecast in an inexpensive and easy to implement fashion.

To evaluate the performance of various z factor prediction methods, such as empirical correlations and equations of state such as those that were discussed in the previous chapters, along with their corrections and modifications a set of experimental compressibility z factor measurements is required. Within the context of the present study, a fluid database consisting of two hundred thirty four gas condensate reservoir fluids from various fields worldwide was utilized to evaluate the accuracy of the most commonly used z factor calculation methods.

5.2 Fluid's Database Properties

Compressibility z factor prediction methods that were described in previous sections were evaluated over a database of experimentally measured data of two hundred thirty four real reservoir condensate gases. The z factor data that were retrieved from the database PVT reports included the composition, reservoir temperature, fluid

characterization data and compressibility factors of 234 gas and condensate gas samples. The latter were obtained from constant composition expansion lab PVT tests. The fluid samples range from lean, rich to slightly sour and highly sour gases. For each gas condensate composition, the data include experimentally measured gas gravity, compositional analysis from methane to C₁₂₊ and molecular weight and specific gravity of the C₁₂₊ fraction. These samples originate from different fields worldwide and vary in their characteristics, composition and properties. Table 5.1 summarizes their properties indicating also the variability of the utilized data.

Table 5.1: Properties of the natural gases of the database (the outliers have been removed)

	Minimum	Maximum	Average
Composition (mole %)			
Hydrogen sulfide	0.0	14.1	0.4
Carbon dioxide	0.0	72.6	3.2
Nitrogen	0.0	10.6	0.9
Methane	12.4	98.3	77.3
Ethane	0.5	14.2	6.6
Propane	0.0	10	3.3
Iso-butane	0.0	2.4	0.7
n-butane	0.0	3.6	1.3
Iso-pentane	0.0	1.6	0.6
n-pentane	0.0	1.6	0.5
Hexane	0.0	2.1	0.8
Eptane	0.0	2.7	0.9
Octane	0.0	3.3	0.9
Nonane	0.0	23.2	0.7
Decane	0.0	1.5	0.4
Undecane	0.0	0.9	0.3
C ₁₂₊	0.0	6.2	1.1
MW of C ₁₂₊	105.3	282.7	137.3
SG of C ₁₂₊	0.718	0.869	0.795
Reservoir pressure (psia)	3000	13000	6527.4
Reservoir temperature (°F)	118.3	352.3	237.3
z factor	0.7009	1.8813	1.0599

5.2.1 Pressure Discretization

The experimental z factor values that had been measured for each gas condensate had been interpolated by specific functions of pressure. In this work, the fitted experimental z factor curves were re-digitized at ten pressure steps varying between the sample's

minimum pressure (P_{min} , which is equal to the sample's dewpoint pressure P_d) and the maximum fluid's pressure which corresponds to the initial reservoir pressure (P_{res}).

The pressure range of each z factor dataset, that is the difference between the maximum (reservoir) and the minimum fluid pressure for each specific fluid, exhibited various values with a maximum difference of approximately 7320 psia, while the minimum pressure difference was found equal to 279 psia. In Fig. 5.1 the frequency distribution of that pressure difference is shown. Those figures indicate that the pressure range in the single phase of each PVT report is quite large, thus justifying the need to divide that range into 10 distinct points for each gas condensate.

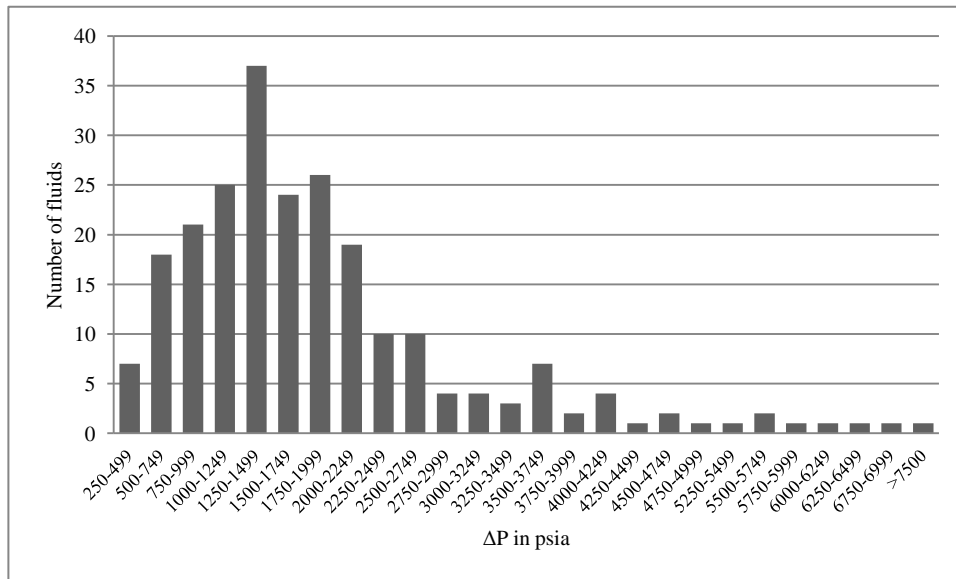


Figure 5.1 – ΔP frequency distribution for the natural gases of the database

5.2.2 Reservoir Temperature Distribution

Reservoir temperature is predominantly determined by the reservoir's depth. For the fluid database under examination, reservoir temperature ranges from approximately 118 °F to 352 °F. Fig. 5.2 below demonstrates a frequency distribution with respect to the reservoir temperature of the fluids of the database under examination. The temperature

distribution is wide enough and can be considered that adequately represents the reservoir temperatures that are encountered worldwide.

5.2.3 Composition Distribution

The composition of the database fluids also varies with respect to concentration of methane, nitrogen, carbon dioxide, hydrogen sulfide and heavy end (C_{7+}). The vast majority (156 natural gases) out of the 234 natural gases of the database are lean with respect to their heavy end content (less than 5%), while 78 of them can be considered rich in heavy hydrocarbons with concentrations greater than 5% mole, and thus more prone to condensation. In Fig. 5.3, the % mole concentration distribution of the heavy end for the natural gases of the database is shown.

With respect to their hydrogen sulfide content, the natural gases under examination are divided into slightly sour gases, containing low concentration of hydrogen sulfide (less than 5%), and highly sour gases having high concentration of hydrogen sulfide (more than 5%). Based on the above categorization and in Fig. 5.4, just five out of the two hundred thirty four natural gases can be considered as highly sour.

Acid natural gases are these gases with significant content of carbon dioxide CO_2 . CO_2 mole concentration distribution is shown in Fig. 5.5 for the natural gases of the database. Methane CH_4 concentration distribution is shown in Fig. 5.6 for the natural gases of the database. Natural gases with high CH_4 content have low CO_2 content and vice versa as verified by Fig. 5.5 and 5.6.

From the discussion above it becomes clear that the PVT reports database that has been utilized in this thesis is quite representative as it contains various types of gas condensate fluids. It is exactly that property that provides validity to the statistics of the obtained deviations between the measured z factor values and those obtained from the various computational methods, as shown in the following chapter.

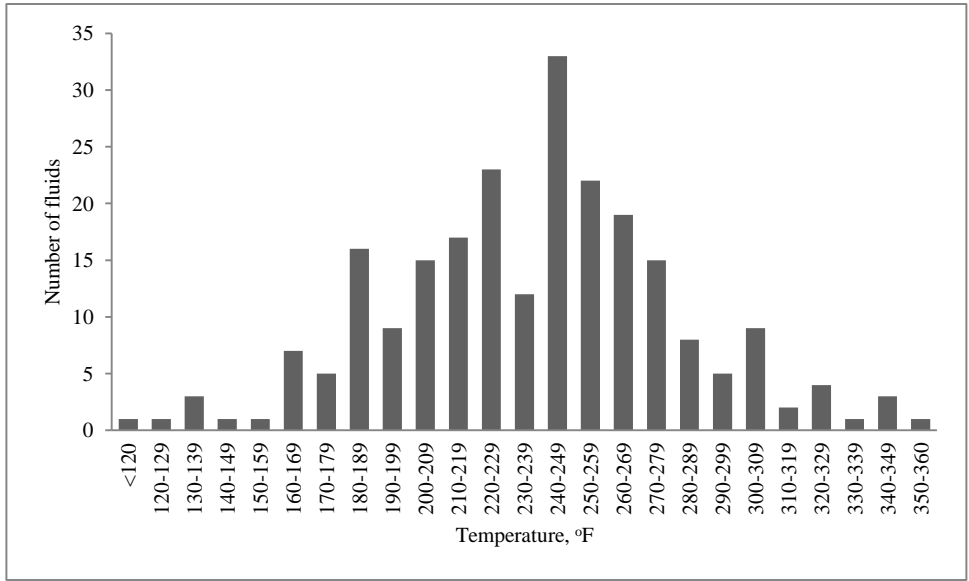


Figure 5.2 – T_{res} frequency distribution for the natural gases of the database ($^{\circ}F$)

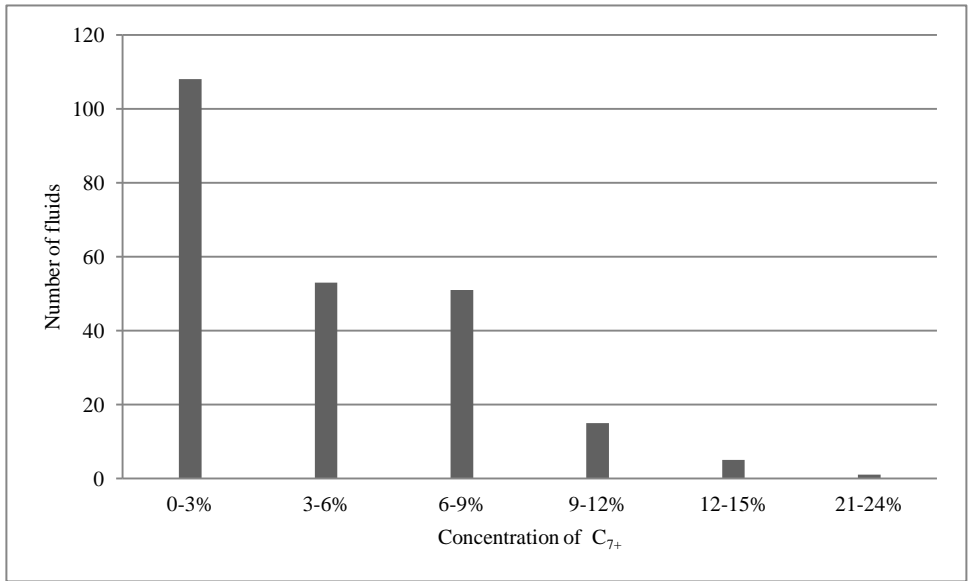


Figure 5.3 – C_{7+} concentration distribution for the natural gases of the database

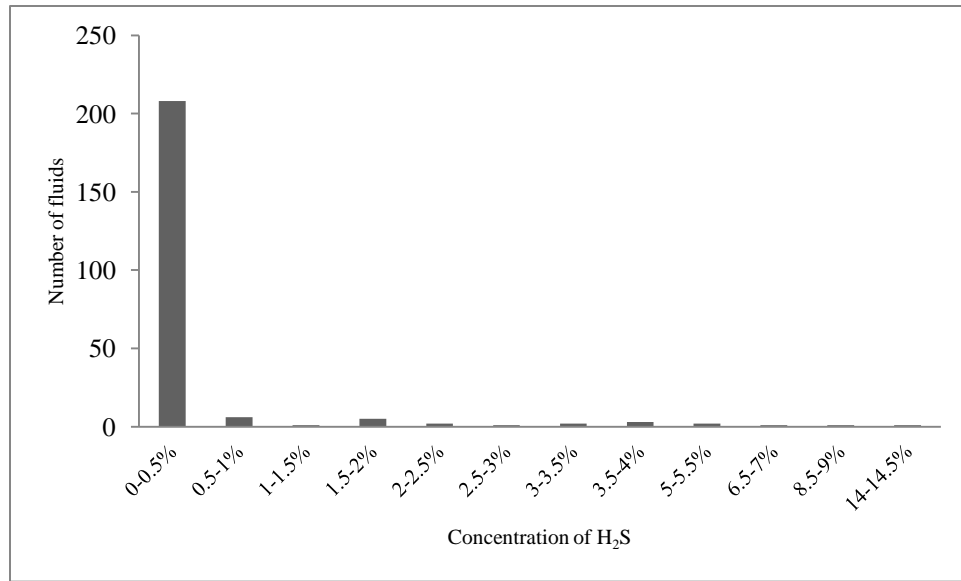


Figure 5.4 – H₂S concentration distribution for the natural gases of the database

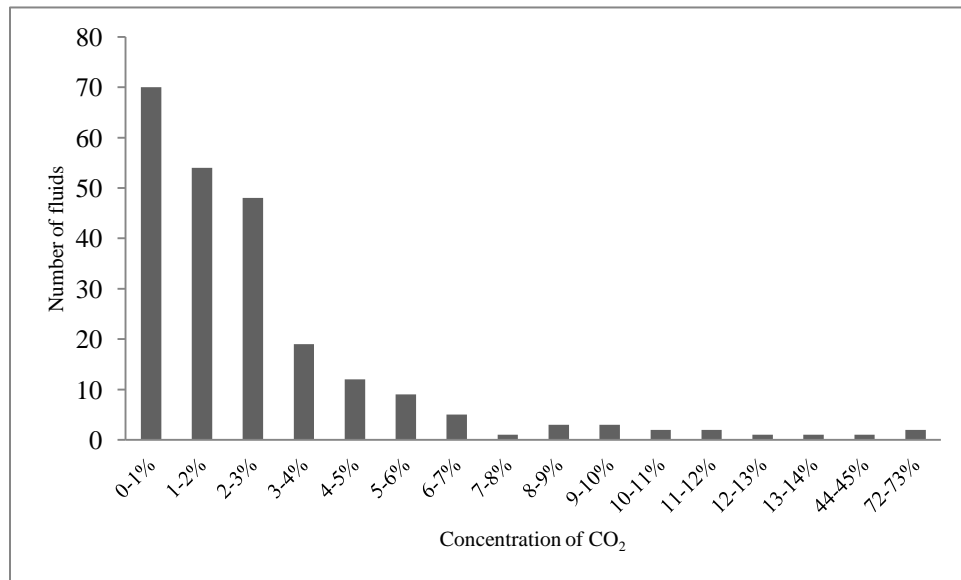


Figure 5.5 – CO₂ concentration distribution for the natural gases of the database

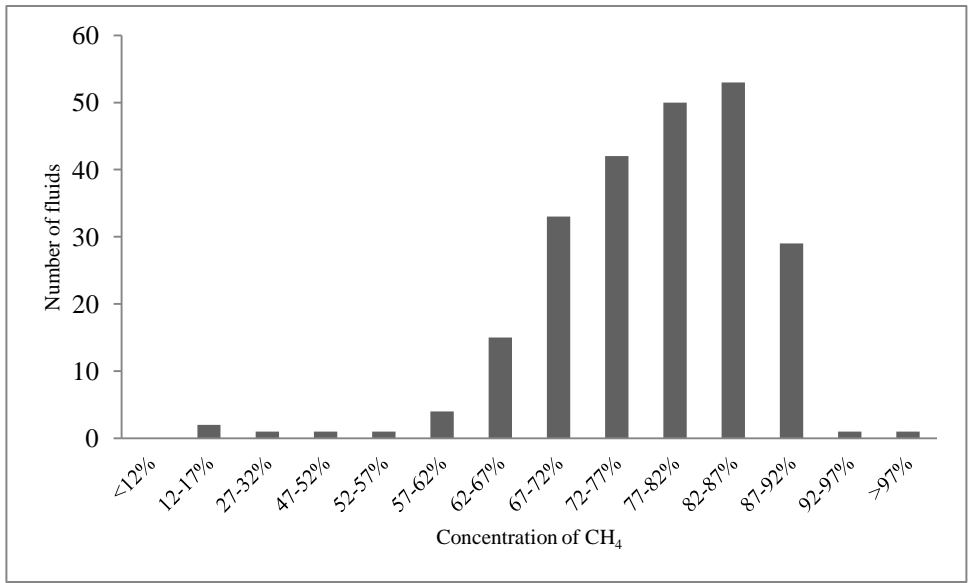


Figure 5.6 – CH₄ concentration distribution for the natural gases of the database

Chapter 6 Results and Discussion

6.1 Statistical Tools

In this section, some of the most commonly used statistical metrics for measuring the accuracy of continuous variables are summarized.

6.1.1 Mean Absolute Deviation

The mean absolute deviation (*MAD* or *MAE* i.e. mean absolute error) is the sum of absolute differences between the actual experimental z factor value and the forecasted value divided by the number of pressure increments. It is given by Eq. 6.1 below:

$$MAD = \frac{\sum_{t=1}^n |A_t - F_t|}{n} \quad (6.1)$$

MAD takes only positive values and constitutes the statistical mean of the absolute deviations, giving thus an estimate of the expected average absolute error between the experimental z factor measurements and the computational method.

6.1.2 Mean Square Error

Mean square error (*MSE* or R^2 , or coefficient of determination) is probably the most commonly used error metric. It penalizes larger errors because squaring larger numbers has a greater impact than squaring smaller ones. The *MSE* is the sum of the squared errors divided by the number of observations (pressure steps) as it is shown in Eq. 6.2. As a statistical metric however, the mean square error has a disadvantage as it lacks any physical meaning due to its squared dimensions.

$$MSE = \frac{\sum_{t=1}^n (A_t - F_t)^2}{n} \quad (6.2)$$

6.1.3 Root Mean Square Error

The root mean square error (*RMSE*) is the square root of the mean square error *MSE* and it is calculated by Eq. 6.3 below.

$$RMSE = \sqrt{\frac{\sum_{t=1}^n (A_t - F_t)^2}{n}} \quad (6.3)$$

RMSE measures the average magnitude of the errors in a set of predictions without considering their direction. Contrary to the MSE, the average model prediction error is expressed in the units of the variable of interest.

6.1.4 Mean Absolute Relative Deviation

Mean absolute relative deviation (*MARD*) is the average of absolute errors divided by the actual experimental compressibility z factor values. It is calculated by Eq. 6.4.

$$MARE = \frac{\sum_{t=1}^n \left| \frac{A_t - F_t}{A_t} \right|}{n} \quad (6.4)$$

6.1.5 Mean Relative Deviation

The mean relative deviation (*MRD*) is the sum of the differences between the experimental z factor values and the forecasted values divided by the number of pressure increments. It is given by Eq. 6.5 below and it is used for checking whether the predictions over or underestimate the actual values.

$$MRD = \frac{\sum_{t=1}^n (A_t - F_t)}{n} \quad (6.5)$$

MRD measures the average magnitude of the deviations occurred in a set of predictions by considering their direction. Ideally, MRD would be equal to zero if a computational method predicts equal values to those of the experimental measurement.

6.1.6 Outliers Removal

An outlier is an observation (i.e. an experimental measurement) that is not alike the other observations. It is rare, or distinct, or it does not fit in some way. Outliers can have many causes such as measurement or input error, data corruption or just being real outliers. There is not a specific way to define and identify outliers in general because of the specific properties of each dataset.

In a Gaussian (and Gaussian-like) distribution within a distance of one standard deviation from the mean, the 68% of the data is covered. Similarly within two standard deviations the 95% of the total data is covered and within three standard deviations the 99.7%. Three standard deviations from the average MRD is a common cut-off in practice for identifying outliers in MRD error distributions. That approach was also adopted from the present work, with respect to the MRD of the implemented z factor calculation methods, given the large volume of available z factor data.

6.2 Results Comparison

6.2.1 Correlations

Results of in total five empirical correlations are presented in this section combined with two of the most commonly used mixing rules and the Wichert-Aziz correction for sour and acid gases, which modifies the pseudo-critical pressure and temperature before introducing them into the correlations. This leads to twenty different combinations that were examined and are presented in this section.

Table 6.1 reports the application range for each correlation in terms of pseudo-reduced pressure and temperature. For the fluid database under examination this range is approximately $1.981 \leq P_{pr} \leq 18.909$ and $1.31 \leq T_{pr} \leq 2.335$. Clearly, some fluid samples

could not be treated by specific methods and they were not taken into account when computing the method statistics.

Table 6.1: Recommended application ranges for the correlations

Correlation	Range, P_{pr}	Range, T_{pr}
Hall and Yarborough	n/a	$1 \leq T_{pr}$
Shell Oil Company	n/a	n/a
Brill and Beggs	$15 \leq P_{pr}$	$1.2 \leq T_{pr} \leq 2$
Azizi et al.	$0.2 \leq P_{pr} \leq 11$	$1.1 \leq T_{pr} \leq 2$
Heidaryan et al.	$0.2 \leq P_{pr} \leq 15$	n/a

6.2.1.1 Azizi-Behbahani-Isazedeh correlation

In Fig 6.1 to 6.4, the frequency distributions of MRD of the different combinations of mixing rules with the inclusion or not of the Wichert-Aziz correction method are shown. The calculation of the z factor is done by the Azizi-Behbahani-Isazedeh correlation which was discussed in chapter 3.2.4. Additionally in Table 6.2 the statistical metrics are reported.

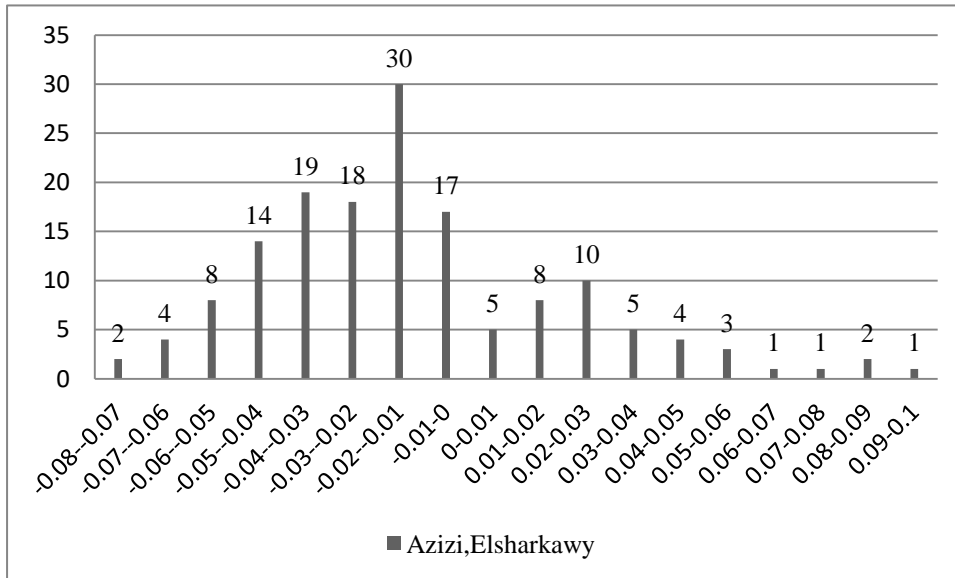


Figure 6.1 – MRD of the Azizi, Elsharkawy combination

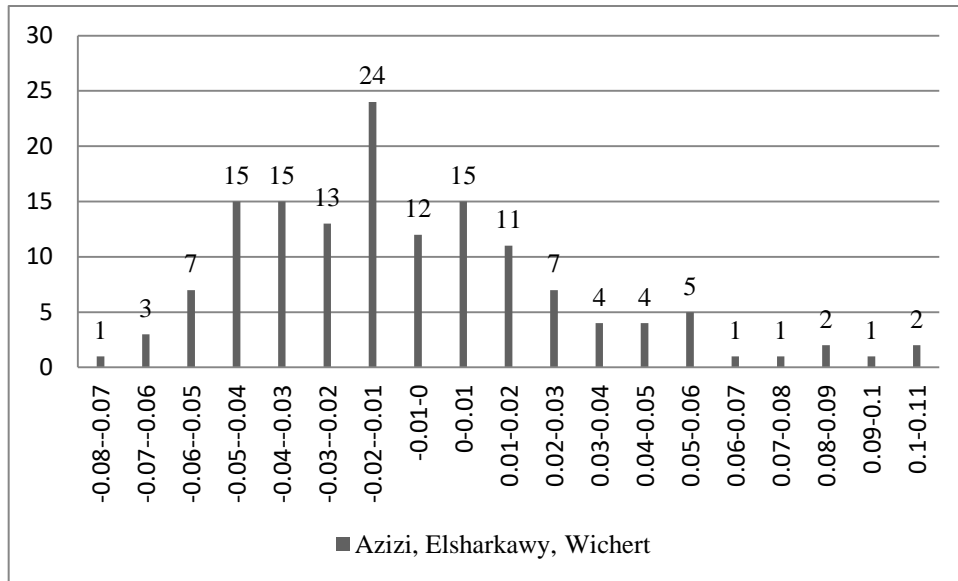


Figure 6.2 – MRD of the Azizi, Elsharkawy, Wichert combination

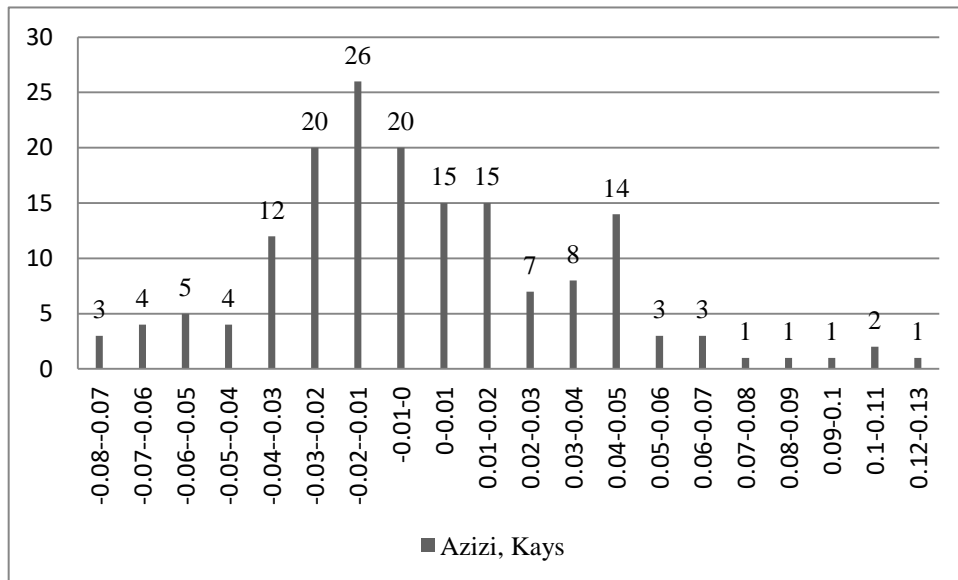


Figure 6.3 – MRD of the Azizi, Kays combination

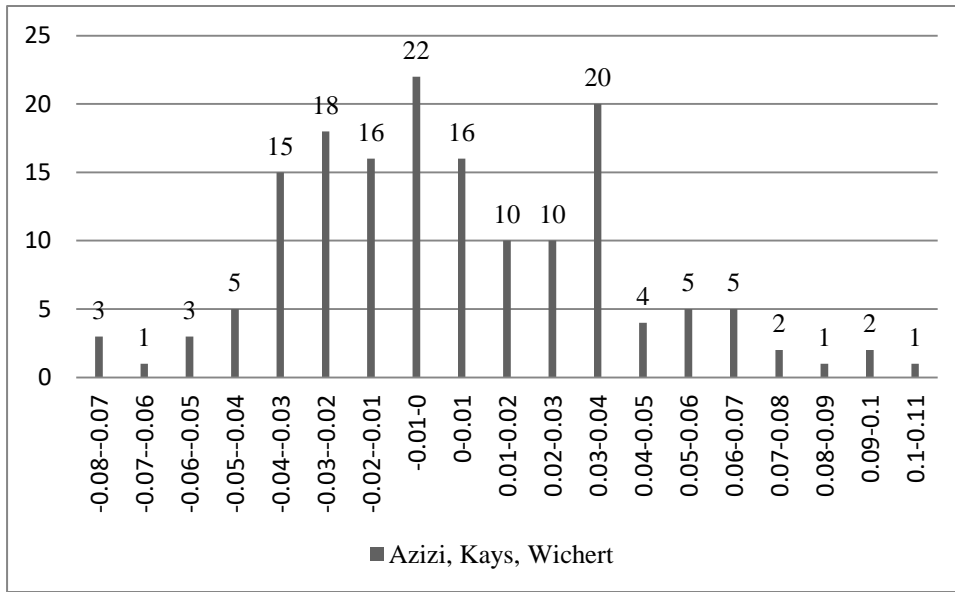


Figure 6.4– MRD of the Azizi, Kays, Wichert combination

Table 6.2: Statistical metrics for the different combinations (Azizi et al.)

Mixing Rule	Correction	Av. MAD	Av. MARD (%)	R ²
Kays	Yes	0.029	3.04	0.98769
Kays	No	0.030	3.08	0.98983
Elsharkawy	Yes	0.030	3.63	0.98184
Elsharkawy	No	0.030	2.88	0.98597

The number of gases that fall into the application range of the method slightly differs for each combination as the choice of the mixing rule and the inclusion or not of the correction slightly changes the pseudo-reduced properties. By examining Fig 6.1 to 6.4, 141 (85.45%) gases out of the 165 that fall into application range have MRD of $\pm 5\%$ with the Azizi, Kay’s combination, 135 (84.91%) out of 159 with the Azizi, Kay’s, Wichert, 105 (73.43%) out of 143 with the Azizi, Elsharkawy, Wichert and 125 (82.24%) out of 152 with the Azizi, Elsharkawy combination.

6.2.1.2 Brill and Beggs correlation

In Fig 6.5 to 6.8, the frequency distributions of MRD of the different combinations of mixing rules with the inclusion or not of the Wichert-Aziz correction method are shown. The calculation of the z factor is done by the Brill and Beggs correlation which was discussed in chapter 3.2.3. In Table 6.3 the statistical metrics are reported.

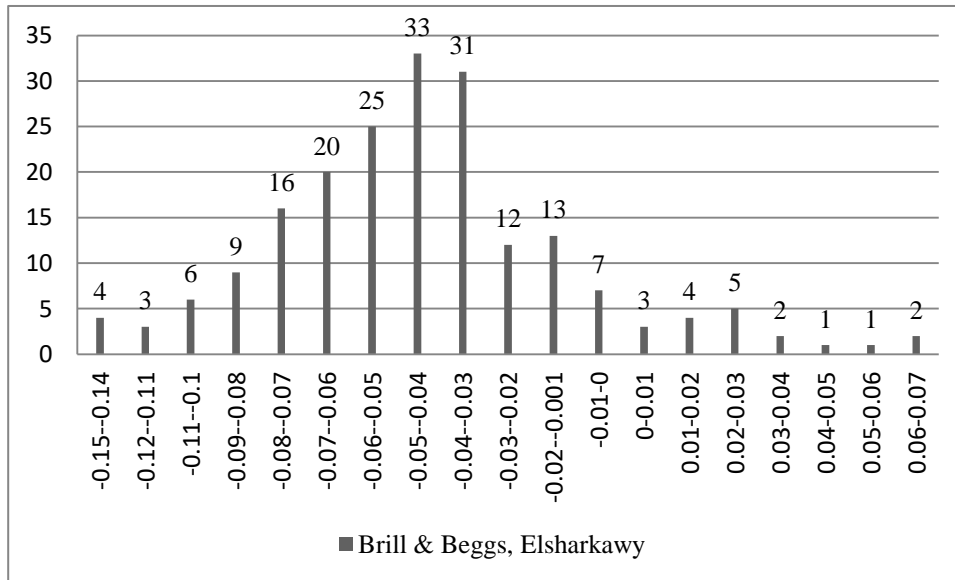


Figure 6.5 – MRD of the Brill and Beggs, Elsharkawy combination

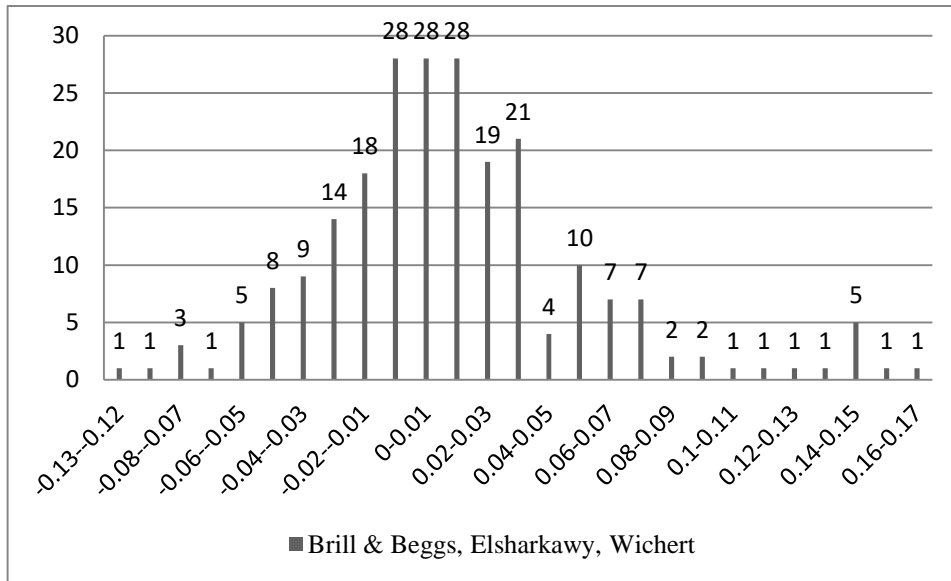


Figure 6.6 – MRD of the Brill and Beggs, Elsharkawy, Wichert combination

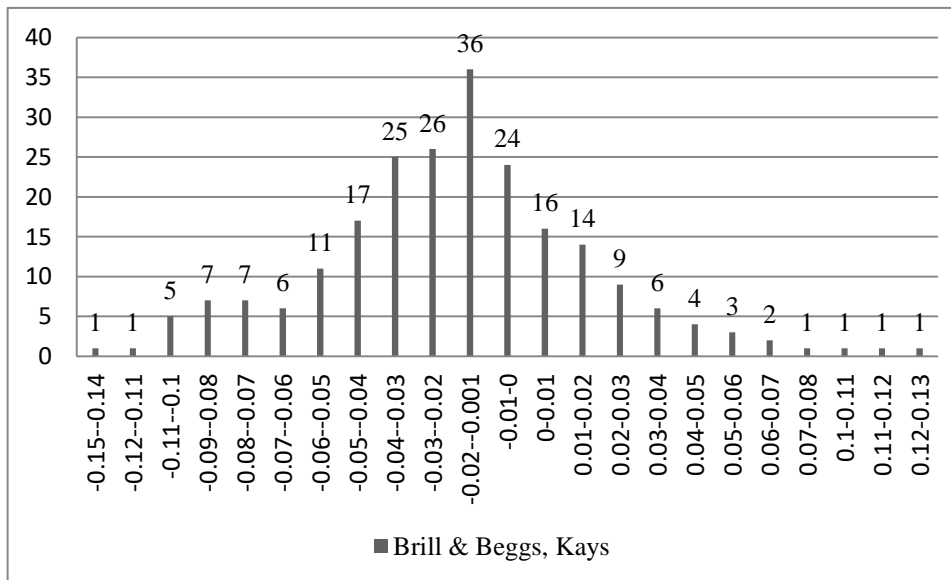


Figure 6.7 – MRD of the Brill and Beggs, Kays combination

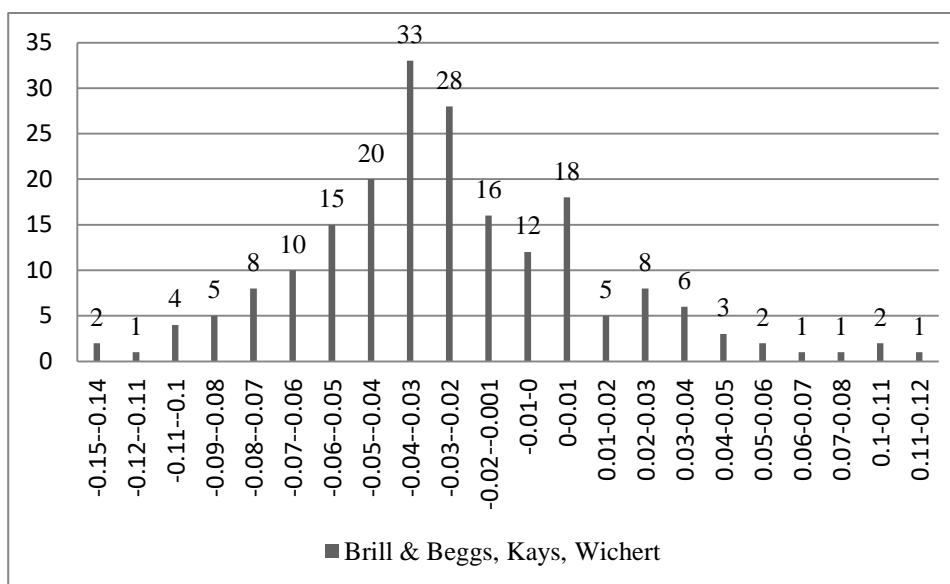


Figure 6.8 – MRD of the Brill and Beggs, Kays, Wichert combination

Table 6.3: Statistical metrics for the different combinations (Brill and Beggs)

Mixing Rule	Correction	Av. MAD	Av. MARD (%)	R ²
Kays	Yes	0.033	3.16	0.99031
Kays	No	0.034	3.29	0.99055
Elsharkawy	Yes	0.030	3.05	0.98943
Elsharkawy	No	0.027	2.68	0.98989

The number of gases that fall into the application range of the method slightly differs for each combination as the choice of the mixing rule and the inclusion or not of the correction slightly changes the pseudo-reduced properties. By examining Fig 6.5 to 6.8, 177 (79.02%) gases out of the 224 that fall into application range have MRD of $\pm 5\%$ with the Brill and Beggs, Kay’s combination, 165 (82.09%) out of 201 with the Brill and Beggs, Kay’s, Wichert, 177 (77.97%) out of 227 with the Brill and Beggs, Elsharkawy, Wichert and 167 (85.39%) out of 197 with the Brill and Beggs, Elsharkawy combination.

6.2.1.3 Shell Oil Company correlation

In Fig 6.9 and 6.12, the frequency distributions of MRD of the different combinations of mixing rules with the inclusion or not of the Wichert-Aziz correction method are shown. The calculation of the compressibility z factor is done by the Shell Oil Company correlation which was discussed in section 3.2.5. Moreover, in Table 6.4 the statistical metrics are reported.

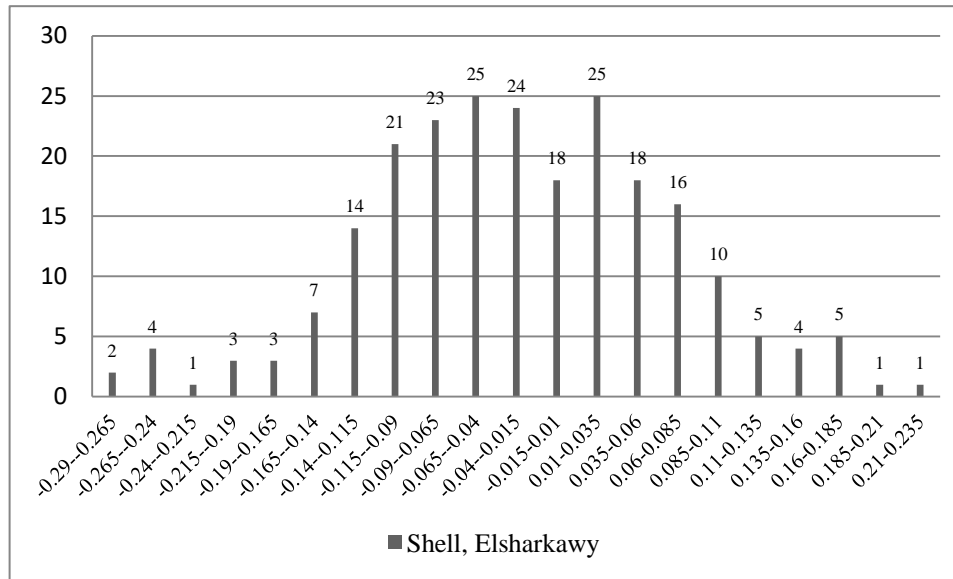


Figure 6.9 – MRD of the Shell, Elsharkawy combination

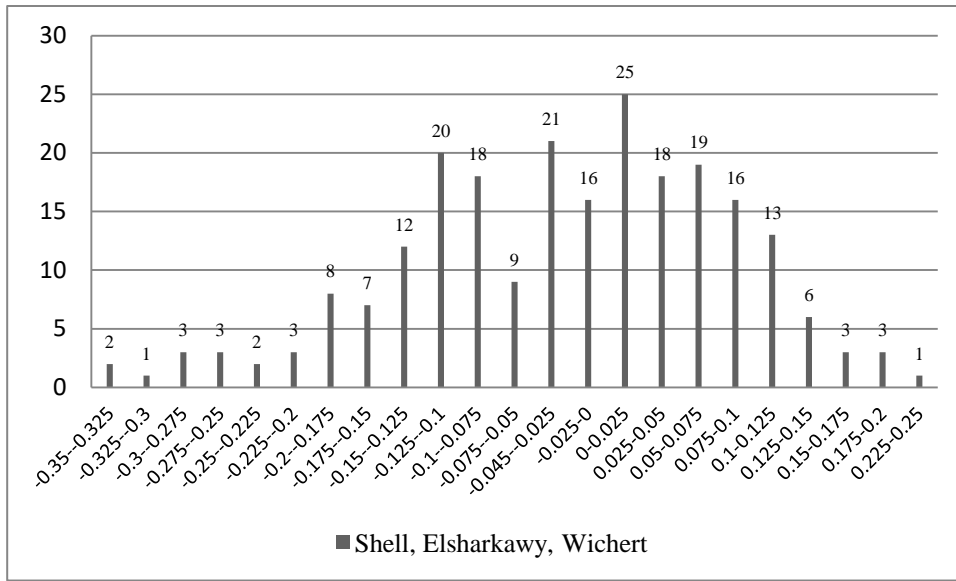


Figure 6.10 – MRD of the Shell, Elsharkawy, Wichert combination

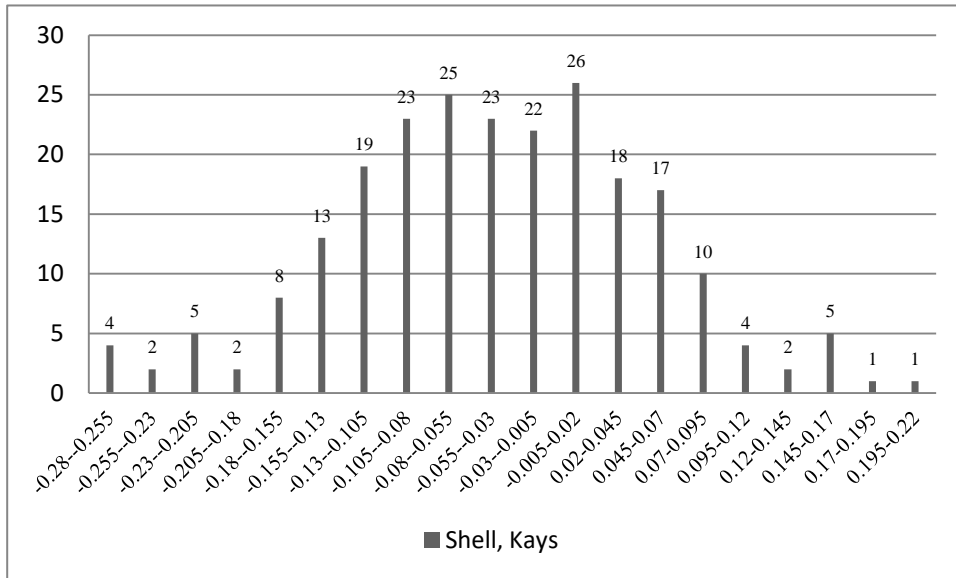


Figure 6.11 – MRD of the Shell, Kays combination

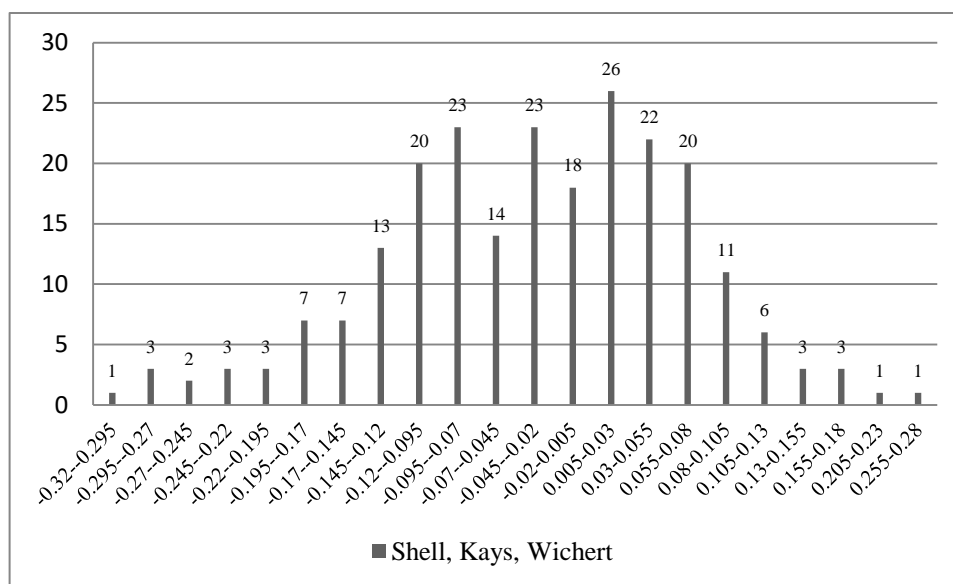


Figure 6.12 – MRD of the Shell, Kays, Wichert combination

Table 6.4: Statistical metrics for the different combinations (Shell correlation)

Mixing Rule	Correction	Av. MAD	Av. MARD (%)	R ²
Kays	Yes	0.089	8.13	0.99519
Kays	No	0.086	7.95	0.99250
Elsharkawy	Yes	0.099	9.02	0.99265
Elsharkawy	No	0.083	7.74	0.99088

For this correlation no application range was found in the literature. By examining Fig 6.9 to 6.12, 89 (38.69%) gases out of 230 exhibit MRD of $\pm 5\%$ with the Shell, Kay’s combination, 89 (38.69%) out of 230 with the Shell, Kay’s, Wichert, 110 (47.82) out of 230 with the Shell, Elsharkawy and 80 (34.93%) out of 229 with the Shell, Elsharkawy, Wichert combination.

6.2.1.4 Heidaryan correlation

In Fig 6.13 to 6.16 the frequency distributions of MRD of the different combinations of mixing rules with the inclusion or not of the Wichert-Aziz correction method are shown. The calculation of the compressibility z factor is done by the Heidaryan et al. correlation which was discussed in section 3.2.7. In Table 6.5 the statistical metrics are reported.

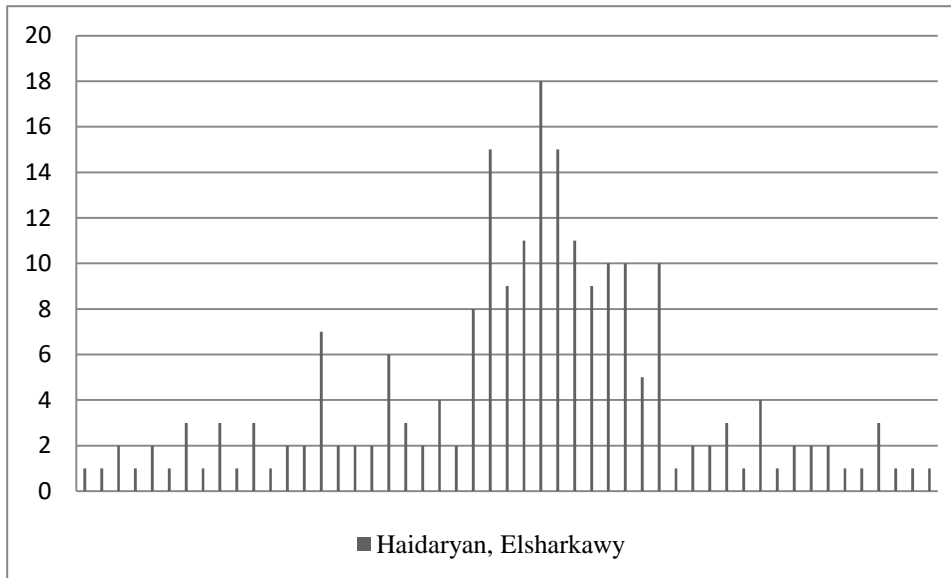


Figure 6.13 – MRD of the Heidaryan, Elsharkawy combination

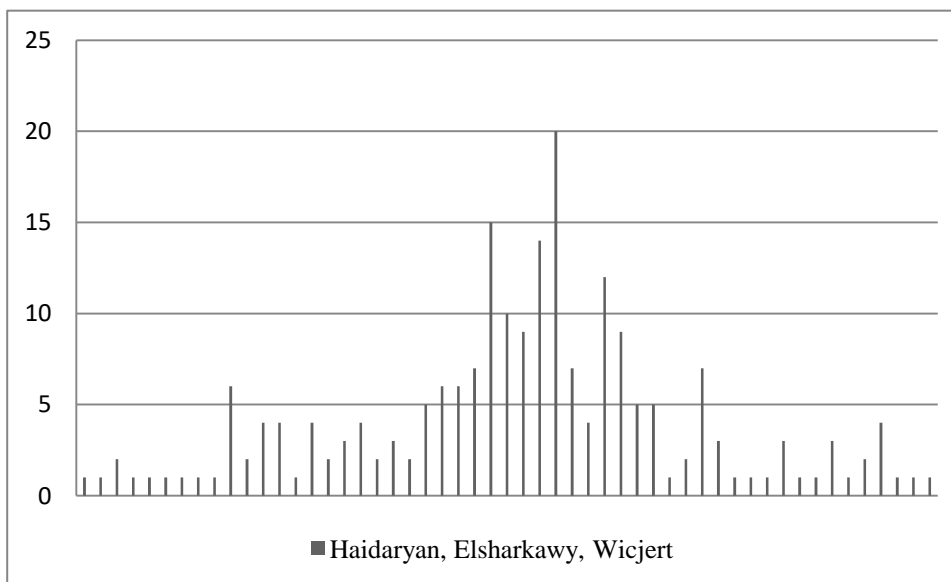


Figure 6.14 – MRD of the Heidaryan, Elsharkawy, Wichert combination

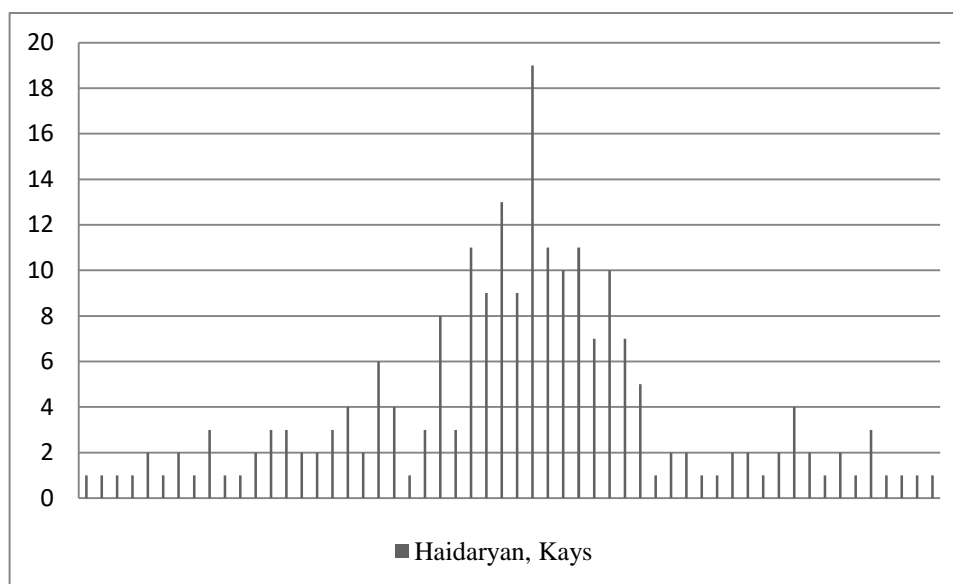


Figure 6.15 – MRD of the Heidaryan, Kays combination

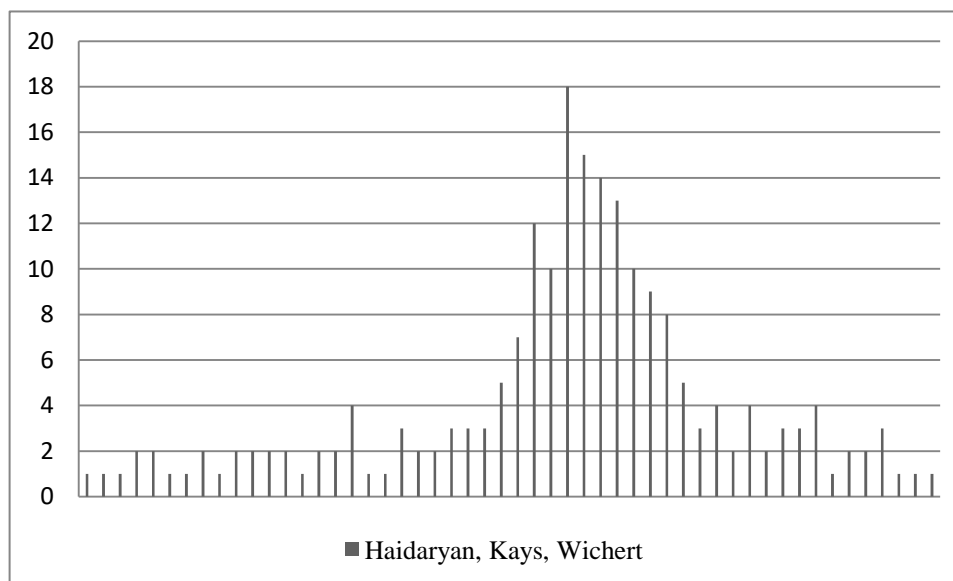


Figure 6.16 – MRD of the Heidaryan, Kays, Wichert combination

Table 6.5: Statistical metrics for the different combinations (Heidaryan et al.)

Mixing Rule	Correction	Av. MAD	Av. MARD (%)	R ²
Kays	Yes	0.088	7.92	0.97209

Kays	No	0.095	8.53	0.96897
Elsharkawy	Yes	0.096	8.63	0.96370
Elsharkawy	No	0.094	8.49	0.96622

By examining Fig 6.13 to 6.16, 110 (51.40%) gases out of 214 exhibit MRD of $\pm 5\%$ with the Heidaryan, Kay's combination, 113 (54.07%) out of 209 with the Heidaryan, Kay's, Wichert, 112 (52.58%) out of 213 with the Heidaryan, Elsharkawy and 110 (5.26%) out of 216 with the Heidaryan, Elsharkawy, Wichert combination.

6.2.1.5 Hall and Yarborough correlation

In Fig 6.17 and 6.20, the frequency distributions of MRD of the different combinations of mixing rules with the inclusion or not of the Wichert-Aziz correction method are shown. The calculation of the compressibility z factor is done by the Hall and Yarborough correlation which was discussed in chapter 3.2.1. In Table 6.6 the statistical metrics are reported and the values in parentheses correspond to the metrics prior to the removal of the outliers.

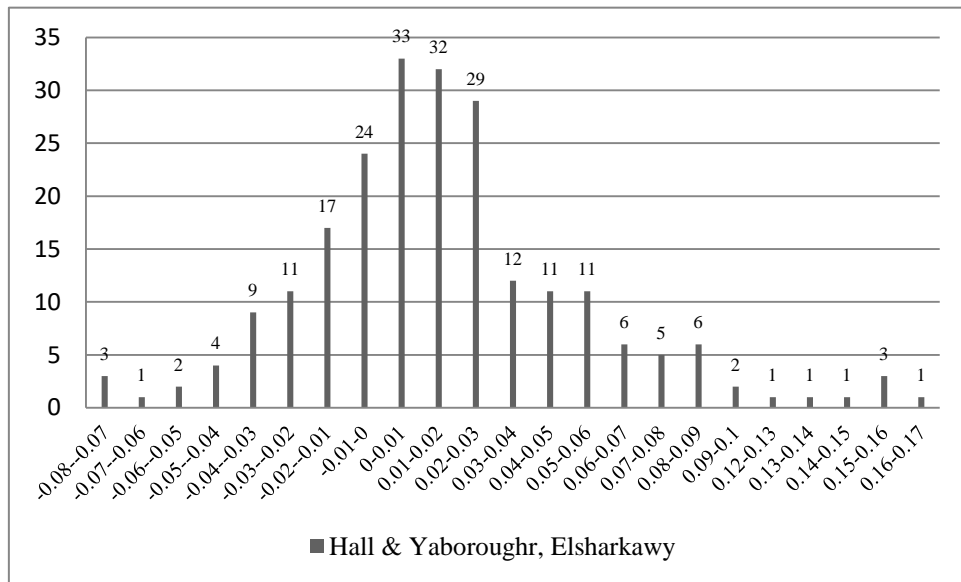


Figure 6.17 – MRD of the Hall and Yarborough, Elsharkawy combination

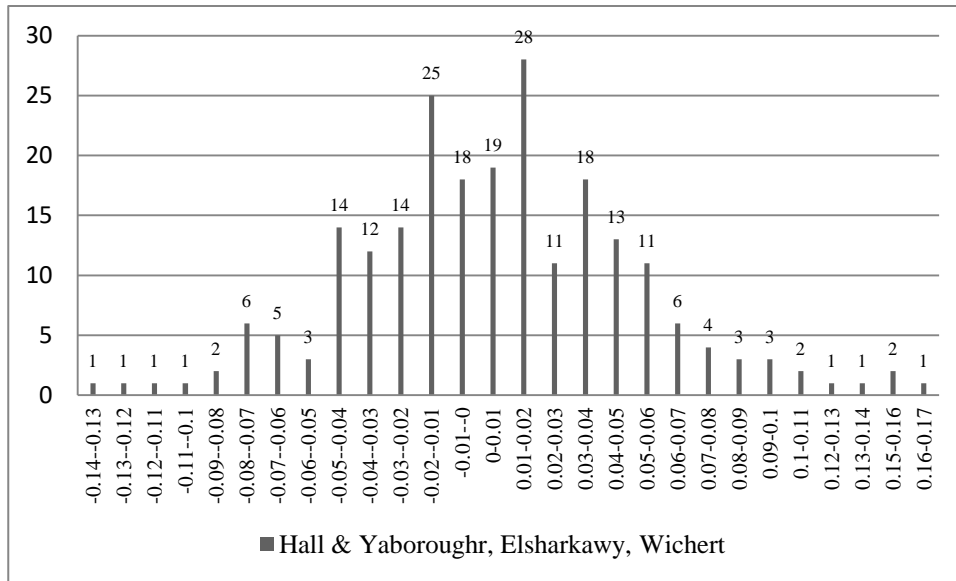


Figure 6.18 – MRD of the Hall and Yarborough, Elsharkawy, Wichert combination

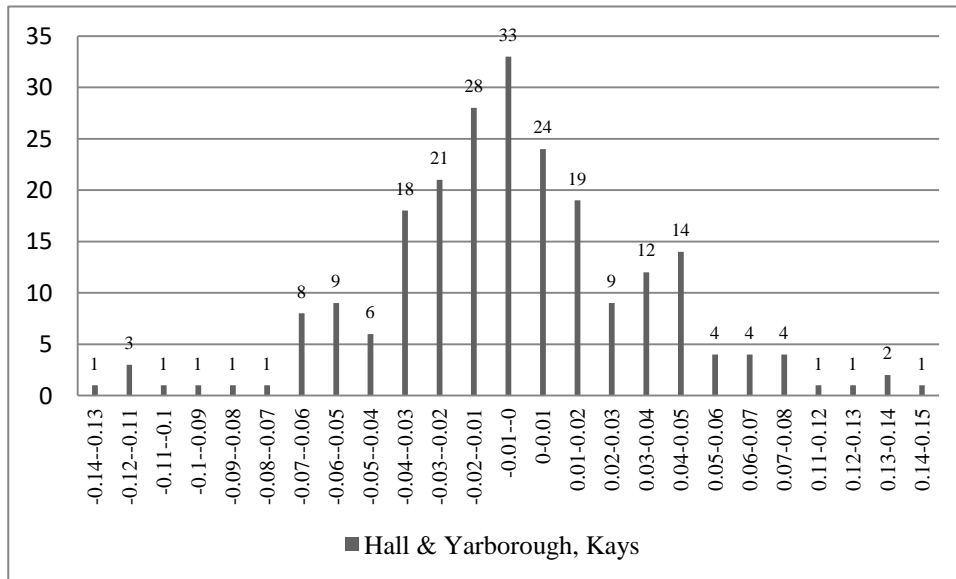


Figure 6.19 – MRD of the Hall and Yarborough, Kays combination

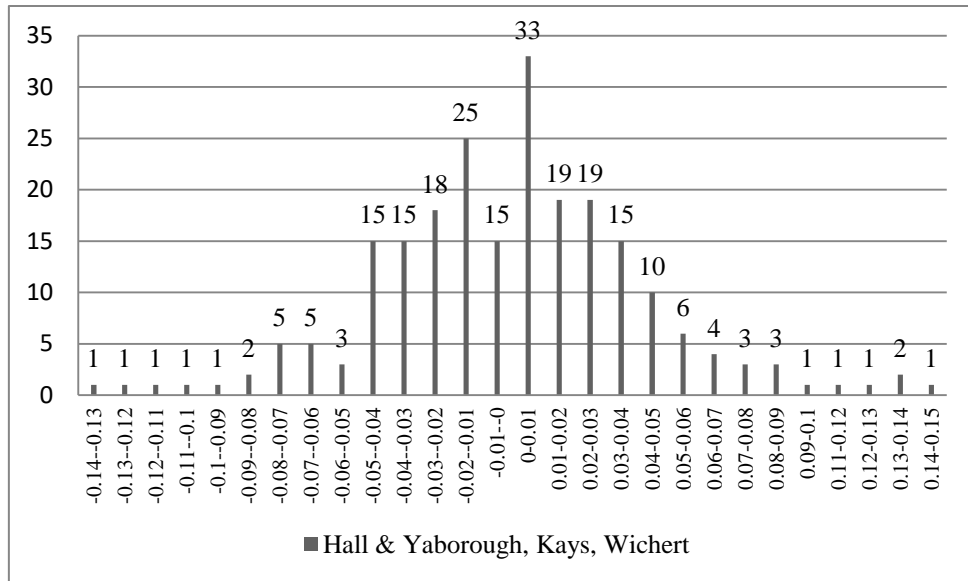


Figure 6.20 – MRD of the Hall and Yarborough, Kays, Wichert combination

Table 6.6: Statistical metrics for the different combinations (Hall and Yarborough)

Mixing Rule	Correction	Av. MAD	Av. MARD (%)	R ²
Kays	Yes	0.036	3.39	0.99468
Kays	No	0.034	3.16	0.99514
Elsharkawy	Yes	0.039	3.72	0.99113
Elsharkawy	No	0.033	3.15	0.99383

By examining Fig 6.17 to 6.20, 184 (81.42%) out of 224 gases have MRD of $\pm 5\%$ with the Hall and Yarborough, Kay’s combination, 184 (81.42%) out of 224 with the Hall and Yarborough, Kay’s, Wichert, 182 (80.89%) out of 225 with the Hall and Yarborough, Elsharkawy and 172 (76.11%) out of 226 with the Hall and Yarborough, Elsharkawy, Wichert combination.

6.2.2 Equation of State Results

The equation of state adopted by the present work was the PR EoS which is one of the most widely used in the petroleum industry. The Peneloux volume translation method was also implemented to identify if it leads to better accuracy results. Moreover,

nonzero binary interaction coefficient values that were discussed in section 4.6 were also incorporated to account for molecular forces.

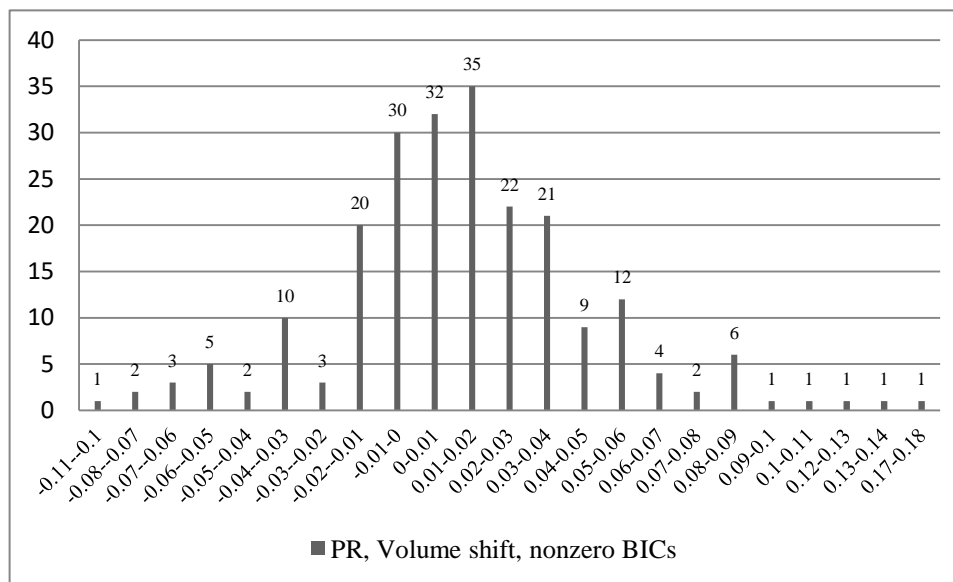


Figure 6.21 – MRD of the PR, Volume shift, nonzero BICs

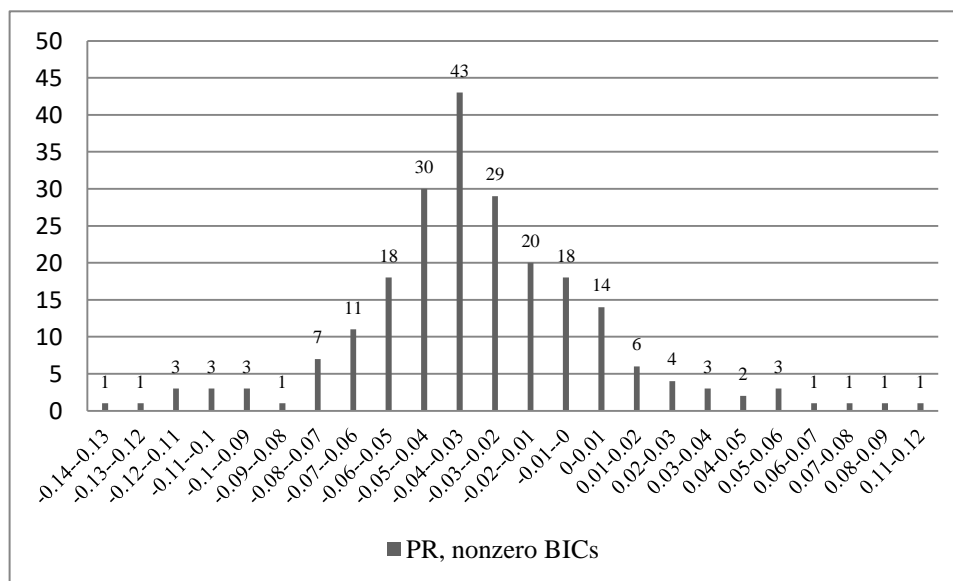


Figure 6.22 – MRD of the PR, nonzero BICs

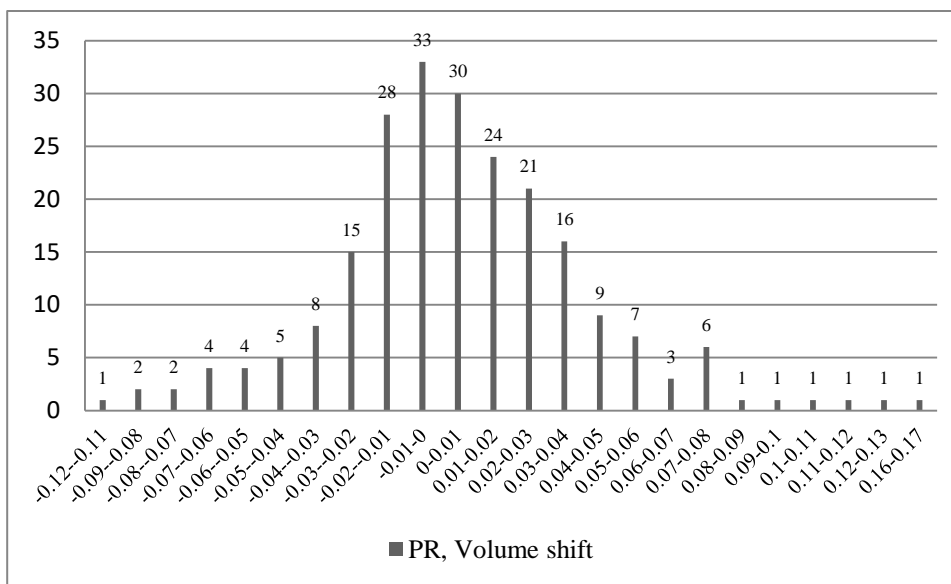


Figure 6.23 – MRD of the PR, Volume shift

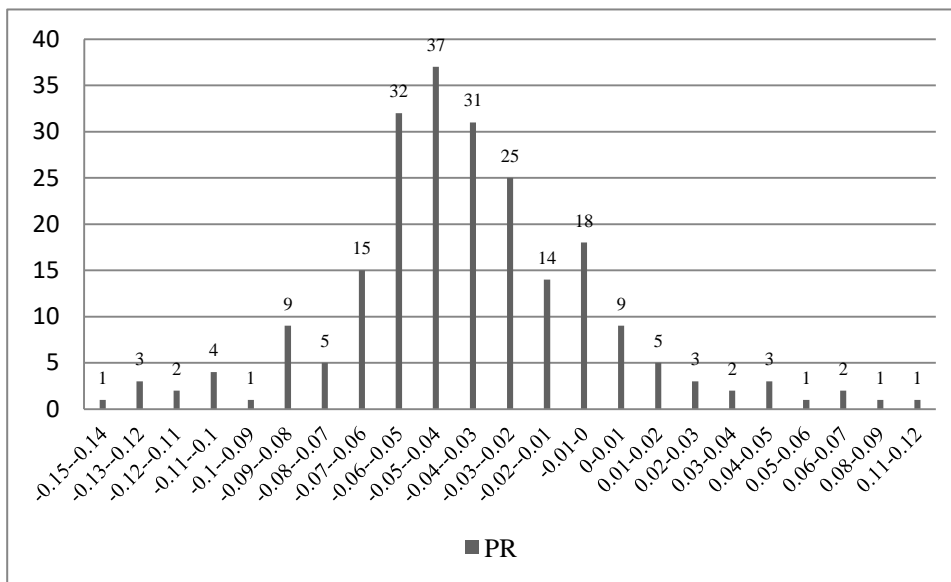


Figure 6.24 – MRD of the PR

By examining Fig 6.21 to 6.24, 189 (84.38%) out of 224 gases have MRD of $\pm 5\%$ with the PR EoS-Volume shift combination, 184 (82.14%) with the PR EoS-Volume

shift-non zero BICs, 169 (75.45%) with the PR EoS-non zero BICs and 147 (65.37%) with the PR EoS without Volume shift or the incorporation of nonzero BICs.

Table 6.7: Statistical metrics for the different combinations of the PR

EoS

Volume shift	Nonzero BICs	Av. MAD	Av. MARD (%)	R ²
No	No	0.048	4.37	0.98249
Yes	No	0.029	2.77	0.97192
No	Yes	0.042	3.86	0.98122
Yes	Yes	0.029	2.83	0.97145

6.2.3 Discussion

This section attempts to discuss particularities and special cases encountered during the calculations. A number of specific (approximately ten) natural gases of the database have been found to systematically have high values of MAD and MARD, regardless of the z factor computational method. These gases do not seem to share any common or similar properties and they are rather irrelevant with each other. Their deviations can therefore be attributed to errors occurred during the experimental measurement procedure. Table 6.8 reports the recorded MARD range for three of these gases.

Table 6.8: MARD range for gases with experimental error

Reference	Method	Min MARD (%)	Max MARD (%)
1	Azizi et al.	16.20	17.28
	Brill and Beggs	13.99	15.87
	Hall and Yarborough	16.15	17.15
	Heidaryan et al.	11.59	13.45
	Shell Oil Company	15.42	16.57
	PR EoS	12.22	17.56
2	Azizi et al.	25.19	28.74
	Brill and Beggs	23.08	26.25
	Hall and Yarborough	22.96	28.25
	Heidaryan et al.	22.71	27.92
	Shell Oil Company	12.30	17.23
	PR EoS	20.96	27.56
3	Azizi et al.	16.36	17.73
	Brill and Beggs	15.02	16.60
	Hall and Yarborough	16.40	17.78
	Heidaryan et al.	16.75	22.69

Shell Oil Company	17.45	19.69
PR EoS	12.00	16.73

Apart from the entries of the database which probably carry experimental error, in the vast majority of the considered natural gases all methods yield comparable results. In some other cases however, certain methods have been proven to be inconsistent in accurately predicting the experimental z factor curves of particular gases. The Heidaryan et al. correlation for instance fails to accurately describe the behavior of z factor in at least seven cases as shown in Table 6.9 below.

Table 6.9: MARD error of selected natural gases

Reference	Method	Min MARD (%)	Max MARD (%)
4	Azizi et al.	2.53	5.36
	Brill and Beggs	0.27	6.33
	Hall and Yarborough	2.55	9.12
	Heidaryan et al.	18.73	21.55
	Shell Oil Company	6.25	10.76
	PR EoS	1.12	3.24
5	Azizi et al.	4.66	5.87
	Brill and Beggs	6.86	8.09
	Hall and Yarborough	5.86	7.15
	Heidaryan et al.	18.61	21.54
	Shell Oil Company	7.05	8.62
	PR EoS	6.59	9.75
6	Azizi et al.	2.45	8.43
	Brill and Beggs	3.78	5.52
	Hall and Yarborough	3.56	6.16
	Heidaryan et al.	12.59	13.33
	Shell Oil Company	6.50	8.72
	PR EoS	1.83	2.32
7	Azizi et al.	3.30	5.70
	Brill and Beggs	5.34	7.47
	Hall and Yarborough	4.84	5.24
	Heidaryan et al.	12.27	14.61
	Shell Oil Company	7.82	9.13
	PR EoS	6.93	8.52
8	Azizi et al.	0.42	4.24
	Brill and Beggs	1.43	3.15
	Hall and Yarborough	4.08	4.12
	Heidaryan et al.	11.06	12.21
	Shell Oil Company	6.45	7.71
	PR EoS	2.78	6.46

9	Azizi et al.	1.47	4.29
	Brill and Beggs	4.19	7.68
	Hall and Yarborough	1.77	7.33
	Heidaryan et al.	12.06	15.78
	Shell Oil Company	7.52	8.72
	PR EoS	6.98	7.35
10	Azizi et al.	4.27	5.03
	Brill and Beggs	2.25	2.81
	Hall and Yarborough	3.48	4.99
	Heidaryan et al.	13.57	15.55
	Shell Oil Company	1.97	2.97
	PR EoS	1.16	4.00

All gases for which the Heidaryan et al. z factor correlation exhibits poor performance have a narrow range of reservoir temperature and pseudo-reduced temperature, $276\text{ }^{\circ}\text{F} < T_{res} < 289\text{ }^{\circ}\text{F}$ and $1.4 < T_{pr} < 1.7$ respectively, while the H_2S concentration is zero for all of them. Most importantly, nearly half of the pseudo-reduced pressures that were introduced into the correlation are greater than the upper limit of the correlation's application range ($P_{pr} \leq 15$) which is shown in Table 6.1.

Application ranges for the Shell Oil Company correlation have not been reported in Table 6.1 as they were not found in the literature. However, the correlation failed in a limited number of cases with the following characteristics: low H_2S content (from 0 to 0.5%), low N_2 content (from 0 to 0.7%), C_{7+} content from 12% to 14%, pseudo-reduced pressure in the range $11.5 \leq P_{pr} \leq 13.5$ and pseudo-reduced temperature in the range $1.31 \leq T_{pr} \leq 1.41$.

6.3 Conclusions

- The Peng-Robinson equation of state with the inclusion of the volume shift method had 189 cases exhibiting a maximum deviation of $\pm 5\%$ from the experimental values.
- Although the volume translation correction method is primarily being used for liquid EoS calculations, when implemented for gases it leads to increased accuracy compared to the utilization of nonzero binary interaction coefficients.

- The Azizi et al. correlation proved to be the most accurate empirical correlation among those examined in this study. Although it is a simple explicit in z formula it provides slightly better accuracy than the also explicit Brill and Beggs correlation and the implicit Hall and Yarborough which needs an iterative solution.
- A fair performance comparison between the PR EoS and the Azizi et al. correlation cannot be established due to their different application range.
- If the Azizi et al. correlation is to be used for the calculation of z factor then it is recommended to be combined to the mixing rule of Kay's instead of that of Elsharkawy. The correlation slightly underestimates z factor.
- If the Brill and Beggs correlation is to be implemented for the calculation of z factor then it is recommended to adopt the Elsharkawy mixing rule and not to apply the Wichert and Aziz correction.
- If the Hall and Yarborough correlation is implemented for the calculation of z factor then the Kay's mixing rule is suggested while the inclusion or not of the Wichert and Aziz correction does not affect accuracy.
- If the Shell Oil Company is to be implemented, the use of Elsharkawy mixing rule is recommended and the combination to the Wichert and Aziz correction is not.
- Databases containing experimental z factor data need to be subjected to detailed screening and quality control in order to be utilized for comparison of z factor calculation methods. Errors during the experimental process are common and lead to data corruption.
- The application range of each z factor computational method should be reviewed and respected in order to ensure accurate and reliable predictions as well as fair performance comparisons.
- There are numerous other z factor calculation methods (e.g. SVM, neural networks) which were not evaluated by the present work.

APPENDIX

Matlab code:

```
clear all
clc
format short e

% Composition which sums at unity
z_i_11 = importdata('Composition.txt') ;
z_i_1 = z_i_11.data ;
% Molecular Weight
MW1 = importdata('MolecularWeight.txt') ;
MW = MW1.data ;
% Molecular Weight of the Heavy End
MW_heavyend1 = importdata('MW_HeavyEnd.txt') ;
MW_heavyend = MW_heavyend1.data ;
% Density STO
Dens_STO1 = importdata('DensitySTO.txt') ;
Dens_STO = Dens_STO1.data ;
% Specific Gravity
SG = (1/1000) * Dens_STO ;

% Constants for the Calculation of Boiling Temperature (Tb)
a_bp = 6.77857 ;
b_bp = 0.401673 ;
c_bp = -1.58262 ;
d_bp = 0.00377409 ;
e_bp = 2.984036 ;
f_bp = -0.00425288 ;
% Boiling Temperature (Tb)
% Preallocation for Speed
Tb_R = zeros(1,size(z_i_1,1));

for i = 1 : size(z_i_1,1)
    Tb_R(i) = a_bp * (MW_heavyend(i)^b_bp) * (SG(i)^c_bp) *
    exp(d_bp*MW_heavyend(i)+e_bp*SG(i)+f_bp*MW_heavyend(i) * SG(i)) ;
end

% Lab Measurements
Plab_psia1 = importdata('PressureSteps.txt') ;
Plab_psia = Plab_psia1.data ;
Tlab_R1 = importdata('ResTemperatures.txt') ;
```

```

Tlab_R      = Tlab_R1.data      ;

% Critical Properties: non-HCs & HCs from C1 to C11 (Katz Table)
Tc_i      = [227.16 547.38 671.76 342.72 549.72 665.64 734.76 765.36 828.72
845.46 923.04 984.96 1036.08 1085.04 1128.06 1166.04 ] ;
Pc_i      = [492 1070 1297 667 708 616 529 551 492 489 483 453 419
383 351 325 ] ;

% Critical Properties: Heavy End
% Preallocation for Speed
Tcp        = zeros(1,size(z_i_1,1)) ;
a_Twu      = zeros(1,size(z_i_1,1)) ;
gama_P     = zeros(1,size(z_i_1,1)) ;
delta_gama_T = zeros(1,size(z_i_1,1)) ;
ef_T       = zeros(1,size(z_i_1,1)) ;
Tc_heavyend = zeros(1,size(z_i_1,1)) ;
delta_gama_P = zeros(1,size(z_i_1,1)) ;
ef_P       = zeros(1,size(z_i_1,1)) ;
Pcp        = zeros(1,size(z_i_1,1)) ;
delta_gama_V = zeros(1,size(z_i_1,1)) ;
ef_V       = zeros(1,size(z_i_1,1)) ;
Vcp        = zeros(1,size(z_i_1,1)) ;
Vcr        = zeros(1,size(z_i_1,1)) ;
Pc_heavyend = zeros(1,size(z_i_1,1)) ;
T_pc_Kays  = zeros(1,size(z_i_1,1)) ;
P_pc_Kays  = zeros(1,size(z_i_1,1)) ;
epsilon    = zeros(1,size(z_i_1,1)) ;
T_pc_Wichert = zeros(1,size(z_i_1,1)) ;
P_pc_Wichert = zeros(1,size(z_i_1,1)) ;

T_pr       = zeros(1,size(z_i_1,1)) ;
P_pr       = zeros(size(Plab_psia)) ;

A          = zeros(size(P_pr)) ;
B          = zeros(size(P_pr)) ;
C          = zeros(size(P_pr)) ;
D          = zeros(size(P_pr)) ;
E          = zeros(size(P_pr)) ;

z_factor   = zeros(size(P_pr)) ;

for i = 1 : size(z_i_1,1)
    % Critical Temperature of the Heavy End (Twu correlation)
    Tcp(i)      = Tb_R(i)*(0.533272 + (0.191017 * 0.001) * Tb_R(i) + (0.779681 *
0.0000001)*(Tb_R(i)^2) -(0.284376 * 0.000000001)*(Tb_R(i)^3) + 0.959468*100 /((0.01 *
Tb_R(i))^13))^-1 ;
    a_Twu(i)    = 1 - (Tb_R(i) / Tcp(i)) ;
    gama_P(i)   = 0.843593 - 0.128624 * a_Twu(i) - 3.36159 * (a_Twu(i)^3) - 13749.5 *
(a_Twu(i)^12) ;
    delta_gama_T(i) = exp(5*(gama_P(i) - SG(i))) - 1 ;
    ef_T(i)     = delta_gama_T(i) * (-0.362456 / (Tb_R(i)^0.5) + (0.0398285 - 0.948125 /
(Tb_R(i)^0.5)) * delta_gama_T(i) ) ;
    Tc_heavyend(i) = Tcp(i) * ((1 + 2 * ef_T(i)) / (1 - 2 * ef_T(i)))^2 ;
    % Critical Pressure of the Heavy End (Twu correlation)

```

```

delta_gama_P(i) = exp(0.5*(gama_P(i) - SG(i)))-1 ;
ef_P(i)         = delta_gama_P(i) * ((2.53262 - 46.1955 / ((Tb_R(i))^0.5) -0.00127885 *
Tb_R(i)) + (-11.4277 + (252.14 / (Tb_R(i))^0.5) + 0.00230535*Tb_R(i))*delta_gama_P(i)) ;
Pcp(i)         = (3.83354 + 1.19629 * (a_Twu(i)^0.5) + 34.8888 * a_Twu(i) + 36.1952 *
(a_Twu(i)^2) +104.193 * (a_Twu(i)^4))^2 ;
delta_gama_V(i) = exp(4*(gama_P(i)^2 - SG(i)^2)) - 1 ;
ef_V(i)         = delta_gama_V(i) * ((0.46659 / (Tb_R(i))^0.5)) + (-0.182421 +
3.01721/(Tb_R(i))^0.5) * delta_gama_V(i)) ;
Vcp(i)         = (1 - (0.419869 - 0.505839 * a_Twu(i) - 1.56436 * (a_Twu(i))^3 - 9481.7
* (a_Twu(i))^14)) ^(-8) ;
Vcr(i)         = Vcp(i) * ((1 + 2 * ef_V(i)) / (1 - 2 * ef_V(i)))^2 ;
Pc_heavyend(i) = (Pcp(i) *(Tc_heavyend(i) / Tcp(i)) *(Vcp(i) / Vcr(i))*((1 + 2 *
ef_P(i))/(1 - 2 * ef_P(i)))^2) ;

% Pseudo-criticals (Kay's mixing rule)
T_pc_Kays(i)   = z_i_1(i,[1:size(z_i_1,2)-1]) * transpose(Tc_i) +
z_i_1(i,size(z_i_1,2))* Tc_heavyend(i) ; % Rankine
P_pc_Kays(i)   = z_i_1(i,[1:size(z_i_1,2)-1]) * transpose(Pc_i) +
z_i_1(i,size(z_i_1,2))* Pc_heavyend(i) ; % psia

% Wichert & Aziz Correction
epsilon(i)     = 120 * ((z_i_1(i,2) + z_i_1(i,3))^0.9-(z_i_1(i,2) + z_i_1(i,3))^1.6 +
15*((z_i_1(i,3))^0.5-(z_i_1(i,3))^4)) ;
T_pc_wichert(i) = T_pc_Kays(i) - epsilon(i) ;
P_pc_wichert(i) = (P_pc_Kays(i) * T_pc_wichert(i)) / (T_pc_Kays(i) + z_i_1(i,3) * (1 -
z_i_1(i,3)) * epsilon(i)) ;

% Pseudo-reduced Properties
T_pr(i) = Tlab_R(i) ./ T_pc_wichert(i) ;

for j = 1 : size(Plab_psia,2)
    P_pr(i,j) = Plab_psia(i,j) / P_pc_wichert(i) ;

% Azizi, Behbahani, Isadebeh Correlation for z factor calculation
% Parameters
a_ABI = 0.0373142485385592 ;
b_ABI = -0.0140807151485369 ;
c_ABI = 0.0163263245387186 ;
d_ABI = -0.0307776478819813 ;
e_ABI = 13843575480.9438 ;
f_ABI = -16799138540.7637 ;
g_ABI = 1624178942.64976 ;
h_ABI = 13702270281.0869 ;
i_ABI = -41645509.8964746 ;
j_ABI = 237249967625.013 ;
k_ABI = -24449114791.1531 ;
l_ABI = 19357955749.3274 ;
m_ABI = -126354717916.607 ;
n_ABI = 623705678.385784 ;
o_ABI = 17997651104.333 ;
p_ABI = 151211393445.064 ;
q_ABI = 139474437997.172 ;

```

```

r_ABI = -24233012984.095 ;
s_ABI = 18938047327.5205 ;
t_ABI = -141401620722.689 ;

A(i,j) = a_ABI * (T_pr(i)^2.16) + b_ABI * (P_pr(i,j)^1.028) + c_ABI * (P_pr(i,j)^1.58) *
(T_pr(i)^-2.1) + d_ABI * log(T_pr(i))^(-0.5) ;
B(i,j) = e_ABI + f_ABI * (T_pr(i)^2.4) + g_ABI * (P_pr(i,j)^1.56) + h_ABI *
(P_pr(i,j)^0.124) * (T_pr(i)^3.033) ;
C(i,j) = i_ABI * log(T_pr(i))^(-1.28) + j_ABI * log(T_pr(i))^(1.37) + k_ABI *
log(P_pr(i,j)) + l_ABI * log(P_pr(i,j))^2 + m_ABI * log(P_pr(i,j)) * log(T_pr(i)) ;
D(i,j) = 1 + n_ABI * (T_pr(i)^5.55) + o_ABI * (P_pr(i,j)^0.68) * (T_pr(i)^0.33) ;
E(i,j) = p_ABI * log(T_pr(i))^1.18 + q_ABI * log(T_pr(i))^2.1 + r_ABI * log(P_pr(i,j)) +
s_ABI * log(P_pr(i,j))^2 + t_ABI * log(P_pr(i,j)) * log(T_pr(i)) ;

z_factor(i,j) = A(i,j) + ((B(i,j) + C(i,j))/(D(i,j) + E(i,j))) ;
end
end

% Cell
h={'Pmin' 'step1' 'step2' 'step3' 'step4' 'step5' 'step6' 'step7' 'step8' 'step9'
'Pmax'} ;
% Add pressure steps labels
z_factor_Table = [h;num2cell(z_factor)] ;

```

[Published with MATLAB® R2017a](#)

```

clear all
clc
format short e

% Composition which sums at unity
z_i_11 = importdata('Composition.txt') ;
z_i_1 = z_i_11.data ;
% Molecular weight
MW1 = importdata('MolecularWeight.txt') ;
MW = MW1.data ;
% Molecular weight of the Heavy End
MW_heavyend1 = importdata('MW_HeavyEnd.txt') ;
MW_heavyend = MW_heavyend1.data ;
% Density STO
Dens_STO1 = importdata('DensitySTO.txt') ;
Dens_STO = Dens_STO1.data ;
% Specific Gravity
SG = (1/1000) * Dens_STO ;

% Constants for the calculation of Boiling Temperature (Tb)
a_bp = 6.77857 ;
b_bp = 0.401673 ;
c_bp = -1.58262 ;
d_bp = 0.00377409 ;

```

```

e_bp = 2.984036 ;
f_bp = -0.00425288 ;
% Boiling Temperature (Tb)
% Preallocation for Speed
Tb_R = zeros(1,size(z_i_1,1));

for i = 1 : size(z_i_1,1)
    Tb_R(i) = a_bp * (MW_heavyend(i)^b_bp) * (SG(i)^c_bp) *
exp(d_bp*MW_heavyend(i)+e_bp*SG(i)+f_bp*MW_heavyend(i) * SG(i)) ;
end

% Lab Measurements
Plab_psia1 = importdata('PressureSteps.txt') ;
Plab_psia = Plab_psia1.data ;
Tlab_R1 = importdata('ResTemperatures.txt') ;
Tlab_R = Tlab_R1.data ;

% Critical Properties: non-HCs & HCs from C1 to C11 (Katz Table)
TC_i = [227.16 547.38 671.76 342.72 549.72 665.64 734.76 765.36 828.72
845.46 923.04 984.96 1036.08 1085.04 1128.06 1166.04 ] ;
PC_i = [492 1070 1297 667 708 616 529 551 492 489 483 453 419
383 351 325 ] ;
% Critical Properties: Heavy End
% Preallocation for Speed
TcP = zeros(1,size(z_i_1,1)) ;
a_Twu = zeros(1,size(z_i_1,1)) ;
gama_P = zeros(1,size(z_i_1,1)) ;
delta_gama_T = zeros(1,size(z_i_1,1)) ;
ef_T = zeros(1,size(z_i_1,1)) ;
Tc_heavyend = zeros(1,size(z_i_1,1)) ;
delta_gama_P = zeros(1,size(z_i_1,1)) ;
ef_P = zeros(1,size(z_i_1,1)) ;
Pcp = zeros(1,size(z_i_1,1)) ;
delta_gama_V = zeros(1,size(z_i_1,1)) ;
ef_V = zeros(1,size(z_i_1,1)) ;
Vcp = zeros(1,size(z_i_1,1)) ;
Vcr = zeros(1,size(z_i_1,1)) ;
PC_heavyend = zeros(1,size(z_i_1,1)) ;
T_pc_Kays = zeros(1,size(z_i_1,1)) ;
P_pc_Kays = zeros(1,size(z_i_1,1)) ;
epsilon = zeros(1,size(z_i_1,1)) ;
T_pc_wichert = zeros(1,size(z_i_1,1)) ;
P_pc_wichert = zeros(1,size(z_i_1,1)) ;

T_pr = zeros(1,size(z_i_1,1)) ;
P_pr = zeros(size(Plab_psia)) ;

A = zeros(size(P_pr)) ;
B = zeros(size(Plab_psia)) ;
C = zeros(size(P_pr)) ;
D = zeros(size(P_pr)) ;

z_factor = zeros(size(P_pr)) ;

```

```

for i = 1 : size(z_i_1,1)
    % Critical Temperature of the Heavy End (Twu correlation)
    Tc_p(i) = Tb_R(i)*(0.533272 + (0.191017 * 0.001) * Tb_R(i) + (0.779681 *
    0.0000001)*(Tb_R(i)^2) -(0.284376 * 0.0000000001)*(Tb_R(i)^3) + 0.959468*100 /((0.01 *
    Tb_R(i))^13))^(-1) ;
    a_Twu(i) = 1 - (Tb_R(i) / Tc_p(i)) ;
    gama_P(i) = 0.843593 - 0.128624 * a_Twu(i) - 3.36159 * (a_Twu(i)^3) - 13749.5 *
    (a_Twu(i)^12) ;
    delta_gama_T(i) = exp(5*(gama_P(i) - SG(i))) - 1 ;
    ef_T(i) = delta_gama_T(i) * (-0.362456 / (Tb_R(i)^0.5) + (0.0398285 - 0.948125 /
    (Tb_R(i)^0.5)) * delta_gama_T(i) ) ;
    Tc_heavyend(i) = Tc_p(i) * ((1 + 2 * ef_T(i)) / (1 - 2 * ef_T(i)))^2 ;
    % Critical Pressure of the Heavy End (Twu correlation)
    delta_gama_P(i) = exp(0.5*(gama_P(i) - SG(i))) - 1 ;
    ef_P(i) = delta_gama_P(i) * ((2.53262 - 46.1955 / ((Tb_R(i))^0.5) - 0.00127885 *
    Tb_R(i) + (-11.4277 + (252.14 / (Tb_R(i))^0.5) + 0.00230535*Tb_R(i))*delta_gama_P(i)) ;
    Pcp(i) = (3.83354 + 1.19629 * (a_Twu(i)^0.5) + 34.8888 * a_Twu(i) + 36.1952 *
    (a_Twu(i)^2) + 104.193 * (a_Twu(i)^4))^2 ;
    delta_gama_V(i) = exp(4*(gama_P(i)^2 - SG(i)^2)) - 1 ;
    ef_V(i) = delta_gama_V(i) * ((0.46659 / (Tb_R(i)^0.5) + (-0.182421 +
    3.01721/(Tb_R(i)^0.5)) * delta_gama_V(i)) ;
    Vcp(i) = (1 - (0.419869 - 0.505839 * a_Twu(i) - 1.56436 * (a_Twu(i))^3 - 9481.7
    * (a_Twu(i))^14)) ^(-8) ;
    Vcr(i) = Vcp(i) * ((1 + 2 * ef_V(i)) / (1 - 2 * ef_V(i)))^2 ;
    Pc_heavyend(i) = (Pcp(i) *(Tc_heavyend(i) / Tc_p(i)) *(Vcp(i) / Vcr(i))*((1 + 2 *
    ef_P(i))/(1 - 2 * ef_P(i)))^2) ;

    % Pseudo-criticals (Kay's mixing rule)
    T_pc_Kays(i) = z_i_1(i,[1:size(z_i_1,2)-1]) * transpose(Tc_i) +
    z_i_1(i,size(z_i_1,2))* Tc_heavyend(i) ; % Rankine
    P_pc_Kays(i) = z_i_1(i,[1:size(z_i_1,2)-1]) * transpose(Pc_i) +
    z_i_1(i,size(z_i_1,2))* Pc_heavyend(i) ; % psia

    % Wichert & Aziz Correction
    epsilon(i) = 120 * ((z_i_1(i,2) + z_i_1(i,3))^0.9 - (z_i_1(i,2) + z_i_1(i,3))^1.6 +
    15*((z_i_1(i,3))^0.5 - (z_i_1(i,3))^4)) ;
    T_pc_Wichert(i) = T_pc_Kays(i) - epsilon(i) ;
    P_pc_Wichert(i) = (P_pc_Kays(i) * T_pc_Wichert(i)) / (T_pc_Kays(i) + z_i_1(i,3) * (1 -
    z_i_1(i,3)) * epsilon(i)) ;

    % Pseudo-reduced Properties
    T_pr(i) = Tlab_R(i) ./ T_pc_Wichert(i) ;

    % Brill and Beggs Correlation for z factor calculation
    A(i) = 1.39 * ((T_pr(i) - 0.92)^(0.5)) - 0.36 * T_pr(i) - 0.101 ;
    C(i) = 0.132 - 0.32 * log10(T_pr(i)) ;
    D(i) = 10^(0.3106 - 0.49 * T_pr(i) + 0.1824 * T_pr(i)^2) ;

    for j = 1 : size(Plab_psia,2)
        P_pr(i,j) = Plab_psia(i,j) / P_pc_Wichert(i) ;

        B(i,j) = (0.62 - 0.23 * T_pr(i)) * P_pr(i,j) + ((0.066 / (T_pr(i) - 0.86)) - 0.037) *

```

```

(P_pr(i,j)^2) + (0.32 / (10000000000 * (T_pr(i)-1))) * (P_pr(i,j)^6) ;

z_factor(i,j) = A(i) + (1 - A(i)) * exp(-B(i,j)) + C(i) * P_pr(i,j)^D(i) ;
end
end

% Cell
h={'Pmin' 'step1' 'step2' 'step3' 'step4' 'step5' 'step6' 'step7' 'step8' 'step9'
'Pmax'} ;
% Add pressure steps labels
z_factor_Table = [h;num2cell(z_factor)] ;

```

Published with MATLAB® R2017a

```

clear all
clc
format short e

% Composition which sums at unity
z_i_11 = importdata('Composition.txt') ;
z_i_1 = z_i_11.data ;
% Molecular weight
MW1 = importdata('MolecularWeight.txt') ;
MW = MW1.data ;
% Molecular weight of the Heavy End
MW_heavyend1 = importdata('MW_HeavyEnd.txt') ;
MW_heavyend = MW_heavyend1.data ;
% Density STO
Dens_STO1 = importdata('DensitySTO.txt') ;
Dens_STO = Dens_STO1.data ;
% Specific Gravity
SG = (1/1000) * Dens_STO ;

% Constants for the calculation of Boiling Temperature (Tb)
a_bp = 6.77857 ;
b_bp = 0.401673 ;
c_bp = -1.58262 ;
d_bp = 0.00377409 ;
e_bp = 2.984036 ;
f_bp = -0.00425288 ;
% Boiling Temperature (Tb)
% Preallocation for Speed
Tb_R = zeros(1,size(z_i_1,1));

for i = 1 : size(z_i_1,1)
    Tb_R(i) = a_bp * (MW_heavyend(i)^b_bp) * (SG(i)^c_bp) *
exp(d_bp*MW_heavyend(i)+e_bp*SG(i)+f_bp*MW_heavyend(i) * SG(i)) ;
end

% Lab Measurements

```

```

Plab_psi1 = importdata('PressureSteps.txt') ;
Plab_psia = Plab_psi1.data ;
Tlab_R1 = importdata('ResTemperatures.txt') ;
Tlab_R = Tlab_R1.data ;

% Critical Properties: non-HCs & HCs from C1 to C11 (Katz Table)
Tc_i = [227.16 547.38 671.76 342.72 549.72 665.64 734.76 765.36 828.72
845.46 923.04 984.96 1036.08 1085.04 1128.06 1166.04 ] ;
Pc_i = [492 1070 1297 667 708 616 529 551 492 489 483 453 419
383 351 325 ] ;

% Critical Properties: Heavy End
% Preallocation for Speed
Tcp = zeros(1,size(z_i_1,1)) ;
a_Twu = zeros(1,size(z_i_1,1)) ;
gama_P = zeros(1,size(z_i_1,1)) ;
delta_gama_T = zeros(1,size(z_i_1,1)) ;
ef_T = zeros(1,size(z_i_1,1)) ;
Tc_heavyend = zeros(1,size(z_i_1,1)) ;
delta_gama_P = zeros(1,size(z_i_1,1)) ;
ef_P = zeros(1,size(z_i_1,1)) ;
Pcp = zeros(1,size(z_i_1,1)) ;
delta_gama_V = zeros(1,size(z_i_1,1)) ;
ef_V = zeros(1,size(z_i_1,1)) ;
Vcp = zeros(1,size(z_i_1,1)) ;
Vcr = zeros(1,size(z_i_1,1)) ;
Pc_heavyend = zeros(1,size(z_i_1,1)) ;
T_pc_Kays = zeros(1,size(z_i_1,1)) ;
P_pc_Kays = zeros(1,size(z_i_1,1)) ;
epsilon = zeros(1,size(z_i_1,1)) ;
T_pc_Wichert = zeros(1,size(z_i_1,1)) ;
P_pc_Wichert = zeros(1,size(z_i_1,1)) ;

T_pr = zeros(1,size(z_i_1,1)) ;
P_pr = zeros(size(Plab_psia)) ;

t_HY = zeros(1,size(z_i_1,1)) ;
a_HY = zeros(1,size(z_i_1,1)) ;

maxIter = 10 ;

F = zeros(size(P_pr,1),size(P_pr,2),maxIter) ;
F_prime = zeros(size(P_pr,1),size(P_pr,2),maxIter) ;
z_factor = zeros(size(P_pr)) ;

% Loop of Fluids
for i = 1 : size(z_i_1,1)
    % Critical Temperature of the Heavy End (Twu correlation)
    Tcp(i) = Tb_R(i)*(0.533272 + (0.191017 * 0.001) * Tb_R(i) + (0.779681 *
0.0000001)*(Tb_R(i)^2) - (0.284376 * 0.0000000001)*(Tb_R(i)^3) + 0.959468*100 /((0.01 *
Tb_R(i))^13))^(-1) ;
    a_Twu(i) = 1 - (Tb_R(i) / Tcp(i)) ;
    gama_P(i) = 0.843593 - 0.128624 * a_Twu(i) - 3.36159 * (a_Twu(i)^3) - 13749.5 *
(a_Twu(i)^12) ;

```

```

delta_gama_T(i) = exp(5*(gama_P(i) - SG(i))) - 1 ;
ef_T(i)         = delta_gama_T(i) * (-0.362456 / (Tb_R(i)^0.5) + (0.0398285 - 0.948125 /
(Tb_R(i)^0.5)) * delta_gama_T(i) ) ;
Tc_heavyend(i) = Tc_p(i) * ((1 + 2 * ef_T(i)) / (1 - 2 * ef_T(i)))^2 ;
    % Critical Pressure of the Heavy End (Twu correlation)
delta_gama_P(i) = exp(0.5*(gama_P(i) - SG(i)))-1 ;
ef_P(i)         = delta_gama_P(i) * ((2.53262 - 46.1955 / ((Tb_R(i))^0.5) -0.00127885 *
Tb_R(i)) + (-11.4277 + (252.14 / (Tb_R(i))^0.5) + 0.00230535*Tb_R(i))*delta_gama_P(i)) ;
Pcp(i)          = (3.83354 + 1.19629 * (a_Twu(i)^0.5) + 34.8888 * a_Twu(i) + 36.1952 *
(a_Twu(i)^2) +104.193 * (a_Twu(i)^4))^2 ;
delta_gama_V(i) = exp(4*(gama_P(i)^2 - SG(i)^2)) - 1 ;
ef_V(i)         = delta_gama_V(i) * ((0.46659 / (Tb_R(i)^0.5)) + (-0.182421 +
3.01721/(Tb_R(i)^0.5)) * delta_gama_V(i)) ;
Vcp(i)          = (1 - (0.419869 - 0.505839 * a_Twu(i) - 1.56436 * (a_Twu(i))^3 - 9481.7
* (a_Twu(i))^14)) ^(-8) ;
Vcr(i)          = Vcp(i) * ((1 + 2 * ef_V(i)) / (1 - 2 * ef_V(i)))^2 ;
Pc_heavyend(i) = (Pcp(i) * (Tc_heavyend(i) / Tc_p(i)) * (Vcp(i) / Vcr(i)) * ((1 + 2 *
ef_P(i))/(1 - 2 * ef_P(i)))^2) ;

% Pseudo-criticals (Kay's mixing rule)
T_pc_Kays(i)    = z_i_1(i,[1:size(z_i_1,2)-1]) * transpose(Tc_i) +
z_i_1(i,size(z_i_1,2))* Tc_heavyend(i) ; % Rankine
P_pc_Kays(i)    = z_i_1(i,[1:size(z_i_1,2)-1]) * transpose(Pc_i) +
z_i_1(i,size(z_i_1,2))* Pc_heavyend(i) ; % psia

% Wichert & Aziz Correction
epsilon(i)      = 120 * ((z_i_1(i,2) + z_i_1(i,3))^0.9-(z_i_1(i,2) + z_i_1(i,3))^1.6 +
15*((z_i_1(i,3))^0.5-(z_i_1(i,3))^4)) ;
T_pc_wichert(i) = T_pc_Kays(i) - epsilon(i) ;
P_pc_wichert(i) = (P_pc_Kays(i) * T_pc_wichert(i)) / (T_pc_Kays(i) + z_i_1(i,3) * (1 -
z_i_1(i,3)) * epsilon(i)) ;

% Pseudo-reduced Properties
T_pr(i) = Tlab_R(i) ./ T_pc_wichert(i) ;

% Hall and Yarborough Correlation for z factor calculation
% Parameters
t_HY(i) = 1 / T_pr(i) ;
a_HY(i) = 0.06125 * t_HY(i) * exp(-1.2 * (1-t_HY(i))^2) ;

% Loop of Pressure-steps
for j = 1 : size(Plab_psia,2)
    P_pr(i,j) = Plab_psia(i,j) / P_pc_wichert(i) ;

y0 = 0.001 ;
y_est = y0 ;
y_old = y0 ;

% Loop of NR
for k = 1 : maxIter
    F(i,j,k) = - a_HY(i) * P_pr(i,j) + ((y_est + y_est^2 + y_est^3 - y_est^4) /
((1-y_est)^3)) - (14.76 * t_HY(i) - 9.76 * t_HY(i)^2 + 4.58 * t_HY(i)^3) * (y_est^2) +
(90.7 * t_HY(i) - 242.2 * t_HY(i)^2 + 42.4 * t_HY(i)^3) * (y_est^(2.18 + 2.82 *

```

```

t_HY(i));
    F_prime(i,j,k) = ((1 + 4 * y_est + 4 * y_est^2 - 4 * y_est^3 + y_est^4)/(1 -
y_est)^4) - (29.52 * t_HY(i) - 19.52 * t_HY(i)^2 + 9.16 * t_HY(i)^3) * y_est + (2.18 +
2.82 * t_HY(i)) * (90.7 * t_HY(i) - 242.2 * t_HY(i)^2 + 42.4 * t_HY(i)^3) * (y_est^(1.18
+ 2.82 * t_HY(i)));

    y_est = y_est - F(i,j,k) / F_prime(i,j,k) ;
    y_old = y_est ;
end

z_factor(i,j) = (a_HY(i) * P_pr(i,j)) / y_est ;

end
end

% Cell
h={'Pmin' 'step1' 'step2' 'step3' 'step4' 'step5' 'step6' 'step7' 'step8' 'step9'
'Pmax'} ;
% Add pressure steps labels
z_factor_Table = [h;num2cell(z_factor)] ;

```

[Published with MATLAB® R2017a](#)

```

clear all
clc
format short e

% Composition which sums at unity
z_i_11 = importdata('Composition.txt') ;
z_i_1 = z_i_11.data ;
% Molecular weight
MW1 = importdata('MolecularWeight.txt') ;
MW = MW1.data ;
% Molecular weight of the Heavy End
MW_heavyend1 = importdata('MW_HeavyEnd.txt') ;
MW_heavyend = MW_heavyend1.data ;
% Density STO
Dens_STO1 = importdata('DensitySTO.txt') ;
Dens_STO = Dens_STO1.data ;
% Specific Gravity
SG = (1/1000) * Dens_STO ;

% Constants for the calculation of Boiling Temperature (Tb)
a_bp = 6.77857 ;
b_bp = 0.401673 ;
c_bp = -1.58262 ;
d_bp = 0.00377409 ;
e_bp = 2.984036 ;
f_bp = -0.00425288 ;
% Boiling Temperature (Tb)
% Preallocation for Speed

```

```

Tb_R = zeros(1,size(z_i_1,1));

for i = 1 : size(z_i_1,1)
    Tb_R(i) = a_bp * (MW_heavyend(i)^b_bp) * (SG(i)^c_bp) *
exp(d_bp*MW_heavyend(i)+e_bp*SG(i)+f_bp*MW_heavyend(i) * SG(i)) ;
end

% Lab Measurements
Plab_psi_a1 = importdata('PressureSteps.txt') ;
Plab_psi_a = Plab_psi_a1.data ;
Tlab_R1 = importdata('ResTemperatures.txt') ;
Tlab_R = Tlab_R1.data ;

% Critical Properties: non-HCs & HCs from C1 to C11 (Katz Table)
Tc_i = [227.16 547.38 671.76 342.72 549.72 665.64 734.76 765.36 828.72
845.46 923.04 984.96 1036.08 1085.04 1128.06 1166.04 ] ;
Pc_i = [492 1070 1297 667 708 616 529 551 492 489 483 453 419
383 351 325 ] ;

% Critical Properties: Heavy End
% Preallocation for Speed
Tcp = zeros(1,size(z_i_1,1)) ;
a_Twu = zeros(1,size(z_i_1,1)) ;
gama_P = zeros(1,size(z_i_1,1)) ;
delta_gama_T = zeros(1,size(z_i_1,1)) ;
ef_T = zeros(1,size(z_i_1,1)) ;
Tc_heavyend = zeros(1,size(z_i_1,1)) ;
delta_gama_P = zeros(1,size(z_i_1,1)) ;
ef_P = zeros(1,size(z_i_1,1)) ;
Pcp = zeros(1,size(z_i_1,1)) ;
delta_gama_V = zeros(1,size(z_i_1,1)) ;
ef_V = zeros(1,size(z_i_1,1)) ;
Vcp = zeros(1,size(z_i_1,1)) ;
Vcr = zeros(1,size(z_i_1,1)) ;
Pc_heavyend = zeros(1,size(z_i_1,1)) ;
T_pc_Kays = zeros(1,size(z_i_1,1)) ;
P_pc_Kays = zeros(1,size(z_i_1,1)) ;
epsilon = zeros(1,size(z_i_1,1)) ;
T_pc_wichert = zeros(1,size(z_i_1,1)) ;
P_pc_wichert = zeros(1,size(z_i_1,1)) ;

T_pr = zeros(1,size(z_i_1,1)) ;
P_pr = zeros(size(Plab_psi_a)) ;

nom = zeros(size(P_pr)) ;
denom = zeros(size(P_pr)) ;

z_factor = zeros(size(P_pr)) ;

for i = 1 : size(z_i_1,1)
    % Critical Temperature of the Heavy End (Twu correlation)
    Tcp(i) = Tb_R(i)*(0.533272 + (0.191017 * 0.001) * Tb_R(i) + (0.779681 *
0.0000001)*(Tb_R(i)^2) -(0.284376 * 0.0000000001)*(Tb_R(i)^3) + 0.959468*100 /((0.01 *
Tb_R(i))^13))^(-1) ;

```

```

a_Twu(i)      = 1 - (Tb_R(i) / Tcp(i)) ;
gama_P(i)     = 0.843593 - 0.128624 * a_Twu(i) - 3.36159 * (a_Twu(i)^3) - 13749.5 *
(a_Twu(i)^12) ;
delta_gama_T(i) = exp(5*(gama_P(i) - SG(i))) - 1 ;
ef_T(i)       = delta_gama_T(i) * (-0.362456 / (Tb_R(i)^0.5) + (0.0398285 - 0.948125 /
(Tb_R(i)^0.5)) * delta_gama_T(i)) ;
Tc_heavyend(i) = Tcp(i) * ((1 + 2 * ef_T(i)) / (1 - 2 * ef_T(i)))^2 ;
    % Critical Pressure of the Heavy End (Twu correlation)
delta_gama_P(i) = exp(0.5*(gama_P(i) - SG(i))) - 1 ;
ef_P(i)        = delta_gama_P(i) * ((2.53262 - 46.1955 / ((Tb_R(i))^0.5) - 0.00127885 *
Tb_R(i)) + (-11.4277 + (252.14 / (Tb_R(i))^0.5) + 0.00230535*Tb_R(i))*delta_gama_P(i)) ;
Pcp(i)        = (3.83354 + 1.19629 * (a_Twu(i)^0.5) + 34.8888 * a_Twu(i) + 36.1952 *
(a_Twu(i)^2) + 104.193 * (a_Twu(i)^4))^2 ;
delta_gama_V(i) = exp(4*(gama_P(i)^2 - SG(i)^2)) - 1 ;
ef_V(i)       = delta_gama_V(i) * ((0.46659 / (Tb_R(i)^0.5)) + (-0.182421 +
3.01721/(Tb_R(i)^0.5)) * delta_gama_V(i)) ;
Vcp(i)        = (1 - (0.419869 - 0.505839 * a_Twu(i) - 1.56436 * (a_Twu(i))^3 - 9481.7
* (a_Twu(i))^14)) ^(-8) ;
Vcr(i)        = Vcp(i) * ((1 + 2 * ef_V(i)) / (1 - 2 * ef_V(i)))^2 ;
Pc_heavyend(i) = (Pcp(i) * (Tc_heavyend(i) / Tcp(i)) * (Vcp(i) / Vcr(i)) * ((1 + 2 *
ef_P(i)) / (1 - 2 * ef_P(i))))^2 ;

% Pseudo-criticals (Kay's mixing rule)
T_pc_Kays(i)  = z_i_1(i,[1:size(z_i_1,2)-1]) * transpose(Tc_i) +
z_i_1(i,size(z_i_1,2))* Tc_heavyend(i) ; % Rankine
P_pc_Kays(i)  = z_i_1(i,[1:size(z_i_1,2)-1]) * transpose(Pc_i) +
z_i_1(i,size(z_i_1,2))* Pc_heavyend(i) ; % psia

% Wichert & Aziz Correction
epsilon(i)    = 120 * ((z_i_1(i,2) + z_i_1(i,3))^0.9 - (z_i_1(i,2) + z_i_1(i,3))^1.6 +
15*((z_i_1(i,3))^0.5 - (z_i_1(i,3))^4)) ;
T_pc_Wichert(i) = T_pc_Kays(i) - epsilon(i) ;
P_pc_Wichert(i) = (P_pc_Kays(i) * T_pc_Wichert(i)) / (T_pc_Kays(i) + z_i_1(i,3) * (1 -
z_i_1(i,3)) * epsilon(i)) ;

% Pseudo-reduced Properties
T_pr(i) = Tlab_R(i) ./ T_pc_Wichert(i) ;

% Heydaryan et al Correlation for z factor calculation
% Parameters
A1_heid = 3.252838 ;
A2_heid = -0.1306424 ;
A3_heid = -0.6449194 ;
A4_heid = -1.518028 ;
A5_heid = -5.391019 ;
A6_heid = -0.01379588 ;
A7_heid = 0.06600633 ;
A8_heid = 0.6120783 ;
A9_heid = 2.317431 ;
A10_heid = 0.1632223 ;
A11_heid = 0.5660595 ;

for j = 1 : size(Plab_psia,2)

```

```

P_pr(i,j) = P_lab_psia(i,j) / P_pc_wichert(i) ;

nom(i,j) = A1_heid + A3_heid * log(P_pr(i,j)) + (A5_heid / T_pr(i)) + A7_heid *
(log(P_pr(i,j)))^2 + (A9_heid / T_pr(i)^2) + (A11_heid / T_pr(i)) * log(P_pr(i,j)) ;
denom(i,j) = 1 + A2_heid * log(P_pr(i,j)) + (A4_heid / T_pr(i)) + A6_heid *
(log(P_pr(i,j)))^2 + (A8_heid / T_pr(i)^2) + (A10_heid / T_pr(i)) * log(P_pr(i,j)) ;

z_factor(i,j) = log(nom(i,j) / denom(i,j)) ;
end
end

% Cell
h={'Pmin' 'step1' 'step2' 'step3' 'step4' 'step5' 'step6' 'step7' 'step8' 'step9'
'Pmax'} ;
% Add pressure steps labels
z_factor_Table = [h;num2cell(z_factor)]
;

```

[Published with MATLAB® R2017a](#)

```

clear all
clc
format short e

% Composition which sums at unity
z_i_11 = importdata('Composition.txt') ;
z_i_1 = z_i_11.data ;
% Molecular weight
MW1 = importdata('MolecularWeight.txt') ;
MW = MW1.data ;
% Molecular weight of the Heavy End
MW_heavyend1 = importdata('MW_HeavyEnd.txt') ;
MW_heavyend = MW_heavyend1.data ;
% Density STO
Dens_STO1 = importdata('DensitySTO.txt') ;
Dens_STO = Dens_STO1.data ;
% Specific Gravity
SG = (1/1000) * Dens_STO ;

% Constants for the calculation of Boiling Temperature (Tb)
a_bp = 6.77857 ;
b_bp = 0.401673 ;
c_bp = -1.58262 ;
d_bp = 0.00377409 ;
e_bp = 2.984036 ;
f_bp = -0.00425288 ;
% Boiling Temperature (Tb)
% Preallocation for Speed
Tb_R = zeros(1,size(z_i_1,1));

for i = 1 : size(z_i_1,1)

```

```

    Tb_R(i) = a_bp * (MW_heavyend(i)^b_bp) * (SG(i)^c_bp) *
exp(d_bp*MW_heavyend(i)+e_bp*SG(i)+f_bp*MW_heavyend(i) * SG(i)) ;
end

% Lab Measurements
Plab_psi1 = importdata('PressureSteps.txt') ;
Plab_psi1 = Plab_psi1.data ;
Tlab_R1 = importdata('ResTemperatures.txt') ;
Tlab_R = Tlab_R1.data ;

% Critical Properties: non-HCs & HCs from C1 to C11 (Katz Table)
Tc_i = [227.16 547.38 671.76 342.72 549.72 665.64 734.76 765.36 828.72
845.46 923.04 984.96 1036.08 1085.04 1128.06 1166.04 ] ;
Pc_i = [492 1070 1297 667 708 616 529 551 492 489 483 453 419
383 351 325 ] ;

% Critical Properties: Heavy End
% Preallocation for Speed
Tcp = zeros(1,size(z_i_1,1)) ;
a_Twu = zeros(1,size(z_i_1,1)) ;
gama_P = zeros(1,size(z_i_1,1)) ;
delta_gama_T = zeros(1,size(z_i_1,1)) ;
ef_T = zeros(1,size(z_i_1,1)) ;
Tc_heavyend = zeros(1,size(z_i_1,1)) ;
delta_gama_P = zeros(1,size(z_i_1,1)) ;
ef_P = zeros(1,size(z_i_1,1)) ;
Pcp = zeros(1,size(z_i_1,1)) ;
delta_gama_V = zeros(1,size(z_i_1,1)) ;
ef_V = zeros(1,size(z_i_1,1)) ;
Vcp = zeros(1,size(z_i_1,1)) ;
Vcr = zeros(1,size(z_i_1,1)) ;
Pc_heavyend = zeros(1,size(z_i_1,1)) ;
T_pc_Kays = zeros(1,size(z_i_1,1)) ;
P_pc_Kays = zeros(1,size(z_i_1,1)) ;
epsilon = zeros(1,size(z_i_1,1)) ;
T_pc_Wichert = zeros(1,size(z_i_1,1)) ;
P_pc_Wichert = zeros(1,size(z_i_1,1)) ;

T_pr = zeros(1,size(z_i_1,1)) ;
P_pr = zeros(size(Plab_psi1)) ;

ZA = zeros(size(P_pr)) ;
ZB = zeros(size(P_pr)) ;
ZC = zeros(size(P_pr)) ;
ZD = zeros(size(P_pr)) ;
ZE = zeros(size(P_pr)) ;
ZF = zeros(size(P_pr)) ;
ZG = zeros(size(Plab_psi1)) ;

z_factor = zeros(size(P_pr)) ;

for i = 1 : size(z_i_1,1)
    % Critical Temperature of the Heavy End (Twu correlation)
    Tcp(i) = Tb_R(i)*(0.533272 + (0.191017 * 0.001) * Tb_R(i) + (0.779681 *

```

```

0.0000001)*(Tb_R(i)^2) -(0.284376 * 0.000000001)*(Tb_R(i)^3) + 0.959468*100 /((0.01 *
Tb_R(i))^13))^1 ;
a_Twu(i)      = 1 - (Tb_R(i) / Tc(i)) ;
gama_P(i)     = 0.843593 - 0.128624 * a_Twu(i) - 3.36159 * (a_Twu(i)^3) - 13749.5 *
(a_Twu(i)^12) ;
delta_gama_T(i) = exp(5*(gama_P(i) - SG(i))) - 1 ;
ef_T(i)       = delta_gama_T(i) * (-0.362456 / (Tb_R(i)^0.5) + (0.0398285 - 0.948125 /
(Tb_R(i)^0.5)) * delta_gama_T(i)) ;
Tc_heavyend(i) = Tc(i) * ((1 + 2 * ef_T(i)) / (1 - 2 * ef_T(i)))^2 ;
    % Critical Pressure of the Heavy End (Twu correlation)
delta_gama_P(i) = exp(0.5*(gama_P(i) - SG(i)))-1 ;
ef_P(i)         = delta_gama_P(i) * ((2.53262 - 46.1955 / ((Tb_R(i))^0.5) -0.00127885 *
Tb_R(i)) + (-11.4277 + (252.14 / (Tb_R(i))^0.5) + 0.00230535*Tb_R(i))*delta_gama_P(i)) ;
Pcp(i)          = (3.83354 + 1.19629 * (a_Twu(i)^0.5) + 34.8888 * a_Twu(i) + 36.1952 *
(a_Twu(i)^2) +104.193 * (a_Twu(i)^4))^2 ;
delta_gama_V(i) = exp(4*(gama_P(i)^2 - SG(i)^2)) - 1 ;
ef_V(i)         = delta_gama_V(i) * ((0.46659 / (Tb_R(i)^0.5)) + (-0.182421 +
3.01721/(Tb_R(i)^0.5)) * delta_gama_V(i)) ;
Vcp(i)          = (1 - (0.419869 - 0.505839 * a_Twu(i) - 1.56436 * (a_Twu(i))^3 - 9481.7
* (a_Twu(i))^14)) ^(-8) ;
Vcr(i)          = Vcp(i) * ((1 + 2 * ef_V(i)) / (1 - 2 * ef_V(i)))^2 ;
Pc_heavyend(i)  = (Pcp(i) * (Tc_heavyend(i) / Tc(i)) * (Vcp(i) / Vcr(i))) * ((1 + 2 *
ef_P(i)) / (1 - 2 * ef_P(i)))^2) ;

% Pseudo-criticals (Kay's mixing rule)
T_pc_Kays(i)    = z_i_1(i,[1:size(z_i_1,2)-1]) * transpose(Tc_i) +
z_i_1(i,size(z_i_1,2))* Tc_heavyend(i) ; % Rankine
P_pc_Kays(i)    = z_i_1(i,[1:size(z_i_1,2)-1]) * transpose(Pc_i) +
z_i_1(i,size(z_i_1,2))* Pc_heavyend(i) ; % psia

% Wichert & Aziz Correction
epsilon(i)      = 120 * ((z_i_1(i,2) + z_i_1(i,3))^0.9-(z_i_1(i,2) + z_i_1(i,3))^1.6 +
15*((z_i_1(i,3))^0.5-(z_i_1(i,3))^4)) ;
T_pc_wichert(i) = T_pc_Kays(i) - epsilon(i) ;
P_pc_wichert(i) = (P_pc_Kays(i) * T_pc_wichert(i)) / (T_pc_Kays(i) + z_i_1(i,3) * (1 -
z_i_1(i,3)) * epsilon(i)) ;

% Pseudo-reduced Properties
T_pr(i) = Tlab_R(i) ./ T_pc_wichert(i) ;

% Brill and Beggs Correlation for z factor calculation
ZA(i) = -0.101 - 0.36 * T_pr(i) + 1.3868 * (T_pr(i) - 0.919)^(0.5) ;
ZB(i) = 0.021 + (0.04275) / (T_pr(i) - 0.65) ;
ZC(i) = 0.6222 - 0.224 * T_pr(i) ;
ZD(i) = (0.0657) / (T_pr(i) - 0.86) - 0.037 ;
ZE(i) = 0.32 * exp(-19.53 * (T_pr(i) - 1)) ;
ZF(i) = 0.122 * exp(-11.3 * (T_pr(i) - 1)) ;

for j = 1 : size(Plab_psia,2)
    P_pr(i,j) = Plab_psia(i,j) / P_pc_wichert(i) ;

ZG(i,j) = P_pr(i,j) * (ZC(i) + ZD(i) * P_pr(i,j) + ZE(i) * P_pr(i,j)^4) ;

```

```

z_factor(i,j) = ZA(i) + ZB(i) * P_pr(i,j) + (1-ZA(i)) * exp(-ZG(i,j)) - ZF(i) *
(P_pr(i,j) / 10)^4 ;
end
end

% Cell
h={'Pmin' 'step1' 'step2' 'step3' 'step4' 'step5' 'step6' 'step7' 'step8' 'step9'
'Pmax'} ;
% Add pressure steps labels
z_factor_Table = [h;num2cell(z_factor)]
;

```

[Published with MATLAB® R2017a](#)

```

clear all
clc
format short e

% Original Composition
z1_100 = [0.10  2.95  0.00  72.18 4.03  4.78  1.44  2.38  1.10  0.99  1.28  2.68  2.13
1.06  0.88  0.36  1.66] ;
z2_100 = [0.01  3.44  0.00  66.95 4.64  5.14  1.59  2.43  1.18  1.08  1.66  2.27  2.91
1.47  0.94  0.59  3.70] ;
z3_100 = [0.33  2.86  0.00  66.49 9.33  5.76  0.82  3.30  1.13  1.64  1.64  2.25  1.75
0.90  0.58  0.33  0.89] ;
% z4_100 = [] ;
% z5_100 = [] ;
% z6_100 = [] ;
% z7_100 = [] ;
% z8_100 = [] ;
% z9_100 = [] ;
% z10_100 = [] ;
% z11_100 = [] ;
% z12_100 = [] ;
% z13_100 = [] ;
% z14_100 = [] ;
% z15_100 = [] ;
% z16_100 = [] ;
% z17_100 = [] ;
z_i_100 = [z1_100 ; z2_100 ; z3_100] ;
% Composition which sums at unity
z_i_1 = (1/100) * z_i_100 ;

% Molecular weight
MW = [32.72491
39.62491
31.4358] ;
% Molecular weight of the Heavy End
MW_heavyend = [224.318
241.5318
215.44] ;

```

```

% Density STO
Dens_STO = [784.421
            796
            757.7] ;
% Specific Gravity
SG = (1/1000) * Dens_STO ;

% Constants for the Calculation of Boiling Temperature (Tb)
a_bp = 6.77857 ;
b_bp = 0.401673 ;
c_bp = -1.58262 ;
d_bp = 0.00377409 ;
e_bp = 2.984036 ;
f_bp = -0.00425288 ;
% Boiling Temperature (Tb)
% Preallocation for Speed
Tb_R = zeros(1,size(z_i_100,1));

for i = 1 : size(z_i_100,1)
    Tb_R(i) = a_bp * (MW_heavyend(i)^b_bp) * (SG(i)^c_bp) *
exp(d_bp*MW_heavyend(i)+e_bp*SG(i)+f_bp*MW_heavyend(i) * SG(i)) ;
end

% Lab Measurements
P_lab_MPa_z1 = [38.1 38.3 38.5 38.7 39.0 39.2 39.4 39.6 39.8 40.0 40.2 40.4
               40.6 40.8 41.0 41.2 41.4 41.6 41.8 42.0 42.2 42.4 42.6 42.8 43.0 43.3
               43.5 43.7 43.9 44.1 44.3 44.5 44.7 44.9 45.1 45.3 45.5 45.7 45.9 46.1
               46.3 46.5 46.7 46.9 47.1 47.3 47.5 47.8 48.0 48.2 48.4] ;
P_lab_MPa_z2 = [37.3 37.6 37.8 38.0 38.2 38.4 38.7 38.9 39.1 39.3 39.5 39.8
               40.0 40.2 40.4 40.6 40.9 41.1 41.3 41.5 41.7 42.0 42.2 42.4 42.6 42.9
               43.1 43.3 43.5 43.7 44.0 44.2 44.4 44.6 44.8 45.1 45.3 45.5 45.7 45.9
               46.2 46.4 46.6 46.8 47.0 47.3 47.5 47.7 47.9 48.1 48.4] ;
P_lab_MPa_z3 = [26.7 26.8 27.0 27.2 27.3 27.5 27.6 27.8 27.9 28.1 28.2 28.4
               28.6 28.7 28.9 29.0 29.2 29.3 29.5 29.6 29.8 30.0 30.1 30.3 30.4 30.6
               30.7 30.9 31.0 31.2 31.4 31.5 31.7 31.8 32.0 32.1 32.3 32.4 32.6 32.8
               32.9 33.1 33.2 33.4 33.5 33.7 33.9 34.0 34.2 34.3 34.5] ;
P_lab_MPa = [P_lab_MPa_z1 ; P_lab_MPa_z2 ; P_lab_MPa_z3] ;
P_lab_psia = 145.038 * P_lab_MPa ;
T_lab_K = [403.65 408.55 377.594] ;
T_lab_R = 1.8 * T_lab_K ;

z_lab_z1 = [1.054621355 1.05754595 1.060476444 1.063412514 1.066353843 1.069300119
            1.072251032 1.075206278 1.078165555 1.081128566 1.084095019 1.087064625 1.090037099
            1.09301216 1.095989532 1.098968943 1.101950124 1.10493281 1.107916742 1.110901663
            1.11388732 1.116873465 1.119859854 1.122846247 1.125832406 1.1288181 1.1318031
            1.134787181 1.137770122 1.140751706 1.14373172 1.146709954 1.149686203 1.152660266
            1.155631942 1.15860104 1.161567366 1.164530735 1.167490962 1.170447867 1.173401274
            1.17635101 1.179296906 1.182238795 1.185176514 1.188109905 1.19103881 1.193963079
            1.19688256 1.199797109 1.202706582] ;
z_lab_z2 = [1.15318002 1.157699905 1.162199764 1.166681794 1.171148041 1.175600406
            1.180040663 1.184470468 1.188891373 1.193304829 1.197712201 1.20211477 1.206513744
            1.210910262 1.215305398 1.219700172 1.224095545 1.228492434 1.232891705 1.237294187
            1.241700667 1.246111895 1.25052859 1.254951438 1.259381097 1.263818198 1.268263348

```

```

1.272717129 1.277180102 1.281652808 1.28613577 1.290629492 1.295134464 1.299651158
1.304180034 1.308721538 1.313276103 1.317844152 1.322426095 1.327022335 1.331633262
1.33625926 1.340900704 1.345557962 1.350231393 1.35492135 1.359628182 1.364352231
1.369093831 1.373853316 1.378631011] ;
zlab_z3 = [0.857043692 0.859472731 0.861909917 0.864355154 0.866808346 0.869269402
0.871738229 0.874214738 0.876698841 0.879190452 0.881689486 0.88419586 0.886709493
0.889230303 0.891758213 0.894293145 0.896835022 0.899383771 0.901939317 0.90450159
0.907070517 0.909646029 0.912228059 0.914816538 0.917411401 0.920012583 0.922620019
0.925233648 0.927853407 0.930479236 0.933111076 0.935748867 0.938392552 0.941042074
0.943697378 0.946358408 0.949025111 0.951697433 0.954375323 0.957058729 0.9597476
0.962441887 0.965141541 0.967846513 0.970556757 0.973272225 0.975992872 0.978718652
0.981449521 0.984185436 0.986926353] ;
zlab = [zlab_z1 ; zlab_z2 ; zlab_z3] ;

% Critical Properties: non-HCs & HCs from C1 to C11 (Katz Table)
Tc_i = [227.16 547.38 671.76 342.72 549.72 665.64 734.76 765.36 828.72
845.46 923.04 984.96 1036.08 1085.04 1128.06 1166.04 ] ;
Pc_i = [492 1070 1297 667 708 616 529 551 492 489 483 453 419
383 351 325 ] ;

% Critical Properties: Heavy End

% Preallocation for Speed
Tcp = zeros(1,size(z_i_100,1)) ;
a_Twu = zeros(1,size(z_i_100,1)) ;
gama_P = zeros(1,size(z_i_100,1)) ;
delta_gama_T = zeros(1,size(z_i_100,1)) ;
ef_T = zeros(1,size(z_i_100,1)) ;
Tc_heavyend = zeros(1,size(z_i_100,1)) ;
delta_gama_P = zeros(1,size(z_i_100,1)) ;
ef_P = zeros(1,size(z_i_100,1)) ;
Pcp = zeros(1,size(z_i_100,1)) ;
delta_gama_v = zeros(1,size(z_i_100,1)) ;
ef_v = zeros(1,size(z_i_100,1)) ;
Vcp = zeros(1,size(z_i_100,1)) ;
Vcr = zeros(1,size(z_i_100,1)) ;
Pc_heavyend = zeros(1,size(z_i_100,1)) ;
J_inf = zeros(1,size(z_i_100,1)) ;
K_inf = zeros(1,size(z_i_100,1)) ;
T_pc_Elshark = zeros(1,size(z_i_100,1)) ;
P_pc_Elshark = zeros(1,size(z_i_100,1)) ;
epsilon = zeros(1,size(z_i_100,1)) ;
T_pc_wichert = zeros(1,size(z_i_100,1)) ;
P_pc_wichert = zeros(1,size(z_i_100,1)) ;
T_pr = zeros(1,size(z_i_100,1)) ;
P_pr = zeros(size(Plab_MPa)) ;
A1 = zeros(1, size(T_pr,2)) ;
A2 = zeros(1, size(T_pr,2)) ;
A3 = zeros(1, size(T_pr,2)) ;

maxIter = 100 ;

rho_r = zeros(size(P_pr,1),size(P_pr,2),maxIter) ;
F = zeros(size(P_pr,1),size(P_pr,2),maxIter) ;

```

```

F_prime      = zeros(size(P_pr,1),size(P_pr,2),maxIter) ;
z_factor     = zeros(size(P_pr)) ;

% Elsharkawy Parameters
a0 = 0.036983 ;
a1 = 1.043902 ;
a2 = 0.894942 ;
a3 = 0.792231 ;
a4 = 0.882295 ;
a5 = 0.018637 ;
b0 = -0.7765003 ;
b1 = 1.0695317 ;
b2 = 0.9850308 ;
b3 = 0.8617653 ;
b4 = 1.0127054 ;
b5 = 0.4014645 ;

% Loop of Fluids
for i = 1 : size(z_i_100,1)
    % Critical Temperature of the Heavy End (Tw correlation)
    Tcp(i)      = Tb_R(i)*(0.533272 + (0.191017 * 0.001) * Tb_R(i) + (0.779681 *
    0.0000001)*(Tb_R(i)^2) - (0.284376 * 0.000000001)*(Tb_R(i)^3) + 0.959468*100 /((0.01 *
    Tb_R(i))^13))^(-1) ;
    aTwu(i)     = 1 - (Tb_R(i) / Tcp(i)) ;
    gamaP(i)    = 0.843593 - 0.128624 * aTwu(i) - 3.36159 * (aTwu(i)^3) - 13749.5 *
    (aTwu(i)^12) ;
    deltagama_T(i) = exp(5*(gamaP(i) - SG(i))) - 1 ;
    efT(i)      = deltagama_T(i) * (-0.362456 / (Tb_R(i)^0.5) + (0.0398285 - 0.948125 /
    (Tb_R(i)^0.5)) * deltagama_T(i) ) ;
    Tc_heavyend(i) = Tcp(i) * ((1 + 2 * efT(i)) / (1 - 2 * efT(i)))^2 ;
    % Critical Pressure of the Heavy End (Tw correlation)
    deltagama_P(i) = exp(0.5*(gamaP(i) - SG(i)))-1 ;
    efP(i)      = deltagama_P(i) * ((2.53262 - 46.1955 / ((Tb_R(i))^0.5) -0.00127885 *
    Tb_R(i) + (-11.4277 + (252.14 / (Tb_R(i))^0.5) + 0.00230535*Tb_R(i))*deltagama_P(i)) ;
    Pcp(i)      = (3.83354 + 1.19629 * (aTwu(i)^0.5) + 34.8888 * aTwu(i) + 36.1952 *
    (aTwu(i)^2) +104.193 * (aTwu(i)^4))^2 ;
    deltagama_V(i) = exp(4*(gamaP(i)^2 - SG(i)^2)) - 1 ;
    efV(i)      = deltagama_V(i) * ((0.46659 / (Tb_R(i)^0.5)) + (-0.182421 +
    3.01721/(Tb_R(i)^0.5)) * deltagama_V(i)) ;
    vcp(i)      = (1 - (0.419869 - 0.505839 * aTwu(i) - 1.56436 * (aTwu(i))^3 - 9481.7
    * (aTwu(i))^14)) ^(-8) ;
    vcr(i)      = vcp(i) * ((1 + 2 * efV(i)) / (1 - 2 * efV(i)))^2 ;
    Pc_heavyend(i) = (Pcp(i) * (Tc_heavyend(i) / Tcp(i)) * (vcp(i) / vcr(i)) * ((1 + 2 *
    efP(i))/(1 - 2 * efP(i)))^2) ;

% Pseudo-criticals (Elsharkawy mixing rule)
Jinf(i) = a0 + (a1*zi_1(i,3)*Tc_i(1,3)/Pc_i(1,3)) +
(a2*zi_1(i,2)*Tc_i(1,2)/Pc_i(1,2)) + (a3*zi_1(i,1)*Tc_i(1,1)/Pc_i(1,1)) +
(a4*zi_1(i,[4:size(z_i_100,2)-1])*transpose(Tc_i(1,[4:size(z_i_100,2)-
1]))./Pc_i(1,[4:size(z_i_100,2)-1])) + (a5*zi_1(i,size(z_i_100,2))*MWheavyend(i)) ;

Kinf(i) = b0 + (b1*zi_1(i,3)*Tc_i(1,3)/Pc_i(1,3).^0.5) +
(b2*zi_1(i,2)*Tc_i(1,2)/Pc_i(1,2).^0.5) + (b3*zi_1(i,1)*Tc_i(1,1)/Pc_i(1,1).^0.5) +

```

```

(b4*z_i_1(i,[4:size(z_i_100,2)-1])*transpose(Tc_i(1,[4:size(z_i_100,2)-
1]))./Pc_i(1,[4:size(z_i_100,2)-1]).^0.5)) + (b5*z_i_1(i,size(z_i_100,2))*Mw_heavyend(i))
;
T_pc_Elshark(i) = K_inf(i)^2 / J_inf(i) ; % Rankine
P_pc_Elshark(i) = T_pc_Elshark(i) / J_inf(i) ; % psia
% Wichert & Aziz Correction
epsilon(i) = 120 * ((z_i_1(i,2) + z_i_1(i,3))^0.9 - (z_i_1(i,2) + z_i_1(i,3))^1.6 +
15*((z_i_1(i,3))^0.5 - (z_i_1(i,3))^4)) ;
T_pc_Wichert(i) = T_pc_Elshark(i) - epsilon(i) ;
P_pc_Wichert(i) = (P_pc_Elshark(i) * T_pc_Wichert(i)) / (T_pc_Elshark(i) + z_i_1(i,3) *
(1 - z_i_1(i,3)) * epsilon(i)) ;
% Pseudo-reduced Properties
T_pr(i) = Tlab_R(i) ./ T_pc_Wichert(i) ;

% Dranchuk and Abou-kassem Correlation for z factor calculation
% Parameters
C1 = 0.3265 ;
C2 = -1.0700 ;
C3 = -0.5339 ;
C4 = 0.01569 ;
C5 = -0.05165 ;
C6 = 0.5475 ;
C7 = -0.7361 ;
C8 = 0.1844 ;
C9 = 0.1056 ;
C10 = 0.6134 ;
C11 = 0.7210 ;

A1(i) = C1 + C2/T_pr(i) + C3/T_pr(i)^3 + C4/T_pr(i)^4 + C5/T_pr(i)^5 ;
A2(i) = C6 + C7/T_pr(i) + C8/T_pr(i)^2 ;
A3(i) = C9 * (C7/T_pr(i) + C8/T_pr(i)^2) ;

% Loop of Pressure-steps
for j = 1 : size(Plab_MPa,2)
    P_pr(i,j) = Plab_psia(i,j) / P_pc_Wichert(i) ;

    z0 = 1 ;
    z_est = z0 ;
    z_old = z0 ;

% Loop of NR
for k = 1 : maxIter

    rho_r(i,j,k) = (0.27 * P_pr(i,j)) / (z_est * T_pr(i)) ;

    F(i,j,k) = A1(i)*rho_r(i,j,k) + A2(i)*rho_r(i,j,k)^2 - A3(i)*rho_r(i,j,k)^5 +
C10*(1+C11*rho_r(i,j,k)^2)*(rho_r(i,j,k)^2/T_pr(i)^3)*3*exp(-C11*rho_r(i,j,k)^2)+1-z_est
;

    F_prime(i,j,k) = (14348907*A3(i)*P_pr(i,j)^5)/(2000000000*T_pr(i)^5*z_est^6) -
(729*A2(i)*P_pr(i,j)^2)/(5000*T_pr(i)^2*z_est^3) -
(27*A1(i)*P_pr(i,j))/(100*T_pr(i)*z_est^2) - (2187*C10*P_pr(i,j)^2*exp(-
(729*C11*P_pr(i,j)^2)/(10000*T_pr(i)^2*z_est^2)))/((729*C11*P_pr(i,j)^2)/(10000*T_pr(i)^2

```

```

*z_est^2) + 1))/(5000*T_pr(i)^5*z_est^3) - (1594323*c10*c11*P_pr(i,j)^4*exp(-
(729*c11*P_pr(i,j)^2)/(10000*T_pr(i)^2*z_est^2)))/(50000000*T_pr(i)^7*z_est^5) +
(1594323*c10*c11*P_pr(i,j)^4*exp(-
(729*c11*P_pr(i,j)^2)/(10000*T_pr(i)^2*z_est^2))*((729*c11*P_pr(i,j)^2)/(10000*T_pr(i)^2
*z_est^2) + 1))/(50000000*T_pr(i)^7*z_est^5) - 1 ;

    z_est = z_est - F(i,j,k) / F_prime(i,j,k) ;
    z_old = z_est ;

end

z_factor(i,j) = z_est ;

end
end

```

Published with MATLAB® R2017a

```

clear all
clc
format short e

% Original Composition
z1_100 = [0.10  2.95  0.00  72.18  4.03  4.78  1.44  2.38  1.10  0.99  1.28  2.68  2.13
          1.06  0.88  0.36  1.66] ;
z2_100 = [0.01  3.44  0.00  66.95  4.64  5.14  1.59  2.43  1.18  1.08  1.66  2.27  2.91
          1.47  0.94  0.59  3.70] ;
z3_100 = [0.33  2.86  0.00  66.49  9.33  5.76  0.82  3.30  1.13  1.64  1.64  2.25  1.75
          0.90  0.58  0.33  0.89] ;
% z4_100 = [] ;
% z5_100 = [] ;
% z6_100 = [] ;
% z7_100 = [] ;
% z8_100 = [] ;
% z9_100 = [] ;
% z10_100 = [] ;
% z11_100 = [] ;
% z12_100 = [] ;
% z13_100 = [] ;
% z14_100 = [] ;
% z15_100 = [] ;
% z16_100 = [] ;
% z17_100 = [] ;
z_i_100 = [z1_100 ; z2_100 ; z3_100] ;
% Composition which sums at unity
z_i_1 = (1/100) * z_i_100 ;

% Molecular weight
MW = [32.72491
      39.62491
      31.4358] ;

```

```

% Molecular weight of the Heavy End
MW_heavyend = [224.318
               241.5318
               215.44] ;
% Density STO
Dens_STO = [784.421
            796
            757.7] ;
% Specific Gravity
SG = (1/1000) * Dens_STO ;

% Constants for the Calculation of Boiling Temperature (Tb)
a_bp = 6.77857 ;
b_bp = 0.401673 ;
c_bp = -1.58262 ;
d_bp = 0.00377409 ;
e_bp = 2.984036 ;
f_bp = -0.00425288 ;
% Boiling Temperature (Tb)
% Preallocation for Speed
Tb_R = zeros(1,size(z_i_100,1));

for i = 1 : size(z_i_100,1)
    Tb_R(i) = a_bp * (MW_heavyend(i)^b_bp) * (SG(i)^c_bp) *
exp(d_bp*MW_heavyend(i)+e_bp*SG(i)+f_bp*MW_heavyend(i) * SG(i)) ;
end

% Lab Measurements
Plab_MPa_z1 = [38.1 38.3 38.5 38.7 39.0 39.2 39.4 39.6 39.8 40.0 40.2 40.4
              40.6 40.8 41.0 41.2 41.4 41.6 41.8 42.0 42.2 42.4 42.6 42.8 43.0 43.3
              43.5 43.7 43.9 44.1 44.3 44.5 44.7 44.9 45.1 45.3 45.5 45.7 45.9 46.1
              46.3 46.5 46.7 46.9 47.1 47.3 47.5 47.8 48.0 48.2 48.4] ;
Plab_MPa_z2 = [37.3 37.6 37.8 38.0 38.2 38.4 38.7 38.9 39.1 39.3 39.5 39.8
              40.0 40.2 40.4 40.6 40.9 41.1 41.3 41.5 41.7 42.0 42.2 42.4 42.6 42.9
              43.1 43.3 43.5 43.7 44.0 44.2 44.4 44.6 44.8 45.1 45.3 45.5 45.7 45.9
              46.2 46.4 46.6 46.8 47.0 47.3 47.5 47.7 47.9 48.1 48.4] ;
Plab_MPa_z3 = [26.7 26.8 27.0 27.2 27.3 27.5 27.6 27.8 27.9 28.1 28.2 28.4
              28.6 28.7 28.9 29.0 29.2 29.3 29.5 29.6 29.8 30.0 30.1 30.3 30.4 30.6
              30.7 30.9 31.0 31.2 31.4 31.5 31.7 31.8 32.0 32.1 32.3 32.4 32.6 32.8
              32.9 33.1 33.2 33.4 33.5 33.7 33.9 34.0 34.2 34.3 34.5] ;
Plab_MPa      = [Plab_MPa_z1 ; Plab_MPa_z2 ; Plab_MPa_z3] ;
Plab_psia     = 145.038 * Plab_MPa ;
Tlab_K        = [403.65 408.55 377.594] ;
Tlab_R        = 1.8 * Tlab_K ;

zlab_z1 = [1.054621355 1.05754595 1.060476444 1.063412514 1.066353843 1.069300119
           1.072251032 1.075206278 1.078165555 1.081128566 1.084095019 1.087064625 1.090037099
           1.09301216 1.095989532 1.098968943 1.101950124 1.10493281 1.107916742 1.110901663
           1.11388732 1.116873465 1.119859854 1.122846247 1.125832406 1.1288181 1.1318031
           1.134787181 1.137770122 1.140751706 1.14373172 1.146709954 1.149686203 1.152660266
           1.155631942 1.15860104 1.161567366 1.164530735 1.167490962 1.170447867 1.173401274
           1.17635101 1.179296906 1.182238795 1.185176514 1.188109905 1.19103881 1.193963079
           1.19688256 1.199797109 1.202706582] ;

```

```

zlab_z2 = [1.15318002  1.157699905 1.162199764 1.166681794 1.171148041 1.175600406
 1.180040663 1.184470468 1.188891373 1.193304829 1.197712201 1.20211477  1.206513744
 1.210910262 1.215305398 1.219700172 1.224095545 1.228492434 1.232891705 1.237294187
 1.241700667 1.246111895 1.25052859  1.254951438 1.259381097 1.263818198 1.268263348
 1.272717129 1.277180102 1.281652808 1.28613577  1.290629492 1.295134464 1.299651158
 1.304180034 1.308721538 1.313276103 1.317844152 1.322426095 1.327022335 1.331633262
 1.33625926  1.340900704 1.345557962 1.350231393 1.35492135  1.359628182 1.364352231
 1.369093831 1.373853316 1.378631011] ;
zlab_z3 = [0.857043692  0.859472731 0.861909917 0.864355154 0.866808346 0.869269402
 0.871738229 0.874214738 0.876698841 0.879190452 0.881689486 0.88419586  0.886709493
 0.889230303 0.891758213 0.894293145 0.896835022 0.899383771 0.901939317 0.90450159
 0.907070517 0.909646029 0.912228059 0.914816538 0.917411401 0.920012583 0.922620019
 0.925233648 0.927853407 0.930479236 0.933111076 0.935748867 0.938392552 0.941042074
 0.943697378 0.946358408 0.949025111 0.951697433 0.954375323 0.957058729 0.9597476
 0.962441887 0.965141541 0.967846513 0.970556757 0.973272225 0.975992872 0.978718652
 0.981449521 0.984185436 0.986926353] ;
zlab    = [zlab_z1 ; zlab_z2 ; zlab_z3] ;

% Critical Properties: non-HCs & HCs from C1 to C11 (Katz Table)
Tc_i    = [227.16 547.38  671.76  342.72  549.72  665.64  734.76  765.36  828.72
 845.46  923.04  984.96  1036.08 1085.04 1128.06 1166.04 ] ;
Pc_i    = [492 1070 1297 667 708 616 529 551 492 489 483 453 419
 383 351 325 ] ;

% Critical Properties: Heavy End
% Preallocation for Speed
Tcp      = zeros(1,size(z_i_100,1)) ;
a_Twu    = zeros(1,size(z_i_100,1)) ;
gama_P   = zeros(1,size(z_i_100,1)) ;
delta_gama_T = zeros(1,size(z_i_100,1)) ;
ef_T     = zeros(1,size(z_i_100,1)) ;
Tc_heavyend = zeros(1,size(z_i_100,1)) ;
delta_gama_P = zeros(1,size(z_i_100,1)) ;
ef_P     = zeros(1,size(z_i_100,1)) ;
Pcp      = zeros(1,size(z_i_100,1)) ;
delta_gama_V = zeros(1,size(z_i_100,1)) ;
ef_V     = zeros(1,size(z_i_100,1)) ;
Vcp      = zeros(1,size(z_i_100,1)) ;
Vcr      = zeros(1,size(z_i_100,1)) ;
Pc_heavyend = zeros(1,size(z_i_100,1)) ;
T_pc_Kays = zeros(1,size(z_i_100,1)) ;
P_pc_Kays = zeros(1,size(z_i_100,1)) ;
epsilon  = zeros(1,size(z_i_100,1)) ;
T_pc_wichert = zeros(1,size(z_i_100,1)) ;
P_pc_wichert = zeros(1,size(z_i_100,1)) ;

T_pr     = zeros(1,size(z_i_100,1)) ;
P_pr     = zeros(size(Plab_MPa)) ;

A1       = zeros(1, size(T_pr,2)) ;
A2       = zeros(1, size(T_pr,2)) ;
A3       = zeros(1, size(T_pr,2)) ;

maxIter = 100 ;

```

```

rho_r      = zeros(size(P_pr,1),size(P_pr,2),maxIter) ;
F          = zeros(size(P_pr,1),size(P_pr,2),maxIter) ;
F_prime   = zeros(size(P_pr,1),size(P_pr,2),maxIter) ;
z_factor   = zeros(size(P_pr)) ;

% Loop of Fluids
for i = 1 : size(z_i_100,1)
    % Critical Temperature of the Heavy End (Twu correlation)
    Tc_p(i)      = Tb_R(i)*(0.533272 + (0.191017 * 0.001) * Tb_R(i) + (0.779681 *
    0.0000001)*(Tb_R(i)^2) - (0.284376 * 0.0000000001)*(Tb_R(i)^3) + 0.959468*100 /((0.01 *
    Tb_R(i))^13))^(-1) ;
    a_Twu(i)     = 1 - (Tb_R(i) / Tc_p(i)) ;
    gama_P(i)    = 0.843593 - 0.128624 * a_Twu(i) - 3.36159 * (a_Twu(i)^3) - 13749.5 *
    (a_Twu(i)^12) ;
    delta_gama_T(i) = exp(5*(gama_P(i) - SG(i))) - 1 ;
    ef_T(i)      = delta_gama_T(i) * (-0.362456 / (Tb_R(i)^0.5) + (0.0398285 - 0.948125 /
    (Tb_R(i)^0.5)) * delta_gama_T(i)) ;
    Tc_heavyend(i) = Tc_p(i) * ((1 + 2 * ef_T(i)) / (1 - 2 * ef_T(i)))^2 ;
    % Critical Pressure of the Heavy End (Twu correlation)
    delta_gama_P(i) = exp(0.5*(gama_P(i) - SG(i))) - 1 ;
    ef_P(i)       = delta_gama_P(i) * ((2.53262 - 46.1955 / ((Tb_R(i))^0.5) - 0.00127885 *
    Tb_R(i) + (-11.4277 + (252.14 / (Tb_R(i))^0.5) + 0.00230535*Tb_R(i))*delta_gama_P(i)) ;
    Pcp(i)       = (3.83354 + 1.19629 * (a_Twu(i)^0.5) + 34.8888 * a_Twu(i) + 36.1952 *
    (a_Twu(i)^2) + 104.193 * (a_Twu(i)^4))^2 ;
    delta_gama_V(i) = exp(4*(gama_P(i)^2 - SG(i)^2)) - 1 ;
    ef_V(i)      = delta_gama_V(i) * ((0.46659 / (Tb_R(i)^0.5) + (-0.182421 +
    3.01721/(Tb_R(i)^0.5)) * delta_gama_V(i)) ;
    Vcp(i)      = (1 - (0.419869 - 0.505839 * a_Twu(i) - 1.56436 * (a_Twu(i))^3 - 9481.7
    * (a_Twu(i))^14)) ^(-8) ;
    Vcr(i)      = Vcp(i) * ((1 + 2 * ef_V(i)) / (1 - 2 * ef_V(i)))^2 ;
    Pc_heavyend(i) = (Pcp(i) * (Tc_heavyend(i) / Tc_p(i)) * (Vcp(i) / Vcr(i)) * ((1 + 2 *
    ef_P(i)) / (1 - 2 * ef_P(i))))^2 ;

% Pseudo-criticals (Kay's mixing rule)
T_pc_Kays(i)   = z_i_1(i,[1:size(z_i_100,2)-1]) * transpose(Tc_i) +
z_i_1(i,size(z_i_100,2))* Tc_heavyend(i) ; % Rankine
P_pc_Kays(i)   = z_i_1(i,[1:size(z_i_100,2)-1]) * transpose(PC_i) +
z_i_1(i,size(z_i_100,2))* Pc_heavyend(i) ; % psia

% Wichert & Aziz Correction
epsilon(i)     = 120 * ((z_i_1(i,2) + z_i_1(i,3))^0.9 - (z_i_1(i,2) + z_i_1(i,3))^1.6 +
15*((z_i_1(i,3))^0.5 - (z_i_1(i,3))^4)) ;
T_pc_Wichert(i) = T_pc_Kays(i) - epsilon(i) ;
P_pc_Wichert(i) = (P_pc_Kays(i) * T_pc_Wichert(i)) / (T_pc_Kays(i) + z_i_1(i,3) * (1 -
z_i_1(i,3)) * epsilon(i)) ;

% Pseudo-reduced Properties
T_pr(i) = Tlab_R(i) ./ T_pc_Wichert(i) ;

% Dranchuk and Abou-kassem Correlation for z factor calculation
% Parameters
C1 = 0.3265 ;

```

```

C2 = -1.0700 ;
C3 = -0.5339 ;
C4 = 0.01569 ;
C5 = -0.05165 ;
C6 = 0.5475 ;
C7 = -0.7361 ;
C8 = 0.1844 ;
C9 = 0.1056 ;
C10 = 0.6134 ;
C11 = 0.7210 ;

A1(i) = C1 + C2/T_pr(i) + C3/T_pr(i)^3 + C4/T_pr(i)^4 + C5/T_pr(i)^5 ;
A2(i) = C6 + C7/T_pr(i) + C8/T_pr(i)^2 ;
A3(i) = C9 * (C7/T_pr(i) + C8/T_pr(i)^2) ;

% Loop of Pressure-steps
for j = 1 : size(Plab_MPa,2)
    P_pr(i,j) = Plab_psia(i,j) / P_pc_wichert(i) ;

    z0 = 1 ;
    z_est = z0 ;
    z_old = z0 ;

% Loop of NR
for k = 1 : maxIter

    rho_r(i,j,k) = (0.27 * P_pr(i,j)) / (z_est * T_pr(i)) ;

    F(i,j,k) = A1(i)*rho_r(i,j,k) + A2(i)*rho_r(i,j,k)^2 - A3(i)*rho_r(i,j,k)^5 +
    C10*(1+C11*rho_r(i,j,k)^2)*(rho_r(i,j,k)^2/T_pr(i)^3)*3*exp(-C11*rho_r(i,j,k)^2)+1-z_est
    ;

    F_prime(i,j,k) = (14348907*A3(i)*P_pr(i,j)^5)/(2000000000*T_pr(i)^5*z_est^6) -
    (729*A2(i)*P_pr(i,j)^2)/(5000*T_pr(i)^2*z_est^3) -
    (27*A1(i)*P_pr(i,j))/(100*T_pr(i)*z_est^2) - (2187*C10*P_pr(i,j)^2*exp(-
    (729*C11*P_pr(i,j)^2)/(10000*T_pr(i)^2*z_est^2))*((729*C11*P_pr(i,j)^2)/(10000*T_pr(i)^2
    *z_est^2) + 1))/(5000*T_pr(i)^5*z_est^3) - (1594323*C10*C11*P_pr(i,j)^4*exp(-
    (729*C11*P_pr(i,j)^2)/(10000*T_pr(i)^2*z_est^2)))/(50000000*T_pr(i)^7*z_est^5) +
    (1594323*C10*C11*P_pr(i,j)^4*exp(-
    (729*C11*P_pr(i,j)^2)/(10000*T_pr(i)^2*z_est^2))*((729*C11*P_pr(i,j)^2)/(10000*T_pr(i)^2
    *z_est^2) + 1))/(50000000*T_pr(i)^7*z_est^5) - 1 ;

    z_est = z_est - F(i,j,k) / F_prime(i,j,k) ;
    z_old = z_est ;

end

z_factor(i,j) = z_est ;

end
end

```

References

‘Phase Behavior’, Curtis H. Whitson and Michael R. Brule, Henry L. Doherty Memorial Fund of AIME Society of Petroleum Engineers Inc.

‘An efficient correlation for calculating compressibility factor of natural gases’, Navid Azizi, Dr. R. Behbahani, Dr. M. A. Isazadeh, Journal of Natural Gas Chemistry 19(2010)642–645.

‘PVT and Phase Behavior of Petroleum Reservoir Fluids’, Ali Danesh, Elsevier Science and Technology Books (ISBN: 0444821961), May 1998.

Kumar, N., 2004. Compressibility Factor for Natural and Sour Reservoir Gases by Correlations and Cubic Equations of State. MSc thesis. Texas Tech University, Lubbock, Texas, USA.

‘Evaluation of Correlations for Libyan Natural Gas Compressibility Factor’, Dr. Ebrahim Ali Mohamed, Dr. Riyad Ageli Saleh, Zawia University, January 2016.

‘An accurate empirical correlation for predicting natural gas compressibility factors’, Ehsan Sanjari, Ebrahim Nemati Lay, Journal of Natural Gas Chemistry 21(2012)184–188.

‘Efficient methods for calculations of compressibility, density and viscosity of natural gases’, Adel M. Elsharkawy, Fluid Phase Equilibria 218 (2004) 1–13.

‘New correlations to predict natural gas viscosity and compressibility factor’, Ehsan Heidaryan, Jamshid Moghadasi, Masoud Rahimi, Journal of Petroleum Science and Engineering, May 2010.

‘A Unified Model for Representing Densities and Viscosities of Hydrocarbon Liquids and Gases based on Peng-Robinson Equation of State’, Li-Sheng Wang, Hui-Chao Lv, The Open Thermodynamics Journal, 2009, 3, 24-33.

‘A New Computerized Approach to z Factor Determination’, Kingdom K. Dune, Oriji Bright N., Transnational Journal of Science and Technology, August 2012.

‘A Review of the Equations of State and their Applicability in Phase Equilibrium Modeling’, Sashay Ramdharee, Edison Muzenda, Mohamed Belaid, International Conference on Chemical and Environmental Engineering (ICCEE 2013), April 2013.

‘Generalized Liquid Volume Shifts for the Peng-Robinson Equation of State for C_1 to C_8 Hydrocarbons’, B. Hoyos, Latin American Applied Research, 2004.

‘Natural Gas Compressibility Factor Measurement and Evaluation for High Pressure High Temperature Gas Reservoirs’, I. I. Azubuike, S. S. Ikiensikimama, O. D. Orodu, International Journal of Scientific & Engineering Research, July 2016.

‘Thermodynamic Models for the Prediction of Petroleum-Fluid Phase Behavior’, Romain Privat, Jean-Noel Jaubert.

‘Natural Gas Compressibility Factor Correlation Evaluation for Niger Delta Gas Fields’, J. Obuba, S. S. Ikiensikimama, S. S. Ubani, C. E. Ekeke, IOSR Journal of Electrical and Electronics Engineering (IOSR-JEEE), August 2013.

Obuba, J., Ikiensikimama, S.S., Ubani, C. E., Ekeke, I. C 2013 Natural Gas Compressibility Factor Correlation Evaluation For Niger Delta Gas Fields IOSR Journal of Electrical and Electronics Engineering (IOSR-JEEE) e-ISSN: 2278-1676,p-ISSN: 2320-3331, Volume 6, Issue 4 (Jul. - Aug. 2013), PP 01-10.

Yarborough L., Hall K.R., 1974. How to Solve Equation of State for z factors Oil & Gas J., Feb 18, 86-88.

Beggs, D.H., Brill, J.P., 1973. A study of two-phase flow in inclined pipes. J. Petrol, Technol. 25 (5), 607e617.

Papay, J. 1985 “A Termelstechnologiai Parameterek Valtozasa a Gazlelepk Muvelese Soran.” OGIL MUSZ, Tud, Kuzl. [Budapest]: 267–273.

Dranchuk, P.M., Abou-Kassem, J.H., 1975. Calculation of z factors for natural gases, using equations of state. J. Can. Petrol. Technol. 14 (3), 34e36.

Brown G. G. The compressibility of Gases, Part I - Pure Gases. Pet Eng, 1940:21.

Brown G. G., Holcomb D. E., The compressibility of Gases, Part II – Gaseous Mixtures. Pet Eng, 1940:23